FEDERAL UNIVERSITY OF MINAS GERAIS

STRUCTURAL ENGINEERING DEPARTMENT

Elayne Marques Silva

Probabilistic Assessment of Serviceability of FRP-Reinforced Concrete Beams

FEDERAL UNIVERSITY OF MINAS GERAIS
STRUCTURAL ENGINEERING DEPARTMENT

"PROBABILISTIC ASSESSMENT OF SERVICEABILITY OF FRP-REINFORCED CONCRETE BEAMS"

Elayne Marques Silva

Dissertation presented to the Graduate Program in Structural Engineering of the Structural Engineering Department of the Federal University of Minas Gerais, being part of the requirements for the "Master in Structural Engineering" degree.

Examination committee:

_____
Prof. Sofia Maria Carrato Diniz – (Advisor)
DEEs – Structural Engineering Department – UFMG

_____
Prof. Sidnea Eliane Campos Ribeiro – (Co-advisor)
DEMC – Department of Materials and Construction - UFMG

_____
Prof. José Márcio Fonseca Calixto
DEEs – Structural Engineering Department – UFMG

_____
Prof. Sebastião Salvador Real Pereira
DEEs – Structural Engineering Department – UFMG

Belo Horizonte, August 2017.

ACKNOWLEDGEMENTS

ABSTRACT

Reinforced concrete (RC) structures are often subjected to deicing salts or in a marine environment; as such, a major problem in the durability of these structures is the corrosion of reinforcing steel. In this light, Fiber Reinforced Polymers (FRP), as noncorrosive materials, provide a promising prospect for use as reinforcement in concrete construction. FRP reinforcement may offer not only greater durability but also higher resistance and, consequently, potential gains throughout the lifecycle of the structure. Although the use of FRP bars as structural reinforcement shows great promise in terms of durability, the characteristics of this material led to new challenges in the design of FRP-RC components. Due to differences between the mechanical properties of steel and FRP, the reliability of FRP-reinforced concrete (RC) beams shall be assessed. While a reasonable body of knowledge has been gathered regarding the reliability of FRP-RC beams with respect to ultimate limit states, the same is not true for serviceability of such beams. Since FRP is characterized by higher values of strength and lower Young's modulus compared to steel, this implies that the design of FRP-RC structures will be influenced almost exclusively by serviceability limit states. In this study, a contribution to the development of semiprobabilistic design recommendations for FRP-RC beams, with respect to the serviceability limit state, is reported. Numerous equations have been proposed for computing the effective moment of inertia of FRP-RC members. This research also aims to select an equation for the calculation of the effective moment of inertia for FRP-RC beams assessed in this study. Since most of the variables involved in the problem (mechanical properties of concrete and FRP, geometric characteristics, model error, loads, etc.) are random, serviceability is established in probabilistic terms. In this context, Monte Carlo simulation is used in the probabilistic description of beam deflections, and in the computation of the probability of failure of designed beams with respect to the limit state of excessive deflections. Large probabilities of failure are found for this serviceability limit state according to current design recommendations. Suggestions are presented on simple, but effective ways to circumvent this limitation.

Keywords: FRP, FRP-Reinforced Structures, Durability, Beams, Effective Moment of Inertia, Design Codes, Deflections, Serviceability Limit State, Reliability, Probability, Monte Carlo Simulation.

TABLE OF CONTENTS

LIST OF FIGURES

LIST OF TABLES

ACRONYMS

ACI – American Concrete Institute;

AFRP – aramid FRP;

COV – coefficient of variation;

CFRP- carbon FRP;

FRP – Fiber-Reinforced Polymers;

FRP-RC – FRP-reinforced concrete;

GFRP – glass FRP;

RC – reinforced concrete;

SLS – serviceability limit state;

ULS – ultimate limit state.

NOTATION

a - depth of equivalent rectangular stress block;

A_f - total area of FRP reinforcement;

$A_{f,min}$ - minimum area of FRP reinforcement;

A'_s - area of compression reinforcement;

b - width of rectangular cross section;

c - depth of the neutral axis;

C_E - environmental reduction factor for various fiber types and exposure conditions;

d - distance from extreme compression fiber to centroid of tension reinforcement;

d_c - thickness of concrete cover measured from extreme tension fiber to center of bar or wire location closest thereto;

d_{FRP} - diameter of FRP bar;

d_s - thickness of stirrups;

DL - random variable "dead load";

E_c - modulus of elasticity of concrete;

E_f - design modulus of elasticity of FRP;

E_{FRP} - random variable "modulus of elasticity of FRP";

$E_{f,ave}$ - average modulus of elasticity of FRP;

E_s - modulus of elasticity of steel;

f_c - concrete compressive strength *in situ*;

f'_c - specified compressive strength of concrete;

f_f - stress in FRP reinforcement in tension;

f_{fu} - design tensile strength of FRP, considering reductions for service environment;

$f_{fu, ave}$ - mean tensile strength of FRP bar;

f^*_{fu} - guaranteed tensile strength of FRP bar;

F_C - random variable "compressive strength of concrete";

F_{FU} - random variable "tensile strength of FRP bar";

f_r - modulus of rupture of concrete;

h - depth of rectangular cross section;

I_{cr} - cracked moment of inertia;

I_e - effective moment of inertia;

I_g - gross moment of inertia;

I_T - moment of inertia of uncracked section transformed to concrete;

I'_e - equivalent moment of inertia;

k - ratio of depth of neutral axis to reinforcement depth;

ℓ - span of beam;

$L1$ - first layer of reinforcement;

$L2$ - second layer of reinforcement;

LL_{SLS} - random variable "live load" (serviceability analysis);

M_a - maximum moment in the beam;

M_{cr} - cracking moment;

M_d - design moment;

M_{Dn} - design moment due to dead load;

M_{Ln} - design moment due to live load;

M_n - nominal moment capacity;

M_u - factored moment at section;

n_f - ratio of the modulus of elasticity of FRP bars to the modulus of elasticity of concrete; number of failures;

n_s - sample size (number of simulations);

p_{serv} - service load;

P_F - probability of failure;

P_s - probability of nonfailure;

r - ratio mean dead load to mean live load;

R_d - design strength;

s - standard deviation;

S_d - design strength;

U_n – unfactored nominal load;

V - coefficient of variation;

y_t - distance from centroidal axis of gross section to tension face.

Greek letters

α_1 - ratio of average concrete stress to concrete strength;

α - bond dependent coefficient;

α_c - reduction factor of concrete compressive strength;

δ_a - allowable deflection;

β_1 - ratio of the depth of the equivalent rectangular stress block to the depth of the neutral axis;

β - reliability index;

β_d - reduction coefficient used in calculating effective moment of inertia;

γ - correction factor used in calculating equivalent moment of inertia;

γ_D - amplification factor of dead load;

γ_L - amplification factor of live load;

$\Delta_{(cp + sh)}$ - additional deflection due to creep and shrinkage under sustained loads;

Δ_b - random variable "beam width";

Δ_c - random variable "concrete cover";

Δ_h - random variable "beam depth";

$\Delta_{i,a}$ - adjusted immediate deflection;

$\Delta_{(i,a)D}$ - adjusted immediate deflection due to dead loads;

$\Delta_{(i,a)L}$ - immediate deflection due to live loads;

$\Delta_{i(sus)}$ - immediate deflection due to sustained loads;

Δ_{total} - total deflection;

ε_c - concrete compressive strain at failure;

ε_{cu} - ultimate strain in concrete;

ε_{fu} - design rupture strain of FRP reinforcement;

ε^*_{fu} - guaranteed rupture strain of FRP reinforcement;

η_s - stiffness reduction coefficient;

η - model error;

λ - multiplier for additional long-term deflection;

λ_r - modification factor used in calculating modulus of rupture of concrete;

μ - mean;

μ_c - average compressive strength of concrete;

μ_{DL} - mean dead load;

$\mu_{LL(SLS)}$ - mean of live loads in the serviceability limit state;

$\mu_{LL(ULS)}$ - mean of live loads in the ultimate limit state;

μ_v - mean nominal load;

ξ - time-dependent factor for sustained loads;

ρ_f - FRP reinforcement ratio;

ρ_{fb} - FRP reinforcement balanced ratio;

ρ' - ratio of steel compression reinforcement;

ϕ - strength reduction factor.

1

INTRODUCTION

1.1 STATEMENT OF THE PROBLEM

Reinforced concrete (RC) structures are often subjected to deicing salts or in a marine environment; as such, a major problem in the durability of these structures is the corrosion of reinforcing steel. In this light, Fiber Reinforced Polymers (FRP), as noncorrosive materials, provide a promising prospect for use as reinforcement in concrete construction.

The use of FRP as internal reinforcement arose from the need to mitigate the corrosion of reinforcing steel. The expansion of the highway systems in the 1950s in United States and the need to provide year-round maintenance, made it common to apply deicing salts on highway bridges during the winter. As a result, reinforcing steel in these structures experienced extensive corrosion, and this problem became a source of concern (ACI 440, 2006). Due to growing interest on high performance materials in recent years, FRP bars have emerged as an alternative to tackling the problem of corrosion.

FRP is a composite material consisting of continuous fibers, usually glass (GFRP), aramid (AFRP) or carbon (CFRP), embedded in a resin matrix then molded and hardened in the intended shape. Examples of FRP bars to be used as internal reinforcement in concrete structures are shown in Figure 1.1 (ACI 440, 2015).

Figure 1.1 - Examples of FRP reinforcing bars (ACI 440, 2015).

FRP reinforcement may offer not only greater durability but also higher resistance and, consequently, potential gains throughout the life-cycle of the structure. Moreover, the specific advantages of this material may be combined in innovative systems, such as FRP reinforced concrete (FRP-RC) beams and slabs.

Although the use of FRP bars as structural reinforcement shows great promise in terms of durability, the characteristics of this material led to new challenges in the design of FRP-RC components. Design of RC beams usually results in under-reinforced beams, where the failure mode is governed by the yielding of steel, while in the design of FRP-RC beams the concrete crushing is the most desirable failure mode (Nanni, 1993). Design recommendations of steel reinforced members are commonly based on limit state design principles, i.e. the member is designed based on its required strength and then checked for serviceability criteria. But in many instances, serviceability criteria may control the flexural design of FRP-RC members (ACI 440, 2006).

Deflections of RC beams have traditionally been computed using an elastic deflection equation that includes an effective moment of inertia (I_e), originally introduced by Branson (1965) for steel reinforced concrete (Bischoff and Gross, 2011b). However, it has been recognized that Branson's empirical equation gives too stiff response for FRP-RC and underestimates deflection of such members (Nawy and Neuwerth, 1977; Yost *et al*., 2003).

Numerous equations have been proposed by many investigators for computing the effective moment of inertia of FRP-RC members.

Due to differences between the mechanical properties of steel and FRP, the reliability of the FRP-RC beams shall be analyzed. While a reasonable body of knowledge has been gathered regarding the reliability of FRP-RC beams with respect to ultimate limit states (ACI 440, 2006; Ribeiro and Diniz, 2013; Shield *et al.*, 2011), the same is not true for serviceability of FRP-RC beams. In this light, this investigation aims to contribute to the development of semi-probabilistic design recommendations for FRP-RC beams with respect to serviceability limit states (excessive deflections).

The basic problem of reliability of structural engineering systems may be cast essentially as a *supply* versus *demand* problem; in other words, as the determination of the capacity (supply) of an engineering system to meet certain requirements (demand) (Ang and Tang, 1990). In this work, the basic problem is formulated from the total deflection of FRP-RC beams (demand) to meet an acceptable deflection limit established in accordance to the use of the structure, i.e. the allowable deflection (supply). Since most of the variables involved in the problem (mechanical properties of concrete and FRP, geometric characteristics, model error, loads, etc.) are random, serviceability of FRP-RC beams is established in probabilistic terms.

In this context, a Monte Carlo simulation procedure is implemented for the probabilistic description of the beam deflections, and the computation of the probability of failure of designed beams with respect to the limit state of excessive deflections. Due to the lack of Brazilian recommendations for FRP-RC member design, the beams assessed in this study are designed according to ACI 440 (2006) design recommendations.

1.2 OBJECTIVES

The main goal of this work is to contribute to the development of semi-probabilistic design recommendations for FRP-RC beams with respect to serviceability limit states (excessive deflections). To this end, the probabilistic assessment of deflections of FRP-RC beams designed according to ACI 440 (2006) is performed.

Other specific objectives have also been pursued:

   – selection of a deterministic equation for calculation of the effective moment of inertia of FRP-RC beams;

   – implementation of a computational procedure using Monte Carlo simulation for the probabilistic description of deflections of FRP-RC beams;

   – probabilistic assessment of serviceability (excessive deflections) of FRP-RC beams designed according to ACI 440 (2006).

1.3 ORGANIZATION

This study is divided into 7 chapters and 2 appendices.

Chapter 1 contains a brief description of FRP composites and the research significance; the objectives of this study are stated, and a description of subsequent chapters is given at the end of the chapter.

Chapter 2 highlights some of the main mechanical properties of concrete and of FRP bars, as related to serviceability checking of FRP-RC beams.

Chapter 3 summarizes ACI 440 (2006) provisions for flexural design of FRP-RC members, for both ultimate strength and serviceability.

Chapter 4 details general considerations regarding deflections of FRP-RC beams. This includes the calculation of the total deflection, and consequently the calculation of the immediate and long-term deflections. Special attention is given to equations used in the computation of the effective moment of inertia of FRP-RC beams.

Chapter 5 presents a brief review of basic reliability concepts (margin of safety, reliability index, probability of failure, performance function, and Monte Carlo simulation).

In Chapter 6, the reliability analysis of deflections of FRP-RC beams is performed. Initially, eighty-one representative beams are selected for the analysis. Then, the deterministic relationship for the performance evaluation is established; the basic variables of the problem are identified, and the corresponding statistics are obtained from the literature. Next, a computational procedure for the reliability analysis of FRP-RC beams with respect to the

serviceability of such beams (excessive deflections) is presented and the corresponding reliability levels are assessed.

Chapter 7 summarizes the main steps along the development of the research presented herein, the main conclusions and recommendations for further researches.

Appendix 1 presents the FRPSERV program for the reliability analysis of serviceability of FRP-RC beams. Monte Carlo simulation is used in order to obtain the statistics of deflections of FRP-RC beams and the corresponding probabilities of failure (and reliability indexes) with respect to the limit state of excessive deflections. This computacional procedure is implemented in the Matlab software, version 7.0.1 (and *Statistics toolbox*).

Appendix 2 presents a complete worked example on the reliability analysis of deflections of a GFRP-RC beam.

2

MECHANICAL PROPERTIES OF MATERIALS

In this chapter, the main mechanical properties of concrete and of FRP bars related to FRP-RC beam deflections are presented.

2.1 CONCRETE

In this study, three specified concrete compressive strengths - 30 and 50 MPa (representing normal strength concrete) and 70 MPa (representing high-strength concrete) - will be evaluated in the probabilistic assessment of deflections of FRP-RC beams.

The use of the high-strength concrete has become very common not only bridges, tunnels or dams, but also in buildings. According to ACI 440 (2006), the high tensile strength of FRP is most efficiently used when paired with high-strength concrete and may increase the stiffness of the cracked region.

Stress-strain diagram of high-strength concrete is different from that presented by normal strength concrete. The curves shown in Figure 2.1 represent stress-strain diagrams of concrete for different strengths, according to the relationship suggested by Thorenfeldt *et al*. (1987). ACI 318 (2014) allows the use of an equivalent rectangular stress block in lieu of the actual stress-strain diagram in the ultimate limit state analysis of RC members.
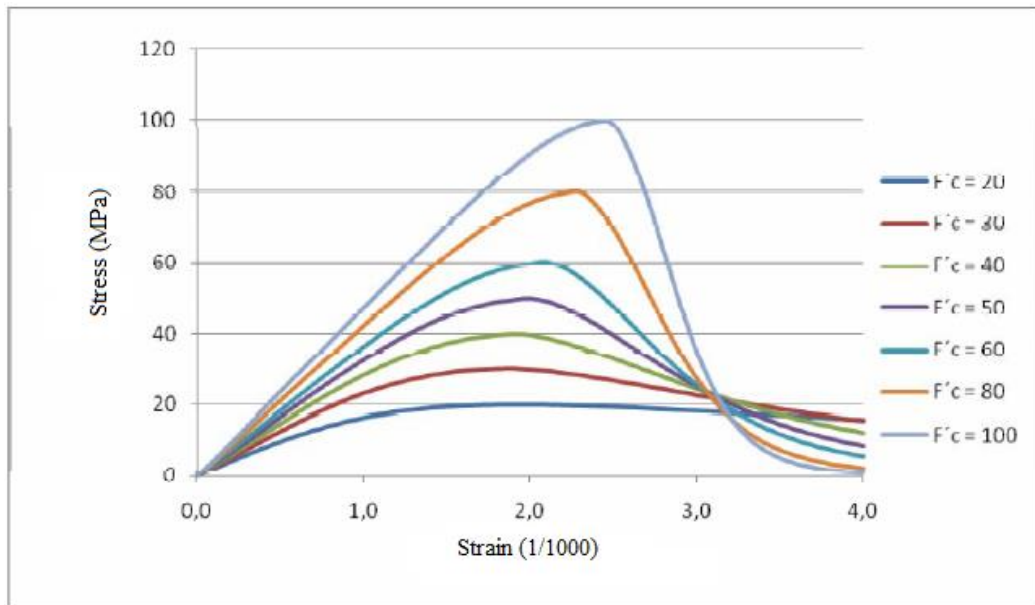
Figure 2.1 - Stress-strain diagram to different strengths of concrete.

From Figure 2.1, it can be observed that:

- maximum strength occurs at a strain between 0.002 and 0.003. ACI 318 (2014) assumes that the concrete has a maximum strain (ε_{cu}) equal to 0.003;

- initial slope of the curves (initial modulus of elasticity) increases with increased compressive strength of the concrete;

- the ascending part of the stress-strain curve is similar to a parabola with vertex at the maximum stress. As the concrete strength increases, the ascending part tends to be linear;

- the higher the concrete strength, the greater the strain at the maximum stress;

- the higher the concrete strength, the lower the maximum strain.

Normal weight concrete typically has a density between 2155 and 2560 kg/m³. The modulus of elasticity (E_c) of normal weight concrete can be computed by the following equation (ACI 318, 2014):

$$E_c = 4700\sqrt{f_c^{'}}$$
(2.1)

where:

f'_c = specified compressive strength of concrete (MPa).

Modulus of rupture, f_r, for concrete shall be calculated by (ACI 318, 2014):

$$f_r = 0.62\,\lambda_r\,\sqrt{f_c^{'}}$$
(2.2)

where λ_r is the modification factor to reflect the reduced mechanical properties of lightweight concrete relative to normal weight concrete of the same compressive strength. For normal weight concrete, λ_r is equal to 1.0.

2.2 FIBER-REINFORCED POLYMERS (FRP)

Mechanical properties of FRP composites can vary significantly from one product to another depending on factors, such as volume and fiber type, resin type, fiber orientation, geometric characteristics, manufacturing process, and quality control during manufacture (ACI 440, 2006). Some of the main mechanical properties of FRP bars are detailed in the following sections.

2.2.1 Tensile behavior of FRP bars

Tensile strength of FRP bars in the longitudinal direction of the fibers is typically greater than the tensile strength of steel reinforcement, and have lower modulus of elasticity, unlike carbon fibers, that may present modulus of elasticity greater than the steel. Tensile properties of FRP bars are summarized in Table 2.1.

Table 2.1 - Usual tensile properties of reinforcing bars* (ACI 440, 2006).

Properties	Steel	GFRP	CFRP	AFRP
Nominal yield stress (MPa)	276 to 517	N/A	N/A	N/A
Tensile strength (MPa)	483 to 690	483 to 1600	600 to 3690	1720 to 2540
Elastic modulus (GPa)	200.0	35.0 to 51.0	120.0 to 580.0	41.0 to 125.0
Yield strain, %	0.14 to 0.25	N/A	N/A	N/A
Rupture strain, %	6.0 to 12.0	1.2 to 3.1	0.5 to 1.7	1.9 to 4.4

* Typical values for fiber volume fraction ranging from 0.5 to 0.7.
N/A: Not applicable.

FRP bars do not exhibit any plastic behavior (yielding) before rupture, and is characterized by a linear-elastic stress-strain relationship up to rupture (ACI 440, 2006). Figure 2.2 shows stress-strain diagrams for steel, GFRP, AFRP, and CFRP bars. While steel presents ductile behavior, FRP exhibits brittle behavior in which the rupture of the bars occurs without any sensitive change in deformation, as can be observed in the diagram.
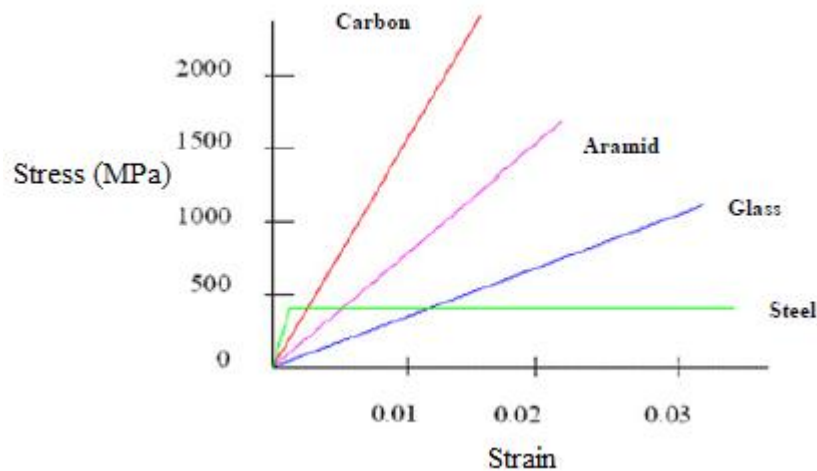
Figure 2.2 - Stress-strain curves of typical reinforcing bars (Fico, 2007).

The tensile strength and stiffness of a FRP bar are dependent on several factors; strength and stiffness variations can occur in bars with different fiber-volume ratios, even in bars with the same diameter, appearance and components. The rate of curing, the manufacturing process, and the manufacturing quality control also affect the mechanical characteristics of the bar (Wu, 1990).

The tensile strength of FRP bars is inversely proportional to the bar diameter: the smaller the bar diameter, the higher the tensile strength of the FRP (ACI 440, 2006), see Table 2.2.

Table 2.2 - Tensile strength of FRP bars.

Metric conversion	Nominal diameter (mm)	Area (mm²)	Minimum tensile strength (MPa)	
			GFRP	CFRP
No. 6	6.4	31.6	760	1450
No. 10	9.5	71	760	1310
No. 13	12.7	129	690	1170
No. 16	15.9	199	655	1100
No. 19	19.1	284	620	1100
No. 22	22.2	387	586	N/A
No. 25	25.4	510	550	N/A
No. 29	28.7	645	517	N/A
No. 32	32.3	819	480	N/A

* N/A: Not applicable.

2.2.2 Compressive behavior of FRP bars

FRP bars with higher tensile strengths usually have higher compressive strengths, except in the case of AFRP, where the fibers present nonlinear behavior in compression at a relatively low level of stress. However, the compressive strength of FRP bars is less than the tensile strength (ACI 440, 2006). Results obtained in studies conducted by Mallick (1988) and Wu (1990) are discussed in ACI 440 (2006). It was found that the compressive strength is approximately 55, 78, and 20% of the tensile strength for GFRP, CFRP, and AFRP, respectively. For this reason, the use of FRP is not recommended to resist compression.

2.2.3 Shear behavior of FRP bars

According to ACI 440 (2006), FRP bars exhibits little shear strength and this is governed by the polymer matrix.

2.2.4 Density

Density of FRP bars is lower than steel density (see Table 2.3). This characteristic should be taken into account while assessing FRP performance as structural reinforcement; reduction of transportation costs, and procedures to facilitate handling and installation of the bars are some of the advantages of the lightweight characteristic of FRP bars (Machado, 2002).

Table 2.3 - Typical densities of reinforcing bars (g/cm³) (ACI 440, 2006).

Steel	GFRP	CFRP	AFRP
7.90	1.25 to 2.10	1.50 to 1.60	1.25 to 1.40

*Typical values for fiber volume fraction ranging from 0.5 to 0.7.

2.2.5 Creep rupture of FRP bars

FRP reinforcing bars can exhibit creep rupture (or static fatigue) when subjected to a constant load over time after a time period called endurance time. The creep rupture endurance time can decrease under adverse environmental conditions such as high temperature, ultraviolet radiation exposure, high alkalinity, wet and dry cycles, or freezing-and-thawing cycles. As the ratio of the sustained tensile stress to the short-term strength of the FRP bar increases, endurance time decreases. Glass fibers are the most susceptible to creep rupture, whereas carbon fibers are the least susceptible to creep rupture (ACI 440, 2006).

2.3 SUMMARY OF THE CHAPTER

In this chapter, some of the main mechanical properties of concrete and FRP bars have been presented. High longitudinal tensile strength and lightweight when compared to steel are some of the advantages of FRP bars. On the other hand, FRP bars have little shear strength, present lower modulus of elasticity than the steel, no yielding before brittle rupture, and should not be used to resist compressive stresses. Additionally, ACI 440 (2006) points out that the use of high-strength concrete allows for better use of high-strength properties of FRP bars.

3

DESIGN CONSIDERATIONS FOR FRP-REINFORCED CONCRETE BEAMS

In this chapter, some of the existing design recommendations for FRP-RC members are listed, and the ACI 440 (2006) procedures for flexural design of FRP-RC beams are reviewed.

3.1 GENERAL DESIGN CONSIDERATIONS

Countries and regions, such as the United States (ACI 440, 2015), Japan (Japan Society of Civil Engineers, 1997), Canada (CAN/ CSA-S6-06, CAN/ CSA-S806-12), and Europe (*fib* 2007, 2010) established design-related documents for FRP-reinforced and externally reinforced concrete members (ACI 440, 2015).

Existing recommendations for FRP-reinforced concrete members are analogous to the design of steel-reinforced concrete members. Modifications are influenced by the mechanical properties of FRP bars, and empirical equations are based on experimental results (Ribeiro, 2009).

Steel-reinforced concrete beams are commonly under-reinforced and the failure mode is governed by steel yielding, resulting in a ductile failure. Design of FRP-RC beams involves two materials of brittle behavior (concrete and FRP), and a brittle failure is unavoidable. Concrete crushing failure mode is marginally more desirable for flexural members reinforced with FRP bars (Nanni, 1993); consequently, a change in the design paradigm for FRP-RC beams is required. However, existing design recommendations for FRP-RC members, do not present an in-depth discussion on the impact of the change in the failure mode (from ductile failure to brittle failure) on the performance of such members (Ribeiro, 2009).

In Brazil, no document exists addressing utilization of FRP in RC construction; therefore, ACI 440 recommendations will be used for FRP-RC beams in this work. ACI 440 (2006) approach for flexural design of FRP-reinforced concrete members is detailed in the following section.

3.2 ACI-440 recommendations for flexural design

ACI 440 (2006) design recommendations for FRP-RC structures are based on limit state design and are similar to the design recommendations for steel-reinforced concrete members. In limit state design principles, a FRP-reinforced concrete member is designed to meet ultimate limit state requirements and then checked for serviceability criteria. Steel-reinforced concrete beams are usually under-reinforced to ensure yielding of steel before the crushing of concrete (ductile failure), providing ductility to the member. If FRP reinforcement ruptures, failure of FRP-RC beams is sudden (Nanni, 1993; Jaeger *et al*., 1997; GangaRao and Vijay, 1997; Theriault and Benmokrane, 1998). Both failure modes (FRP rupture and concrete crushing) are fragile but acceptable if strength and serviceability criteria are met. Because FRP does not yield, ACI 440 (2006) recommendations prescribes a higher margin of safety than that used in traditional steel-reinforced concrete design to compensate for the lack of ductility. Thus, the member should possess a higher strength reserve.

Calculation of the strength of cross sections should be based on the following assumptions (ACI 440, 2006):

(i)   strain in the concrete and FRP reinforcement is proportional to the distance from neutral axis;

(ii)   the maximum usable compressive strain in the concrete is assumed to be 0.003;

(iii)   the tensile strength of concrete is ignored;

(iv)   the tensile behavior of the FRP reinforcement is linearly elastic until failure; and

(v)   perfect bond exists between concrete and FRP reinforcement.

ACI 440 (2006) establishes that the flexural strength (reduced strength) of the beam must be greater than or equal to the factored moment calculated by the factored loads (increased loads):

$$\phi M_n \geq M_u \tag{3.1}$$

where:

ϕ = strength reduction factor;

M_n = nominal moment capacity;

M_u = factored moment at section, result of increased load. (Coefficients of increased loads of ACI 440 – 2006 recommendations are the same as those prescribed in ACI 318 – 2014.)

The nominal flexural strength of FRP-RC beams can be determined based on strain compatibility, internal force equilibrium, and failure mode. Failure mode (FRP rupture and concrete crushing) can be determined by comparing the FRP reinforcement ratio to the balanced reinforcement ratio (i.e., a ratio where concrete crushing and FRP rupture occur simultaneously). Because the nonductile behavior of FRP reinforcement, the balanced ratio of FRP reinforcement is computed using its design tensile strength. The FRP reinforcement ratio and the balanced FRP reinforcement ratio can be computed by Eqs. (3.2) and (3.3), respectively:

$$\rho_f = \frac{A_f}{b\,d} \tag{3.2}$$

where:

ρ_f = FRP reinforcement ratio;

A_f = total area of FRP reinforcement;

b = width of rectangular cross section;

d = distance from extreme compression fiber to centroid of tension reinforcement.

$$\rho_{fb} = 0.85\,\beta_1 \frac{f_c^{'}}{f_{fu}} \left(\frac{E_f\,\varepsilon_{cu}}{E_f\,\varepsilon_{cu} + f_{fu}} \right) \tag{3.3}$$

where:

ρ_{fb} = FRP reinforcement balanced ratio;

β_1 = factor taken as 0.85 for concrete strength (f'_c) up to and including 27.6 MPa. For strengths above 27.6 MPa, this factor is reduced continuously at a rate of 0.05 per each 6.9 MPa of strength in excess of 27.6 MPa, but is not taken less than 0.65;

f'_c = specified compressive strength of concrete (MPa);

f_{fu} = design tensile strength of FRP, considering reductions for service environment (MPa);

E_f = design modulus of elasticity of FRP defined as mean modulus of sample test specimens;

ε_{cu} = ultimate strain in concrete.

If the reinforcement ratio is less than the balanced ratio ($\rho_f < \rho_{fb}$), failure mode is governed by FRP rupture. Otherwise ($\rho_f > \rho_{fb}$), concrete crushing governs the failure mode. When $\rho_f > \rho_{fb}$, failure mode of the structure is initiated by concrete crushing and stress distribution in the concrete can be given by ACI 318 rectangular stress block. Based on the equilibrium of forces and strain compatibility, the nominal flexural strength can be calculated by:

$$M_n = A_f \, f_f \left(d - \frac{a}{2} \right) \tag{3.4}$$

where a is the depth of equivalent rectangular stress block given by:

$$a = \frac{A_f \, f_f}{0.85 \, f'_c \, b} \tag{3.5}$$

and the stress in FRP reinforcement in tension, f_f, is computed by:

$$f_f = E_f \, \varepsilon_{cu} \frac{\beta_1 \, d - a}{a} \quad \text{(MPa)} \tag{3.6}$$

Substituting Eq. (3.5) into Eq. (3.6), f_f can be obtained by:

$$f_f = \left(\sqrt{\frac{(E_f \, \varepsilon_{cu})^2}{4} + \frac{0.85 \, \beta_1 \, f'_c}{\rho_f} E_f \, \varepsilon_{cu}} - 0.5 E_f \, \varepsilon_{cu} \right) \leq f_{fu} \tag{3.7}$$

The nominal flexural strength can also be calculated in terms of FRP reinforcement ratio as given in Eq. (3.8) to replace Eq. (3.4):

$$M_n = \rho_f \, f_f \left(1 - 0.59 \, \frac{\rho_f \, f_f}{f_c'} \right) b \, d^2 \qquad (3.8)$$

When $\rho_f < \rho_{fb}$, the failure of the member is initiated by rupture of FRP bar, and ACI 318 stress block is not applicable because the maximum concrete strain (0.003) may not be reached. In this case, an equivalent stress block would need to be used that approximates the stress distribution in the concrete at the particular strain level reached. This analysis incorporates two unknowns: the concrete compressive strain at failure, ε_c, and the depth of the neutral axis, c. In addition, the rectangular stress block factors, α_1 and β_1, are unknown. The factor α_1 is the ratio of the average concrete stress to the concrete strength; factor β_1 is given by the ratio of the depth of the equivalent rectangular stress block to the depth of the neutral axis. The analysis involving all these unknowns is complex. Nominal flexural strength can be calculated by the following equation:

$$M_n = A_f \, f_{fu} \left(d - \frac{\beta_1 c}{2} \right) \qquad (3.9)$$

For a given section, the product $(\beta_1 c)$ in Eq. (3.9) varies depending on material properties and FRP reinforcement ratio. The maximum value for this product is equal to $(\beta_1 c_b)$ and is reached when the maximum concrete strain (0.003) is attained. Nominal flexural strength of the member can be calculated by a simplified and conservative mode by Eqs. (3.10) and (3.11) as follows:

$$M_n = A_f \, f_{fu} \left(d - \frac{\beta_1 c_b}{2} \right) \qquad (3.10)$$

$$c_b = \left(\frac{\varepsilon_{cu}}{\varepsilon_{cu} + \varepsilon_{fu}} \right) d \qquad (3.11)$$

3.2.1 Strength reduction factors

Because FRP bars do not exhibit ductile behavior, a conservative strength reduction factor ϕ must be adopted to provide a higher reserve strength for the member.

The strength reduction factors suggested by ACI 440 (2006) are given by:

$$\phi = 0.55 \text{ for } \rho_f \leq \rho_{fb} \tag{3.12a}$$

$$\phi = 0.3 + 0.25 \frac{\rho_f}{\rho_{fb}} \quad \text{for } \rho_{fb} < \rho_f < 1.4\,\rho_{fb} \tag{3.12b}$$

$$\phi = 0.65 \text{ for } \rho_f \geq 1.4\rho_{fb} \tag{3.12c}$$

where ρ_f and ρ_{fb} are computed by Eqs. (3.2) and (3.3).

The reduction factor equal to 0.55 represents under-reinforced concrete beams where failure mode is governed by FRP rupture; 0.65 for over-reinforced beams where concrete crushing governs the failure mode; and the reduction factor given by Eq. (3.12b) represents beams in a transition zone.

3.2.2 Minimum FRP reinforcement

ACI 440 (2006) prescribes a minimum amount of reinforcement that should be adopted if failure of a member is controlled by FRP rupture, i.e., when $\rho_f < \rho_{fb}$. The minimum reinforcement area for FRP-reinforced members is given by:

$$A_{f,\min} = \frac{4.9\sqrt{f_c'}}{f_{fu}}\,b\,d \geq \frac{360}{f_{fu}}\,b\,d \text{ (psi)} \tag{3.13}$$

where:

$A_{f,min}$ = minimum area of FRP reinforcement;

f'_c = specified compressive strength of concrete;

f_{fu} = design tensile strength of FRP, considering reductions for service environment;

b = width of rectangular cross section;

d = distance from extreme compression fiber to centroid of tension reinforcement.

If concrete crushing governs the failure mode ($\rho_f > \rho_{fb}$) the minimum reinforcement area of FRP is achieved.

3.2.3 Design material properties

The material properties values of FRP bars provided by the manufacturer, such as tensile strength, should be taken as initial values because they do not include the effects of long-term exposure to the environment. This exposure can reduce the strength capacity of FRP bars; therefore, it is necessary to consider in design equations the reduction of the values of the material properties according to the type and level of environmental exposure (ACI 440, 2006).

In order to account for the effects of the environmental exposure, ACI 440 (2006) reduces the tensile strength of FRP bars according to the following expression:

$$f_{fu} = C_E \, f^*_{fu} \tag{3.14}$$

where:

f_{fu} = design tensile strength of FRP, considering reductions for service environment;
C_E = environmental reduction factor for various fiber types and exposure conditions, given in Table 3.1;
f^*_{fu} = guaranteed tensile strength of FRP bar.

Table 3.1 - Environmental reduction factor for various fibers and exposure conditions (ACI 440, 2006).

Exposure condition	Fiber type	Environmental reduction fator C_E
Concrete not exposed to earth and weather	Carbon	1.0
	Glass	0.8
	Aramid	0.9
Concrete exposed to earth and weather	Carbon	0.9
	Glass	0.7
	Aramid	0.8

The environmental reduction factors given in Table 3.1 are conservative values that take into account the durability of each fiber type and include the temperature effects.

ACI 440 (2006) recommendations also define a reduced design rupture strain that should be used in the design process Eq. (3.15):

$$\varepsilon_{fu} = C_E \ \varepsilon^*_{fu} \tag{3.15}$$

where:

ε_{fu} = design rupture strain of FRP reinforcement;

ε^*_{fu} = guaranteed rupture strain of FRP reinforcement.

3.2.4 Serviceability

Serviceability can be defined as satisfactory performance under service load conditions; with deflection calculations being one of the main tasks in a serviceability analysis. FRP-reinforced concrete members have a relatively small stiffness after cracking. Consequently, permissible deflections under service loads can control the design (ACI 440, 2006). Moreover, FRP bars are characterized by higher values of strength and lower modulus of elasticity compared to steel, and this implies that the design of FRP-RC structures will be influenced almost exclusively by the serviceability limit state (Mota *et al*., 2006; Tegola, 1998). According to ACI 440 (2006), FRP-reinforced cross sections designed for failure by concrete crushing (more desirable failure mode) satisfies serviceability criteria for deflection.

The serviceability provisions given in existing recommendations for steel-reinforced members need to be modified for FRP-RC members due to differences in properties between steel and FRP, such as lower stiffness, bond strength, and corrosion resistance. At the same longitudinal reinforcement ratio, the replacement of steel with FRP, would typically result in larger deflections (Gao *et al*., 1998; Tighiouart *et al*., 1998).

ACI 440 (2006) provisions for deflection control are interested with deflections that occur at service levels under immediate and sustained static loads, and do not apply to dynamic loads such as earthquakes, transient winds, or vibration of machinery. Two methods are presented in ACI 440 (2006), in accordance with ACI 318-05, for control of deflections of one-way flexural members: (i) the indirect method of mandating the minimum thickness of the member; and (ii) the direct method of limiting computed deflections.

The direct method of deflection control, as presented in ACI 440 (2006) recommendations, is described in the following section.

3.2.4.1 Calculation of deflection (direct method)

According ACI 440 (2006), the control of deflection by direct method is given by comparison of the computed deflections with acceptable limits (allowable deflections) set as part of the design criteria for the project.

3.2.4.1.1   Immediate deflection

Immediate deflection (calculated under service loads) of an FRP one-way flexural member can be calculated using the effective moment of inertia (I_e) of the FRP-RC beam and the usual structural analysis techniques.

When maximum moment (M_a) of a beam is less than cracking moment (M_{cr}), i.e., $M_a < M_{cr}$, the section is uncracked and the effective moment of inertia (I_e) is taken to be equal to the gross moment of inertia (I_g). Otherwise, when $M_a > M_{cr}$, cracking occurs, causing a reduction in the stiffness of the beam. In this case, the effective moment of inertia, I_e, is based on the cracked moment of inertia (I_{cr}). Thus, separation between behavior of the cracked and the uncracked section is defined by the cracking moment, M_{cr}. I_g is calculated according to the cross section geometry, while I_{cr} can be calculated using an elastic analysis. The concept that involves the elastic analysis to calculate I_{cr} of FRP-RC is similar to the analysis used for steel-reinforced concrete, where concrete in tension is ignored (ACI 440, 2006). The elastic analysis is given by Eq. (3.16) to (3.18):

$$M_{cr} = \frac{f_r\, I_g}{y_t} \tag{3.16}$$

where:

f_r = modulus of rupture of concrete (MPa), defined by Eq. (2.2);
I_g = gross moment of inertia;
y_t = distance from centroidal axis of gross section to tension face.

$$I_{cr} = \frac{b\,d^3}{3}k^3 + n_f\,A_f\,d^2\,(1-k)^2 \tag{3.17}$$

and k is given by:

$$k = \sqrt{2\,\rho_f\,n_f + (\rho_f\,n_f)^2} - \rho_f\,n_f \tag{3.18}$$

where:

b = width of rectangular cross section;

d = distance from extreme compression fiber to centroid of tension reinforcement;

k = ratio of depth of neutral axis to reinforcement depth;

n_f = ratio of the modulus of elasticity of FRP bars (E_f) to the modulus of elasticity of concrete

(E_c), $n_f = \dfrac{E_f}{E_c}$;

A_f = total area of FRP reinforcement;

ρ_f = FRP reinforcement ratio, defined by Eq. (3.2).

The overall flexural stiffness E_cI of a flexural member that has experienced cracking at service varies between E_cI_g and E_cI_{cr}, depending on magnitude of the applied moment. Branson (1965) derived an equation to express transition from I_g to I_{cr}. This equation is adopted by ACI 318 (2014) to calculate the effective moment of inertia I_e for steel-reinforced beams and is given by the following equation (ACI 440, 2006):

$$I_e = \left\{ \left(\frac{M_{cr}}{M_a}\right)^3 I_g + \left[1 - \left(\frac{M_{cr}}{M_a}\right)^3\right] I_{cr} \right\} \le I_g \tag{3.19}$$

where:

M_{cr} = cracking moment;

M_a = maximum moment in the beam;

I_g = gross moment of inertia;

I_{cr} = cracked moment of inertia.

This equation was based on the behavior of steel-reinforced beams at service load levels and reflects two different phenomena: the variation of stiffness (*EI*) along the member and the effect of concrete tension stiffening (ACI 440, 2006). Branson's equation, however, has been found to overestimate the effective moment of inertia of FRP-RC beams, especially for lightly reinforced beams, implying a lesser degree of tension stiffening than in comparable steel-reinforced beams (Nawy and Neuwerth, 1977; Benmokrane *et al.*, 1996; Toutanji and Saafi, 2000). According to ACI 440 (2006), this reduced tension stiffening may be attributed to the lower modulus of elasticity and different bond stress levels for the FRP reinforcement as compared with those of steel.

Gao *et al.* (1998) proposed a modified equation for the effective moment of inertia to account for reduced tension stiffening in FRP-RC beams. This equation is recommended by ACI 440 (2006) and is given by:

$$I_e = \left\{ \left(\frac{M_{cr}}{M_a} \right)^3 \beta_d I_g + \left[1 - \left(\frac{M_{cr}}{M_a} \right)^3 \right] I_{cr} \right\} \leq I_g \tag{3.20}$$

where β_d is a reduction coefficient related to the reduced tension stiffening exhibited by FRP-RC members.

Research has demonstrated that the degree of tension stiffening is affected by the amount and stiffness of the flexural reinforcement and by the relative reinforcement ratio (ratio of ρ_f to ρ_{fb}) (Toutanji and Saafi, 2000; Yost *et al.*, 2003). Based on an evaluation of experimental results from several studies, ACI 440 (2006) recommends the following relationship for β_d:

$$\beta_d = \left(\frac{1}{5} \right) \cdot \left(\frac{\rho_f}{\rho_{fb}} \right) \leq 1.0 \tag{3.21}$$

where:

ρ_f = FRP reinforcement ratio, defined by Eq. (3.2);
ρ_{fb} = FRP reinforcement balanced ratio, defined by Eq. (3.3).

ACI 440 (2006) recommendations establishes that Eq. (3.20) is valid if the maximum moment in the member is equal to or greater than cracking moment, $M_a \geq M_{cr}$. If M_a is significantly

lower than M_{cr}, then the calculated deflection should be based on I_g. In cases where M_a is slightly less than M_{cr}, the section can be considered as cracked because factors such as shrinkage and temperature may cause the section to crack even if $M_a < M_{cr}$; and $M_a = M_{cr}$ must be assumed.

Several researchers have proposed other equations of computing the effective moment of inertia for FRP-RC beams. Some of these equations are presented in Chapter 4.

3.2.4.1.2   Long-term deflection

Long-term increase in deflection is a function of member geometry (reinforcement area and member size), load characteristics (age of concrete when loading is applied, and magnitude and duration of sustained loading), and material properties (modulus of elasticity of concrete and FRP reinforcement, creep and shrinkage of concrete, formation of new cracks, and widening of existing cracks) (ACI 440, 2006).

Study performed by Brown (1997) shows that data on time-dependent deflections of FRP-RC members due to creep and shrinkage indicate that the time-versus-deflection curves of FRP-reinforced and steel-reinforced members have the same basic shape, indicating that the same fundamental approach for estimating the long-term deflection can be used.

Long-term deflection due to creep and shrinkage, $\Delta_{(cp + sh)}$, for steel-reinforced concrete beams can be computed according to the following equations (ACI 440, 2006):

$$\Delta_{(cp + sh)} = \lambda \, (\Delta_i)_{sus} \qquad (3.22)$$

and the factor λ is given by:

$$\lambda = \frac{\xi}{1 + 50\rho'} \qquad (3.23)$$

where:

$\Delta_{i(sus)}$ = immediate deflection due to sustained loads;
ξ = time-dependent factor for sustained loads, given in Table 3.2;

ρ' = ratio of steel compression reinforcement, given by $\rho' = \dfrac{A'_s}{b\,d}$, where A'_s is the area of compression reinforcement, b is the width of rectangular cross section, and d is the distance from extreme compression fiber to centroid of tension reinforcement.

Table 3.2 - Time-dependent factor for sustained loads (ACI 318, 2014).

Sustained load duration (months)	Time-dependent factor (ξ)
3	1.0
6	1.2
12	1.4
60 or more	2.0

ACI 440 (2006) recommendations defines that for FRP-RC beams the factor λ reduces to ξ because the compression reinforcement is not considered for FRP-RC members ($\rho'_f = 0$). Therefore, long-term deflections for FRP-RC beams are computed by:

$$\Delta_{(cp\,+\,sh)} = \xi\,(\Delta_i)_{sus} \tag{3.24}$$

Brown (1997) observed that the long-term deflection of FRP-RC beams with no compression reinforcement with a sustained load over a period of 6 months was 60 to 90% of the initial deflection. The measured additional long-term deflection was only 50 to 75% of the deflection suggested by Eqs. (3.22) and (3.23). Other studies performed by Vijay *et al*. (1998) and Arockiasamy *et al*. (1998) found similar results for both GFRP and CFRP beams (ACI 440, 2006).

Based on these results, ACI 440 (2006) recommends a modification factor of 0.6 in Eq. (3.24). Therefore, for typical applications, the calculation of the long-term deflection of FRP-RC beams can be determined from Eq. (3.25):

$$\Delta_{(cp\,+\,sh)} = 0.6\,\xi\,(\Delta_i)_{sus} \tag{3.25}$$

3.3 SUMMARY OF THE CHAPTER

Recommendations of ACI 440 (2006) for flexural design and serviceability criteria related to deflections of FRP-RC members were described in this chapter. The design approach in ACI 440 for FRP-RC members are similar to the design recommendations for steel-reinforced

concrete members and are based on limit state design principles. In this method, the resistance capacity of the member is reduced and loading is increased. The changing of the ductile failure (steel-reinforced beams) to brittle failure mode (FRP-reinforced beams) is an important issue which must be dealt with in more detail in existing design recommendations for FRP-RC members. Similarly, differences in the mechanical properties between steel and FRP grant a thorough investigation on the performance levels resulting from serviceability provisions for FRP-RC beams.

4

DEFLECTIONS OF FRP-RC BEAMS

This chapter begins with general considerations on deflections of FRP-RC beams. The approach used in the calculation of the total deflection (sum of immediate and long-term deflection) is presented. Particular attention is given to the equations for the calculation of the effective moment of inertia of FRP-RC beams.

4.1 GENERAL CONSIDERATIONS

Deflections of FRP-RC beams tend to be greater in magnitude compared to deflections in traditional steel-reinforced beams because of the lower stiffness associated with commercially available FRP reinforcement (ACI 440, 2006). Because of the variable stiffness, brittle-elastic nature, and particular bond features of FRP reinforcement, deflections of FRP-RC members are more sensitive to the variables affecting deflection than steel-reinforced members of identical size and reinforcement layout (ACI 440, 2006).

As seen in Section 3.2.4, ACI 440 (2006) recommendations establish that control of deflections are made by the direct method, detailed in Section 3.2.4.1.

The total deflection is given by the sum of the long-term deflection due to all sustained loads and the immediate deflection due to any additional live loads. The calculation procedure for the long-term deflection for FRP-RC beams was described in Section 3.2.4.1.2. Although ACI 440 (2006) recommends the equation proposed by Gao *et al.* (1998) [Eq. (3.20)] for the calculation of the effective moment of inertia to be used in the estimation of the immediate deflection of FRP-RC beams, that document also reminds that other equations for the same purpose have been proposed. Most of the proposed equations involve changes in the original Branson's equation; some of these equations are presented in chronological order in the following section.

4.2 EQUATIONS FOR THE EFFECTIVE MOMENT OF INERTIA

4.2.1 Benmokrane *et al.* (1996)

To calibrate the original Branson's equation for FRP-RC beams [Eq. (3.19)], Benmokrane *et al.* (1996) proposed α and β coefficients derived from experimental programs. According to that study, the effective moment of inertia I_e can be computed by Eq. (4.1):

$$I_e = \left\{ \left(\frac{M_{cr}}{M_a} \right)^3 \frac{I_g}{\beta} + \alpha \left[1 - \left(\frac{M_{cr}}{M_a} \right)^3 \right] I_{cr} \right\} \leq I_g \tag{4.1}$$

In this equation, α and β coefficients are taken as 0.84 and 7, respectively.

4.2.2 Brown and Bartholomew (1996)

Brown and Bartholomew (1996) have suggested a variation of Branson's equation that consists of changing the exponent value in Eq. (3.19) to five, thus resulting in the following equation for the calculation of the effective moment of inertia I_e:

$$I_e = \left\{ \left(\frac{M_{cr}}{M_a} \right)^5 I_g + \left[1 - \left(\frac{M_{cr}}{M_a} \right)^5 \right] I_{cr} \right\} \leq I_g \tag{4.2}$$

4.2.3 Toutanji and Saafi (2000)

Toutanji and Saafi (2000) proposed a different variation of the Branson's equation related to the order of the exponent in the original equation. While Brown and Bartholomew (1996) suggested that the value of the exponent of I_e is equal to 5 [Eq. (4.2)], Toutanji and Saafi defines that this exponent depends on both the FRP modulus of elasticity (E_f) and FRP reinforcement ratio (ρ_f). In this way, the equation to calculated I_e is defined by:

$$I_e = \left\{ \left(\frac{M_{cr}}{M_a} \right)^m I_g + \left[1 - \left(\frac{M_{cr}}{M_a} \right)^m \right] I_{cr} \right\} \leq I_g \tag{4.3}$$

with exponent *m* varying as follows:

- if $\dfrac{E_f}{E_s}\rho_f > 0.3$, $m = 6-10\dfrac{E_f}{E_s}\rho_f$;

- if $\dfrac{E_f}{E_s}\rho_f < 0.3$, $m = 3$.

where:

E_f = design modulus of elasticity of FRP;

E_s = modulus of elasticity of steel;

ρ_f = FRP reinforcement ratio.

4.2.4 Rizkalla and Mufti (2001)

Rizkalla and Mufti (2001) have suggested an equation for I_e derived from the effective moment of inertia equation proposed by CEB-FIP MC-90 (CEB-FIP 1990). This equation is given by:

$$I_e = \frac{I_T\,I_{cr}}{I_{cr} + \left[1 - 0.5\left(\dfrac{M_{cr}}{M_a}\right)^2\right]\left(I_T - I_{cr}\right)} \le I_g \tag{4.4}$$

where I_T is the moment of inertia of uncracked section transformed to concrete.

4.2.5 Yost *et al.* (2003)

As already mentioned, Eq. (3.20) proposed by Gao *et al.* (1998) was adopted by ACI 440 (2003) (see Section 3.2.4.1.1). The reduction coefficient β_d introduced in that equation is given by:

$$\beta_d = \alpha\left(\frac{E_f}{E_s} + 1.0\right) \tag{4.5}$$

where E_f is the modulus of elasticity of FRP, E_s is the modulus of elasticity of steel, and α is a bond dependent coefficient.

The coefficient α was proposed by Yost *et al.* (2003) as follows:

$$\alpha = 0.064\left(\frac{\rho_f}{\rho_{fb}}\right) + 0.13 \tag{4.6}$$

where ρ_f is FRP reinforcement ratio and ρ_{fb} is FRP reinforcement balanced ratio.

4.2.6 Bischoff and Scanlon (2007)

Limitations of Branson's equation for FRP-RC members led Bischoff and Scanlon (2007) to develop an alternative equation for I_e defined by:

$$I_e = \frac{I_{cr}}{1 - \eta_s\left(\dfrac{M_{cr}}{M_a}\right)^2} \leq I_g \tag{4.7}$$

where η_s is the stiffness reduction coefficient equal to $1 - \left(\dfrac{I_{cr}}{I_g}\right)$.

4.2.7 Bischoff and Gross (2011)

Bischoff and Gross (2011a, 2011b) developed an equation from the integration of curvature using Eq. (4.7), resulting in the following expression for the equivalent moment of inertia, I'_e:

$$I'_e = \frac{I_{cr}}{1 - \gamma\,\eta\left(\dfrac{M_{cr}}{M_a}\right)^2} \leq I_g \tag{4.8}$$

Equation (4.8) takes into account the integration of curvature of the beam by inclusion of a correction factor γ related to variations in stiffness along the member length. The factor γ depends on the boundary conditions and type of loading on the beam, as shown in Figure 4.1.
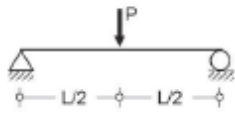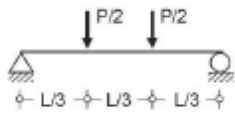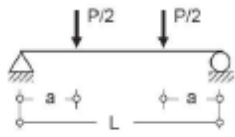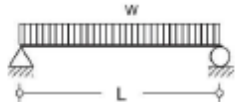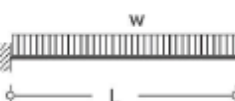
Beam and loading type	Moment and elastic deflection equations	I'_e based on integration of curvature using Eq. (1) $$I'_e = I_{cr}\,/[1 - \gamma\eta(M_{cr}/M_a)^2]$$ with $\eta = 1 - I_{cr}/I_g$
	$M_a = PL/4$ $\Delta = PL^3/48E_cI'_e$	$\gamma = 3 - 2(M_{cr}/M_a)$
	$M_a = PL/6$ $\Delta = 23PL^3/1296E_cI'_e$	$\gamma = 1.7 - 0.7(M_{cr}/M_a)$
	$M_a = Pa/2$ $\Delta = \alpha PL^3/48E_cI'_e$ $\alpha = 3(a/L) - 4(a/L)^3$	$\gamma = \dfrac{3(a/L) - 4\xi(a/L)^3}{3(a/L) - 4(a/L)^3}$ $\xi = 4(M_{cr}/M_a) - 3$
	$M_a = wL^2/8$ $\Delta = 5wL^4/384E_cI'_e$	$\gamma = \dfrac{1.6\xi^3 - 0.6\xi^4}{(M_{cr}/M_a)^2} + 2.4\ln(2 - \xi)$ $\approx 1.72 - 0.72(M_{cr}/M_a)$ $\xi = 1 - \sqrt{1 - M_{cr}/M_a}$
	$M_a = PL$ $\Delta = PL^3/3E_cI'_e$	$\gamma = 3 - 2(M_{cr}/M_a)$
	$M_a = wL^2/2$ $\Delta = wL^4/8E_cI'_e$	$\gamma = 1 - 2\ln(M_{cr}/M_a)$

Figure 4.1 - Equivalent moment of inertia values for calculating deflection (Bischoff and Gross, 2011b).

4.3 SUMMARY OF THE CHAPTER

Deflections of FRP-RC beams are expected to be greater than those of steel-reinforced beams because of the lower stiffness of FRP bars. Both immediate and long-term deflections under service loads shall be considered in the design process and the total deflection (given by the sum of immediate and long-term deflection) of FRP-RC beams shall be computed. Long-term deflections of FRP-RC beams have been discussed in Section 3.2.4.1.2.

In this chapter, the main issue involving the calculation of the immediate deflection of FRP-RC beams, i.e. the determination of the effective moment of inertia equation, has been

discussed. Studies available in the literature report that traditional Branson's equation used to compute the effective moment of inertia of steel-reinforced beams is not recommended for FRP-RC beams. As a consequence, several equations have been proposed for the computation of the effective moment of inertia of FRP-RC beams and were presented in this chapter. The further scrutiny in the selection of the equation for the effective moment of inertia to be used in the probabilistic serviceability assessment of FRP-RC beams is discussed in Chapter 6.

5

RELIABILITY BASICS

5.1 INTRODUCTION

In the development of engineering projects, engineers often make decisions based on available information, using analytical methods and evaluation that include improved modeling and mathematical analysis, such as numerical simulation and optimization techniques. However, regardless of the level of sophistication of such models (including models of laboratory), they are predictions, assumptions or idealized conditions; hence, information obtained from these models may or may not reflect the reality. However smaller, there is always a probability of a structure to underperform. This probability relies upon the information obtained, which are deduced from models in similar or different situations. Therefore, estimating an accurate probability of underperformance is difficult due to inherent variability of these informations.

A number of uncertainties are present in the structural design problem. These may be related to inherent variability such as material properties (steel yield strength, steel ultimate strength, concrete compressive strength, concrete modulus of elasticity, etc.), dimensions (beam width and depth, concrete cover, etc.), loads (dead loads, live loads, wind, earthquake, etc.) or epistemic uncertainties, i.e., those related to the lack (or limited) knowledge. In this latter category are the errors associated to predictive models, sampling errors, and measurement errors. These errors may be reduced as more information is gained (Diniz, 2008).

These uncertainties may be modeled from mathematical basis set by probability principles, statistics and decision theory, and then the effects on the engineering design may be assessed.

5.2 METHODS OF RELIABILITY ANALYSIS

5.2.1 Basic problem

The basic problem of structural reliability may be cast as a problem of *supply* versus *demand*. In Structural Engineering, the basic problem is to ascertain that the strength, *X*, will be larger than the load (or load effects), *Y*, throughout the life of the structure, i.e., ($X > Y$). This assurance is possible only in terms of the probability $P(X > Y)$. This probability, therefore, represents a realistic measure of the reliability of the structural component (Ang and Tang, 1990).

Assuming that the probability distributions of *X* and *Y* are known, that is, $F_X(x)$ or $f_X(x)$ and $F_Y(y)$ or $f_Y(y)$, and random variables *X* (strength) and *Y* (load effects) are continuous and statistically independent, the probability of failure P_F is given by:

$$P_F = \int_0^\infty F_X(y)\, f_Y(y)\, dy \tag{5.1}$$

Equation (5.1) is the convolution with respect to *y* and may be explained from Figure 5.1 as follows. If $Y = y$, the conditional probability of failure would be $F_X(y)$; however, in terms of continuous variables, the probability that $y < Y \leq y + dy$ is associated with probability $f_Y(y)$ dy, and integration over all values of *Y* yields Eq. (5.1). Alternatively, the reliability may be formulated also by the convolution with respect to *x* (Ang and Tang, 1990).
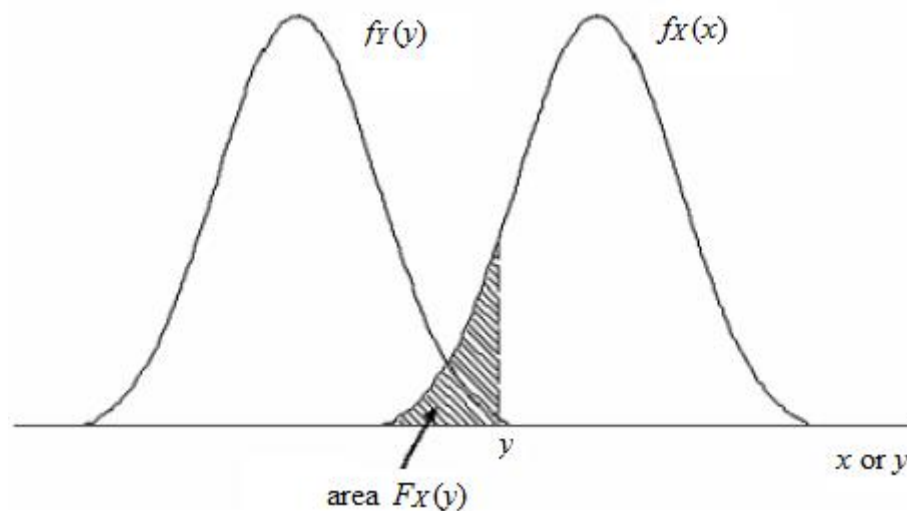
Figure 5.1 - Probability density functions $f_X(x)$ and $f_Y(y)$.

According to Ang and Tang (1990), the corresponding probability of nonfailure P_s is:

$$P_S = 1 - P_F \qquad (5.2)$$

As seen in Figure 5.1, the overlapping of the curves $f_X(x)$ and $f_Y(y)$ represents a qualitative measure of the probability of failure P_F. In general, the probability of failure may be expressed in terms of joint probability density function of X and Y, $f_{X,Y}(x, y)$ as follows (Ang and Tang, 1990):

$$P_F = \int_0^\infty \left[\int_0^y f_{X,Y}(x, y)\, dx \right] dy \qquad (5.3)$$

and the corresponding probability of nonfailure P_s is given by:

$$P_S = \int_0^\infty \left[\int_0^x f_{X,Y}(x, y)\, dy \right] dx \qquad (5.4)$$

Knowledge of the probability density functions $f_X(x)$ and $f_Y(y)$ for statistically independent random variables, - or the joint probability density function $f_{X,Y}(x, y)$-, is required in the computation of the probability of failure via Eqs. (5.1) and (5.3), respectively. However, as discussed in most textbooks on Structural Reliability (e.g. Ang and Tang, 1990) the use of these equations to compute the probability of failure is limited. In the following sections some basic concepts in Structural Reliability theory are reviewed and Monte Carlo simulation (Ang and Tang, 1990) is briefly presented.

5.2.2 Margin of safety

The *supply-demand* problem may be formulated in terms of the margin of safety, $M = X - Y$. Since X and Y are random variables, M is also a random variable with corresponding probability density function $f_M(m)$. Failure corresponds to the condition ($M < 0$) and the corresponding probability of failure could be computed by the following equation if the probability distribution associated to M is known (Ang and Tang, 1990):

$$P_F = \int_{-\infty}^{0} f_M(m)\,dm = F_M(0) \tag{5.5}$$

Graphically, this is represented by the area below 0 under the curve $f_M(m)$, as show in Figure 5.2.
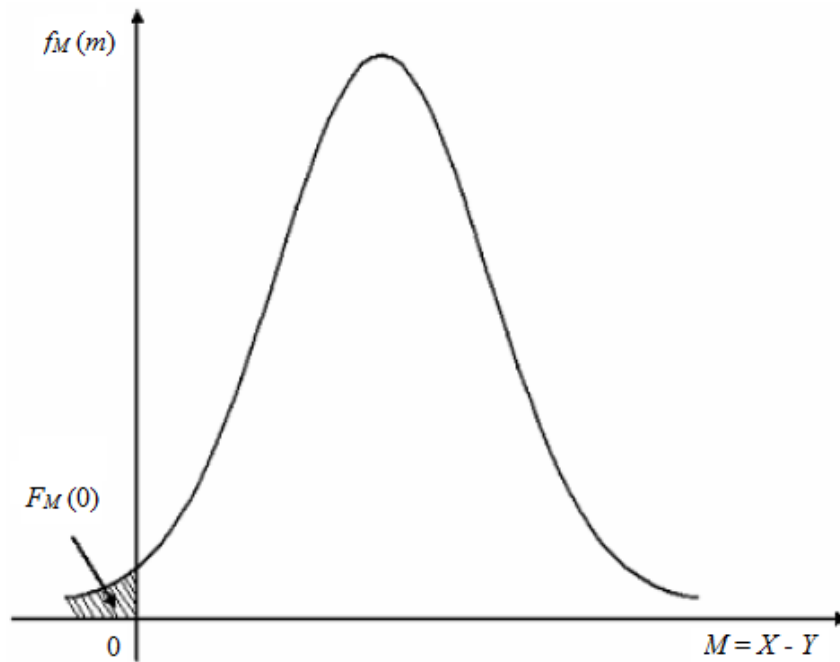
Figure 5.2 - Probability density function of safety margin *M*.

For a structure whose strength, R, and load, Q, are statistically independent random variables following Normal distributions, i.e., $N(\mu_R, \sigma_R)$ and $N(\mu_Q, \sigma_Q)$, respectively, the margin of safety M is also a normal random variable $N(\mu_M, \sigma_M)$. The notation $N(\mu, \sigma)$ represents a normal variable with mean μ and standard deviation σ. The mean and standard deviation of the margin of safety is given by (Ang and Tang, 1990):

$$\mu_M = \mu_R - \mu_Q \tag{5.6}$$

$$\sigma_M = \sqrt{\sigma_R^2 + \sigma_Q^2} \tag{5.7}$$

The probability of failure P_F can be computed by the following equation:

$$P_F = F_M(0) = \Phi\left(\frac{-\mu_M}{\sigma_M}\right) = 1 - \Phi\left(\frac{\mu_M}{\sigma_M}\right) \tag{5.8}$$

where Φ is the standard normal cumulative distribution function, $N(0, 1)$, and the probability of nonfailure P_S is:

$$P_S = 1 - P_F = \Phi\left(\frac{\mu_M}{\sigma_M}\right) \qquad (5.9)$$

It may be observed that reliability is a function of the ratio μ_M / σ_M, which is the safety margin expressed in units of σ_M and is known as "reliability index" and denoted by β, as follows:

$$\beta = \frac{\mu_M}{\sigma_M} = \frac{\mu_R - \mu_Q}{\sqrt{\sigma_R^2 + \sigma_Q^2}} \qquad (5.10)$$

In this case, linear performance function (see Section 5.3) and normal variables, the reliability index can be computed based solely on the information on the means and the standard deviations of the basic variables pertaining to the problem.

The probability of nonfailure, therefore, can be calculated in terms of the reliability index as follows:

$$P_s = \Phi(\beta) \qquad (5.11)$$

and the corresponding probability of failure:

$$P_F = 1 - \Phi(\beta) = \Phi(-\beta) \qquad (5.12)$$

5.3 PERFORMANCE FUNCTION

The reliability of an engineering system may involve multiple variables. In particular, the supply and demand may be a function of many variables. For such cases, the supply-demand problem described in Section 5.2.1 must be generalized. This generalization is often necessary in engineering, particularly when the problem must be formulated in terms of the basic design variables (Ang and Tang, 1990).

 In a broader sense, the reliability of an engineering system (or component) may be defined as the probability of performing its intended function or mission. The level of performance of a

system will obviously depend on the properties of the system. In this context, the performance function can be generalized as follows (Ang and Tang, 1990):

$$g(\mathbf{X}) = g(X_1, X_2, \ldots, X_n) \tag{5.13}$$

where $\mathbf{X} = (X_1, X_2, \ldots, X_n)$ is a vector of basic state (or design) variables of the system, and the function $g(\mathbf{X})$ determines the performance or state of the system. Accordingly, the limiting performance requirement may be defined as $g(\mathbf{X}) = 0$, which is the "limit-state" of the system. It follows, therefore, that when $g(\mathbf{X}) > 0$ the "safe state" is reached; and when $g(\mathbf{X}) < 0$ the "failure state" occurs (Ang and Tang, 1990).

5.4 MONTE CARLO SIMULATION

In engineering, simulation allows the study the effectiveness of a project. From a set of values prescribed for the parameters (or variables of the problem), the simulation process produces a specific measure for the performance of the structure (e.g. probability of excessive deflections). Through repeated simulations, the sensitivity of the system performance to variation in the system parameters may be examined or assessed. This simulation procedure can be used to appraise alternative designs (Ang and Tang 1990).

Monte Carlo simulation involves repeating a simulation process, using in each simulation a particular set of values of the random variables generated in accordance with the corresponding probability distributions. By repeating the process, a sample of realizations, each corresponding to a different set of values of the random variables is obtained. A sample from Monte Carlo simulation is similar to a sample of experimental observations (Ang and Tang, 1990).

Results obtained via Monte Carlo simulation usually are not exact (unless the sample size is infinitely large). Monte Carlo simulation is a sampling procedure; as such, it is subjected to sampling errors. Therefore, the use of samples with a large number of elements is required for more accurate and reliable results. A discussion on sampling errors is presented in Section 5.5.

Two items are required for a Monte Carlo simulation: (i) a deterministic relation to describe the response of the structure, and (ii) the probability distributions of all variables involved in calculation of the response (Diniz, 2008).

Monte Carlo simulation in the evaluation of structural performance may be used to compute:

- the statistics (mean, standard deviation, and type of distribution) of the system response. In this case, first a sample of the structure's response is obtained, then a probability distribution is fitted to the sample data and the distribution parameters are estimated;

- the probability of unsatisfactory performance of the structure. In this case, a performance function is established and a sample of the possible outcomes is simulated. The number of unsatisfactory performances is counted, and the probability of failure is obtained by the rate of unsatisfactory performances, that is, ratio of the number of unsatisfactory performances to the number of simulations.

A key task in the Monte Carlo simulation is the generation of appropriate values of the random variables (i.e., random numbers). Random numbers are generated according to the prescribed probability distribution for each basic variable pertaining to the problem at hand and the corresponding parameters. Currently, generation of random numbers according to several probability distributions can be easily achieved by using built-in functions in commercial softwares, e.g. Matlab version 7.0.1.

5.5 SAMPLING ERROR

Monte Carlo simulation is often used in the estimation of the probability of failure of a structural component (or system). Knowledge of the error related to this estimation, or the required number of simulations (or sample size) in order to achieve a prescribed accuracy, are of interest. Shooman (1968) developed the following equation for the percentage error:

$$\% \, error = 200 \sqrt{\frac{1 - P_F}{n \, P_F}} \qquad (5.14)$$

where P_F is the estimated probability of failure and n is the sample size.

There is a 95 % chance that the percent error in the estimated probability will be less than that given by Eq. (5.14) (Ang and Tang, 1990). For example, assuming that in 100,000 simulations a probability of failure equal to 0.0065 is obtained, for this probability of failure Eq. (5.14) provides a 7.8 %, i.e., the probability of failure is in the range 0.0065 ± 0.000507.

5.6 SUMMARY OF THE CHAPTER

In this chapter, a brief review of reliability concepts was presented. This literature review was intended to enable the understanding of basic concepts in Structural Reliability theory and attendant tools, as required in the probabilistic assessment of deflections of FRP-RC beams. A detailed discussion on this subject is beyond the scope of this dissertation and can be found in a number of textbooks (e.g. Ang and Tang, 1990; Melchers, 1999; Nowak and Collins, 2000).

The research work presented herein is aimed at the probabilistic description of total deflections of FRP-RC beams and the assessment of performance levels resulting from current design recommendations. To this end, the concepts and tools presented in this Chapter will be used in the implementation of a Monte Carlo simulation computational procedure aimed at the reliability analysis of the FRP-RC beams with respect to the limit state of excessive deflections. This latter topic is dealt with in the following chapter.

6

RELIABILITY ANALYSIS OF SERVICEABILITY OF FRP-RC BEAMS

In this chapter, the reliability of eighty-one FRP-RC beams with respect to serviceability limit states (excessive deflections) is assessed. Monte Carlo simulation is used for the probabilistic description of the beam deflection, and in the computation of the probability of failure (and corresponding reliability indexes) of beams designed according to ACI 440 (2006) provisions. The number of simulations is taken as 100,000.

As shown in Chapter 5, Monte Carlo simulation requires information on the probability distributions of all random variables involved in the problem and a deterministic relationship between these variables. In this work, the following variables are assumed as random: dead and live loads, cross section geometry, compressive strength of concrete, tensile strength and modulus of elasticity of FRP, and model error. The variables assumed as deterministic are: span of the beam ($\ell = 3000$ mm), FRP reinforcement area (taken as the nominal area of FRP), and allowable deflection.

This chapter begins with a description of the eighty-one FRP-RC beams assessed in this work. In the sequence, the deterministic relationship for the performance evaluation of the beams is presented; in particular, the selection of the equation to calculate the effective moment of inertia of FRP-RC beams is discussed. The probabilistic description of the basic variables involved in this study is presented in Section 6.3; special attention is given to the definition of the statistics of the service loads. Finally, the reliability results associated to the limit state of excessive deflections, i.e. probabilities of underperformance, obtained via Monte Carlo simulation, are presented and discussed.

6.1 DESIGNED BEAMS

Eighty-one FRP-RC beams, designed according to ACI 440 (2006) recommendations for flexure, were selected for analysis. All beams are simply-supported, with 3-m span, 20 x 30 cm^2 rectangular cross-sections, and subjected to uniformly distributed load. Due to lower cost of the three types of fibers most used in construction (carbon - CFRP, aramid – AFRP, and glass - GFRP) the beams analyzed in this study are reinforced with GFRP.

Three specified concrete compressive strengths - 30, 50, and 70 MPa -, and three FRP tensile strengths - 485 MPa, 850 MPa, and 1275 MPa -, were chosen. The selected FRP tensile strengths are consistent with values suggested in ACI 440 (2006) for GFRP.

FRP reinforcement ratios in the range 0.82-2.10 ρ_{fb} have been used, thus representing under-reinforced, in the transition region, and over-reinforced beams (ρ_f and ρ_{fb} limits were defined by Eqs. (3.2) and (3.3), respectively). The selected FRP bars have diameters ranging from 6.3 to 22.5 mm. Three mean dead load to mean live load ratios ($\mu_{DL} / \mu_{LL} = 0.5, 1.0$, and 2.0) have been selected.

To facilitate analysis of data and results, each beam is identified by four groups of numbers and/ or letters. The first group, - C30, C50, and C70 -, stands for the specified concrete compressive strength in MPa. The second group is related to the tensile strength of FRP bars (P1: 485 MPa, P2: 850 MPa, and P3: 1275 MPa). The third group is related to the load ratio (R5, R1 and R2 correspond to $\mu_{DL} / \mu_{LL} = 0.5, 1.0$, and 2.0, respectively). The fourth group is related to the FRP longitudinal ratio (UR: under-reinforced beams; OR: over-reinforced beams; and TR: transition region). For example, beam C70-P1-R5-OR has a specified concrete cylinder strength of 70 MPa, FRP tensile strength of 485 MPa, load ratio equal to 0.5, and is over-reinforced.

Table 6.1 presents the details of the designed beams (R* indicates that groups R5, R1, and R2 have the same geometrical and mechanical properties). The 54 beams corresponding to P2 and P3 are the same as those investigated by Ribeiro and Diniz (2013).

Table 6.1 - Details of the designed beams.

Beam identification	Cross section (cm²)	f'_c (MPa)	f^*_{fu} (MPa)	A_f (cm²)	Ratio ρ_f / ρ_{fb}
C30-P1-R*-UR	20 x 30	30	485	3 φ 12.5	0.63
C30-P1-R*-TR	20 x 30	30	485	3 φ 16	1.05
C30-P1-R*-OR	20 x 30	30	485	3 φ 22.5	2.10
C30-P2-R*-UR	20 x 30	30	850	3 φ 9.5	0.86
C30-P2-R*-TR	20 x 30	30	850	4 φ 9.5	1.15
C30-P2-R*-OR	20 x 30	30	850	3 φ 12.5	1.50
C30-P3-R*-UR	20 x 30	30	1275	4 φ 6.3	0.93
C30-P3-R*-TR	20 x 30	30	1275	5 φ 6.3	1.16
C30-P3-R*-OR	20 x 30	30	1275	3 φ 9.5	1.59
C50-P1-R*-UR	20 x 30	50	485	4 φ 12.5	0.61
C50-P1-R*-TR	20 x 30	50	485	3 φ 19	1.08
C50-P1-R*-OR	20 x 30	50	485	4 φ 22.5	2.03
C50-P2-R*-UR	20 x 30	50	850	4 φ 9.5	0.83
C50-P2-R*-TR	20 x 30	50	850	3 φ 12.5	1.09
C50-P2-R*-OR	20 x 30	50	850	4 φ 12.5	1.45
C50-P3-R*-UR	20 x 30	50	1275	5 φ 6.3	0.84
C50-P3-R*-TR	20 x 30	50	1275	3 φ 9.5	1.15
C50-P3-R*-OR	20 x 30	50	1275	4 φ 9.5	1.54
C70-P1-R*-UR	20 x 30	70	485	4 φ 16	0.77
C70-P1-R*-TR	20 x 30	70	485	4 φ 19	1.09
C70-P1-R*-OR	20 x 30	70	485	4 φ 25	1.90
C70-P2-R*-UR	20 x 30	70	850	3 φ 12.5	0.82
C70-P2-R*-TR	20 x 30	70	850	4 φ 12.5	1.10
C70-P2-R*-OR	20 x 30	70	850	6 φ 12.5	1.64
C70-P3-R*-UR	20 x 30	70	1275	3 φ 9.5	0.87
C70-P3-R*-TR	20 x 30	70	1275	4 φ 9.5	1.16
C70-P3-R*-OR	20 x 30	70	1275	3 φ 12.5	1.52

6.2 DETERMINISTIC RELATIONSHIP FOR PERFORMANCE VERIFICATION OF GFRP-RC BEAMS

In the serviceability checking of the eighty-one GFRP-RC beams dealt with in this work, a performance function must be specified, which is given by:

$$g(\Delta) = \delta_a - \Delta_{total} \tag{6.1}$$

where δ_a is the allowable deflection and Δ_{total} is the total deflection.

6.2.1 Allowable deflection

To meet the serviceability criteria related to deflections, estimated values of deflection must be within acceptable limits established for the intended use of the structure. ACI 440 (2006) requires that the control of deflections be made from verification if the estimated deflection is less than an allowable deflection, usually equal to a percentage of the beam span (ℓ). Values of permissible deflections for FRP-RC beams are the same for steel-reinforced beams (*fib*, 2007). Table 6.2 shows the maximum permissible values of deflections set by ACI 318 (2014).

Table 6.2 - Maximum permissible calculated deflections (ACI 318, 2014).

Member	Condition		Deflection to be considered	Deflection limitation
Flat roofs	Not supporting or attached to nonstructural elements likely to be damaged by large deflections		Immediate deflection due to maximum of L_r, S and R	$\ell/180$[1]
Floors			Immediate deflection due to L	$\ell/360$
Roof or floors	Supporting or attached to nonstructural elements	Likely to be damaged by large deflections	The part of the total deflection occurring after attachment of nonstructural elements, which is the sum of the time-dependent deflection due to all sustained loads and the immediate deflection due to any additional live load [2]	$\ell/480$[3]
		Not likely to be damaged by large deflections		$\ell/240$[4]

[1] Limit not intended to safeguard against ponding. Ponding shall checked by calculations of deflection, including added deflections due to ponded water, and considering time-dependent effects of sustained loads, camber, construction tolerances, and reliability of provisions for drainage.

[2] Time-dependent deflection shall be calculated in accordance with 24.2.4 in ACI 318 (2014), but shall be permitted to be reduced by amount of deflection calculated to occur before attachment of nonstructural elements. This amount shall be calculated on basis of accepted engineering data relating to time-deflection characteristics of members similar to those being considered.

[3] Limit shall be permitted to be exceed if measures are taken to prevent damage to supported or attached elements.

[4] Limit shall not exceed tolerance provided for nonstructural elements.

The allowable deflection, δ_a, adopted in this study is a deterministic variable taken equal to $\ell/240$.

6.2.2 Total deflection

Total deflection is calculated by the sum of the immediate deflection, Δ_i, and the long-term deflection due to creep and shrinkage, $\Delta_{(cp + sh)}$. It is a random variable that is function of a set of other random variables, as presented in the following sections.

6.2.2.1 Immediate deflection of FRP-RC beams

Immediate deflection, Δ_i, of FRP-RC beams is calculated by an elastic equation that takes into account the load type of the structure, the modulus of elasticity of concrete (E_c), and the effective moment of inertia (I_e). For simply-supported beams subjected to uniformly distributed load, the deterministic equation to compute the immediate deflection is given by:

$$\Delta_i = \frac{5\, p_{serv}\, \ell^4}{384\, E_c\, I_e} \tag{6.2}$$

where:

p_{serv} = service load;
ℓ = span length of the beam;
E_c = modulus of elasticity of concrete, defined by Eq. (2.1).

In addition to uncertainties inherent in the variables relevant to the problem at hand, the reliability analysis must include the uncertainty in the model predictions, calculation of the effective moment of inertia (I_e). Therefore, a main problem related to Eq. (6.2) is the selection of the equation for the calculation of the effective moment of inertia (I_e) and the incorporation of the attendant uncertainty in the immediate deflection prediction into the analysis. As presented in Section 4.2, several equations have been proposed for calculation of the effective moment of inertia of FRP-RC beams.

Studies performed by Mota *et al.* (2006) obtained the statistics of the random variable "model error", i.e., the ratio "experimental deflection/ calculated deflection", $\eta = \Delta_{exp}/ \Delta_{calc}$, corresponding to immediate deflections for some of the available equations for computation of I_e. Table 6.3 lists the mean (μ), and the coefficient of variation (COV) of the model error in the prediction of deflections at the service load level for GFRP-RC beams according to those authors.

Table 6.3 - Statistics of the model error (mean and COV) associated to predicted immediate deflections at service of GFRP-RC beams according to different proposals (Mota *et al.*, 2006).

Author	Equation	μ	COV
Gao *et al.*	3.20	1.24	0.0740
Benmokrane *et al.*	4.1	0.49	0.0677
Brown and Bartholomew	4.2	1.45	0.0809
Toutanji and Saafi	4.3	1.28	0.0817
Rizkalla and Mufti	4.4	0.60	0.0638
Yost *et al.*	4.6	0.95	0.0698

These results indicate the ranges 0.49-1.45 and 0.0638-0.0817 for the mean values (μ) and coefficients of variation (COV) of the model error, respectively. In the evaluation of these equations, a mean value close to 1.0 and a small coefficient of variation correspond to desirable features. Considering that the equation suggested by Yost *et al.* (2003) [Eq. (4.5) and (4.6)] has a mean $\mu = 0.95$ and COV = 0.0698, this equation has been selected for the calculation of the effective moment of inertia (I_e) for GFRP-RC beams assessed in this study.

From the previous considerations, the model error, η, is used as a multiplier of the immediate deflection given by Eq. (6.2), thus providing the adjusted immediate deflection, $\Delta_{i,a}$:

$$\Delta_{i,a} = \frac{5\,p_{serv}\,\ell^4}{384\,E_c\,I_e}\,\eta \qquad (6.3)$$

6.2.2.2 Long-term deflection of FRP-RC beams

Long-term deflections due to creep and shrinkage, $\Delta_{(cp + sh)}$, of FRP-RC beams can be computed according to Eq. (3.25). In this equation, the time-dependent factor for sustained loads, ξ, is taken as 2.0 (sustained load duration of 5 years or more), according to Table 3.2. This value is consistent with the 8-yr reference period for live loads adopted in this study for the serviceability analysis (see Section 6.3.5). Furthermore, it is assumed that 20 % of the live load is sustained loading. In this way, the long-term deflection of GFRP-RC beams is calculated by:

$$\Delta_{(cp + sh)} = 1.2\,[(\Delta_{i,a})_D + 0.2\,(\Delta_{i,a})_L] \qquad (6.4)$$

where:

$(\Delta_{i,a})_D$ = immediate deflection due to dead loads;

$(\Delta_{i,a})_L$ = immediate deflection due to live loads.

Thus, the total deflection is computed by the following equation:

$$\Delta_{total} = [0.8\ (\Delta_{i,a})_L] + \Delta_{(cp + sh)} \tag{6.5}$$

This deterministic procedure for the computation of the beam total deflection is illustrated by the flowchart presented in Figure 6.1.

Performance Function

$$g(\Delta) = \delta_a - \Delta_{total}$$

$$\delta_a = \ell/240$$

$$\Delta_{total} = \Delta_{(cp+sh)} + \left[0.8\,(\Delta_{i,a})_L\right]$$

$$\Delta_{(cp+sh)} = 1.2\left[0.8\,(\Delta_{i,a})_D + 0.2\,(\Delta_{i,a})_L\right]$$

$$(\Delta_{i,a})_D = \frac{5\,DL\,\ell^4}{384\,E_c\,I_e}$$

$$(\Delta_{i,a})_L = \frac{5\,LL_{SLS}\,\ell^4}{384\,E_c\,I_e}$$

$\mu_{LL(ULS)}$ and $\mu_{LL(SLS)}$: see Section 6.5

$$\mu_{LL(ULS)} \rightarrow \mu_{LL(SLS)} \rightarrow LL_{SLS}$$

Eq. (6.24)   Eq. (6.25b)

$$r = \frac{\mu_{DL}}{\mu_{LL(ULS)}} \rightarrow \mu_{DL} = r\,\mu_{LL(ULS)} \rightarrow DL$$

$$E_c = 4700\sqrt{F_c}$$

$$I_e = \left\{\left(\frac{M_{cr}}{M_a}\right)^3 \beta_d\,I_g + \left[1 - \left(\frac{M_{cr}}{M_a}\right)^3\right]I_{cr}\right\}$$

$$M_a = \frac{(DL + LL_{SLS})\,\ell^2}{8}$$

$$M_{cr} = \frac{f_r\,I_g}{y_t}$$

$$I_g = \frac{b\,h^3}{12}$$

$$f_r = 0.62\sqrt{F_c}$$

$$\beta_d = \alpha\left(\frac{E_f}{E_s} + 1.0\right)$$

$$\alpha = 0.064\left(\frac{\rho_f}{\rho_{fb}}\right) + 0.13$$

$$\rho_{fb} = 0.85\,\beta_1\,\frac{F_c}{F_{FU}}\left(\frac{E_f\,\varepsilon_{cu}}{E_f\,\varepsilon_{cu} + F_{FU}}\right)$$

$$\rho_f = \frac{A_f}{b\,d} \qquad d = h - d_c$$

$$I_{cr} = \frac{b\,d^3}{3}\,k^3 + n_f\,A_f\,d^2(1 - k)^2$$

$$k = \sqrt{2\,\rho_f\,n_f + (\rho_f\,n_f)^2} - \rho_f\,n_f$$

$$n_f = \frac{E_f}{E_c} \qquad \rho_f = \frac{A_f}{b\,d} \qquad d = h - d_c$$

Deterministic variable

Random variable

Derived random variable

Figure 6.1 - Flowchart of the deterministic procedure for computation of beam total deflection.

6.3 STATISTICS OF THE BASIC VARIABLES

6.3.1 Compressive strength, modulus of elasticity of concrete, and cracking moment

An important concept in semi-probabilistic design recommendations for steel-reinforced concrete members is the specified strength. Compressive strength of concrete in a structure is different from the strength specified in design; this difference is due to usual procedures in the design, production methods, tests, and quality control during manufacturing of concrete. Variations in material properties, proportions of components, mixing methods, transport, casting of concrete, curing methods, and test procedures are the main sources of variability in concrete strength. Variations also occur in the strength of concrete because it is in a structure, and not in specimens (Ribeiro, 2009).

Specified compressive strength of concrete, f'_c, is obtained by statistical treatment of test results of a sample and shall be calculated in accordance with following equation (ACI 318, 2014):

$$f'_c = \mu_c \, (1\text{-}1.34 \; V) \tag{6.6}$$

where:

μ_c = average compressive strength of concrete;
V = coefficient of variation, calculated by $V = s \, / \, \mu_c$, and s is the standard deviation.

For a given specified strength, the mean and the corresponding standard deviation can be computed if the coefficient of variation is known. According to Mirza and MacGregor (1979), the coefficient of variation can be taken as practically constant for concrete compressive strengths below 28 MPa, represented by 0.10, 0.15, and 0.20 for excellent, medium, and low quality control, respectively. Recent researches have shown that evolution of quality control worldwide has resulted in coefficients of variation close to 0.10 for a wide range of compressive strengths (Azevedo and Diniz, 2008; Szerszen and Nowak, 2003).

ACI 318 (2008) recommendations adopt a Normal distribution to describe the variability of the compressive strength of concrete; nevertheless, other researchers refer to Lognormal

distribution as a more adequate type of distribution in the representation of this variable (Azevedo and Diniz, 2008; Diniz and Frangopol, 1997).

In this study, the Lognormal distribution is assumed in the description of the concrete compressive strength variability. Three specified concrete compressive strengths are consideres (30 MPa, 50 MPa, and 70 MPa); the coefficient of variation is assumed as 0.10. Twenty-seven beams are analyzed for each concrete compressive strength class.

The above information refers to compressive strength of concrete evaluated from cylindrical specimens. Computation of the *in situ* concrete compressive strength (f_c) is given by (Diniz and Frangopol, 1997):

$$f_c = f'_c \, \alpha_c \qquad (6.7)$$

where:

f'_c = specified concrete compressive strength;
α_c = reduction factor of concrete compressive strength, equal to 0.85 when $f'_c \leq 55$ MPa; or α_c = 0.85 − 0.004 (f'_c - 55) ≥ 0.75, when $f'_c > 55$ MPa.

Modulus of elasticity of concrete, E_c, is taken as a random variable derived from the specified compressive strength of concrete, f'_c, and calculated by Eq. (2.1).

Cracking moment, M_{cr}, can be calculated by Eq. (3.16) and is taken as a random variable derived from the modulus of rupture of concrete, f_r, and the gross moment of inertia, I_g. In this equation, the distance from centroidal axis of gross section to tension face, y_t, is a deterministic variable.

Modulus of rupture of concrete, f_r, in its turn, is taken as a random variable derived from the specified compressive strength of concrete, f'_c, calculated by Eq. (2.2).

Gross moment of inertia, I_g, is assumed as random variable (see Section 6.3.3 for the variability of beam depth and beam width). For rectangular cross sections, I_g is given by:

$$I_g = \frac{b \, h^3}{12} \qquad (6.8)$$

6.3.2 Mechanical properties of FRP bars

According to ACI 440 (2006), variations of the strength, diameter and material properties of FRP bars can influence variation of the tensile strength of FRP. A Normal distribution is recommended by ACI 440 (2006) in the modeling of the tensile strength of FRP. Pilakoutas *et al*. (2002) also recommend a Normal distribution to represent the tensile strength of FRP bars and suggest a coefficient of variation of 0.05.

In this work, a Normal distribution is assumed to describe the variability of the tensile strength of FRP bars; three mean tensile strengths were adopted - 570.59 MPa, 1000 MPa, and 1500 MPa -, and the coefficient of variation is taken as 0.05. Thus, the nominal tensile strength of FRP can be determined by (ACI 440, 2006):

$$f^*_{fu} = f_{fu, ave} - 3\,s \tag{6.9}$$

where:

f^*_{fu} = guaranteed tensile strength of FRP bar;
$f_{fu, ave}$ = mean tensile strength of FRP bar;
s = standard deviation.

Twenty-seven beams were analyzed for each level of FRP tensile strength.

The design modulus of elasticity of FRP, E_f, is the same as the value reported by the manufacturer, i.e. it is equal to the mean elastic modulus (nominal value), $E_{f,ave}$, of a sample of test specimens (ACI 440, 2006):

$$E_f = E_{f, ave} \tag{6.10}$$

For this study, it is assumed that the modulus of elasticity of FRP is a random variable with averages of 35 GPa, 42.5 GPa, and 50 GPa for the strengths of 485 MPa, 850 MPa, and 1275 MPa, respectively. This variable follows a Normal distribution and has coefficient of variation of 0.05 (Pilakoutas *et al*., 2002). It is also assumed that the modulus of elasticity and the tensile strength of FRP are perfectly correlated variables.

6.3.3 Cross section geometry

Geometric imperfections in steel-reinforced concrete members occur during different construction stages, and cause variations in cross section dimensions. Geometric imperfections vary from country to country, region to region, and even from structure to structure, depending on quality, construction techniques, equipments and training of local staff (Mirza and Macgregor, 1979).

Following Mirza and Macgregor (1979), a Normal distribution is adopted herein for the variability of cross section dimensions. It is considered that the variability of the deviations in the nominal depth (Δ_h) and the nominal width (Δ_b) follow a Normal distribution with mean of 1.524 mm and standard deviation of 6.35 mm. Concrete cover is also a random variable and the deviation in the nominal value, Δ_c, is given by (Mirza and MacGregor, 1979):

$$\Delta_c = 6.35 + 0.004\, h \tag{6.11}$$

and standard deviation equal to 4.22 mm.

6.3.4 Model error

The random variable "model error", η, i.e. ratio experimental/ calculated deflection has been defined in Section 6.2.2.1. According to the information presented in that section, the model error associated to Yost *et al.* (2003) equation for the effective moment of inertia of GFRP-RC beams has mean $\mu = 0.95$ and COV = 0.0698 (see Table 6.3). It is assumed that the model error may be described by a Normal distribution.

6.3.5 Loading

In a reliability analysis, it is necessary to know the statistics of the loads under consideration, that is, the type of the probability distribution and the corresponding parameters. Table 6.4 presents the statistics for the dead and live load in the ultimate limit state – ULS- (Galambos *et al.*, 1982), and for the live load in the serviceability limit state – SLS- (Galambos *et al.*, 1986).

Table 6.4 - Statistics of loads.

Type	μ_v / U_n*	Coefficient of variation (COV)	Probability Distribution
Dead load	1.05	0.10	Normal
Live load (ULS)	1.00	0.25	Type I
Live load (SLS)	0.65	0.32	Type I

* Ratio of mean to unfactored nominal load.

Three mean dead load to mean live load ratios (μ_{DL} / μ_{LL}) equal to 0.5, 1.0, and 2.0 have been selected for the analysis. The statistics of the live load for the serviceability limit state is taken for an eight-year reference period, as suggested by Galambos *et al*. (1986).

6.4 STATISTICS OF THE BASIC VARIABLES: SUMMARY

The statistics of the basic variables considered in this study are summarized in Table 6.5.

Table 6.5 - Statistics of the basic variables.

Basic variable	Mean (μ)	Standard Deviation (σ)	Coefficient of variation (COV)	Probability Distribution
Dimensions *				
Δ_h, Δ_b	1.524 mm	6.35 mm	0.0417	Normal
Cover, Δ_c	6.35 + 0.004 h (mm)	4.22 mm	-	Normal
Concrete compressive strength (f'_c)				
f'_c = 30 MPa	34.64 MPa	3.46 MPa	0.10	Lognormal
f'_c = 50 MPa	57.74 MPa	5.77 MPa	0.10	Lognormal
f'_c = 70 MPa	80.83 MPa	8.08 MPa	0.10	Lognormal
GFRP tensile strength (f^*_{fu})				
f^*_{fu} = 485 MPa	570.59 MPa	28.53 MPa	0.05	Normal
f^*_{fu} = 850 MPa	1000 MPa	50 MPa	0.05	Normal
f^*_{fu} = 1275 MPa	1500 MPa	75 MPa	0.05	Normal
GFRP modulus of elasticity (E_f)				
E_f = 35 GPa	35 GPa	1750 MPa	0.05	Normal
E_f = 42.5 GPa	42.5 GPa	2125 MPa	0.05	Normal
E_f = 50 GPa	50 GPa	2500 MPa	0.05	Normal
Model error				
η	0.95	0.066	0.0698	Normal
Loads				
Type	μ_v / U_n ***		Coefficient of variation (COV)	Probability Distribution
Dead load	1.05		0.10	Normal
Live load (ULS)	1.00		0.25	Type I
Live load (SLS)	0.65		0.32	Type I

* Deviations from nominal values; ** Cylinder strength; *** Ratio of mean to unfactored nominal load.

6.5 PROCEDURE FOR CALCULATION OF MEANS OF DEAD AND LIVE LOADS

Statistics for dead and live loads to be used in the reliability of FRP-RC beams with respect to excessive deflections are presented in Table 6.5. However, the corresponding mean values for both dead load and live load at service must be defined for each of the 81 beams considered in this study. In the following, the procedure adopted in this study for the definition of the mean dead load and mean service live load is presented.

ACI 440 (2006) recommendations:

- First, design load, S_d, is assumed as identical to the FRP-RC beam design strength, R_d :

$$S_d = R_d \tag{6.12}$$

- Considering the flexural strength of a FRP-RC beam, as prescribed by ACI 440 (2006) provisions, then Eq. (6.12) becomes:

$$\phi M_n = M_d \tag{6.13}$$

where:

ϕ = strength reduction factor;

M_n = nominal moment capacity;

M_d = design moment.

In this work, it is considered that only dead load (*DL*) and live load (*LL*) are acting on the FRP-RC beams. The design moment is computed by:

$$M_d = \gamma_D M_{Dn} + \gamma_L M_{Ln} \tag{6.14}$$

where:

γ_D = amplification factor of dead load, equal to 1.2;

M_{Dn} = design moment due to dead load;

γ_L = amplification factor of live load, equal to 1.6;

M_{Ln} = design moment due to live load.

Substituting Eq. (6.14) into Eq. (6.13), ϕM_n can be obtained by:

$$\phi M_n = \gamma_D\, M_{Dn} + \gamma_L\, M_{Ln} \tag{6.15}$$

For simply-supported beams subjected to uniformly distributed dead and live loads (*DL* and *LL*, respectively), M_{Dn} and M_{Ln} are given by:

$$M_{Dn} = \frac{DL\,\ell^2}{8} \tag{6.16}$$

$$M_{Ln} = \frac{LL\,\ell^2}{8} \tag{6.17}$$

Substituting Eqs. (6.16) and (6.17) into (6.15), results:

$$\phi M_n = \gamma_D\, \frac{DL\,\ell^2}{8} + \gamma_L\, \frac{LL\,\ell^2}{8} \tag{6.18}$$

According to the load statistics in Table 6.4 (ratio of mean to unfactored nominal load, μ_v / U_n), it is obtained:

$$DL = \frac{\mu_{DL}}{1.05} \tag{6.19}$$

$$LL = \frac{\mu_{LL(ULS)}}{1.00} \tag{6.20}$$

where μ_{DL} and $\mu_{LL(ULS)}$ are the means of dead and live loads in the ultimate limit state analysis, respectively.

Substituting Eq. (6.19) and (6.20) into (6.18):

$$\phi M_n = \frac{\ell^2}{8} \left(\gamma_D \frac{\mu_{DL}}{1.05} + \gamma_L \, \mu_{LL(ULS)} \right) \tag{6.21}$$

In terms of the mean dead load to mean live load ratios, $r = \mu_{DL} / \mu_{LL}$, Eq. (6.21) can be rewritten as:

$$\phi M_n = \frac{\ell^2}{8} \mu_{LL(ULS)} \left(\gamma_D \frac{r}{1.05} + \gamma_L \right) \tag{6.22}$$

Thus resulting for the mean live load at the ultimate limit state:

$$\mu_{LL(ULS)} = \frac{8}{\ell^2} \frac{\phi M_n}{\left(\gamma_D \dfrac{r}{1.05} + \gamma_L \right)} \tag{6.23}$$

According to Eq. (6.13), Eq. (6.23) can be rewritten as:

$$\mu_{LL(ULS)} = \frac{8}{\ell^2} \frac{M_d}{\left(\gamma_D \dfrac{r}{1.05} + \gamma_L \right)} \tag{6.24}$$

The mean live load at serviceability, $\mu_{LL(SLS)}$, is computed from the data in Table 6.4:

$$\frac{\mu_{LL(SLS)}}{\mu_{LL(ULS)}} = 0.65 \tag{6.25a}$$

or

$$\mu_{LL(SLS)} = 0.65 \ \mu_{LL(ULS)} \qquad\qquad (6.25b)$$

This deterministic procedure to eighty-one beams analyzed led to results presented in Table 6.6. In this table, design moment, M_d, mean dead load, μ_{DL}, mean live load at ultimate limit state, $\mu_{LL(ULS)}$, and mean live load at service, $\mu_{LL(SLS)}$ are presented for R5, R1 and R2 beams ($r = 0.5, 1.0,$ and 2.0, respectively).

Table 6.6 - Design moment, M_d, mean dead load, μ_{DL}, mean live load at ultimate state, $\mu_{LL(ULS)}$, and mean live load at service, $\mu_{LL(SLS)}$, of GFRP-RC beams.

Beam	M_d (kNxm)	R5			R1			R2		
		μ_{DL} (kN)	$\mu_{LL(ULS)}$ (kN)	$\mu_{LL(SLS)}$ (kN)	μ_{DL} (kN)	$\mu_{LL(ULS)}$ (kN)	$\mu_{LL(SLS)}$ (kN)	μ_{DL} (kN)	$\mu_{LL(ULS)}$ (kN)	$\mu_{LL(SLS)}$ (kN)
C30-P1-R*-UR	18.48	3.78	7.56	4.92	5.99	5.99	3.89	8.45	4.23	2.75
C30-P1-R*-TR	28.84	5.90	11.81	7.67	9.35	9.35	6.08	13.19	6.60	4.29
C30-P1-R*-OR	42.26	8.65	17.30	11.24	13.70	13.70	8.90	19.33	9.67	6.28
C30-P2-R*-UR	18.81	3.85	7.70	5.01	6.10	6.10	3.96	8.61	4.30	2.80
C30-P2-R*-TR	24.48	5.01	10.02	6.51	7.93	7.93	5.16	11.20	5.60	3.64
C30-P2-R*-OR	29.94	6.13	12.25	7.97	9.70	9.70	6.31	13.70	6.85	4.45
C30-P3-R*-UR	16.78	3.43	6.87	4.46	5.44	5.44	3.53	7.68	3.84	2.49
C30-P3-R*-TR	20.61	4.22	8.44	5.48	6.68	6.68	4.34	9.43	4.71	3.06
C30-P3-R*-OR	25.72	5.27	10.53	6.84	8.34	8.34	5.42	11.77	5.88	3.82
C50-P1-R*-UR	24.93	5.10	10.21	6.63	8.08	8.08	5.25	11.41	5.70	3.71
C50-P1-R*-TR	40.97	8.38	16.77	10.90	13.28	13.28	8.63	18.74	9.37	6.09
C50-P1-R*-OR	58.88	12.05	24.10	15.67	19.08	19.08	12.40	26.94	13.47	8.76
C50-P2-R*-UR	25.38	5.20	10.39	6.75	8.23	8.23	5.35	11.61	5.81	3.77
C50-P2-R*-TR	32.16	6.58	13.17	8.56	10.42	10.42	6.77	14.71	7.36	4.78
C50-P2-R*-OR	41.27	8.45	16.89	10.98	13.37	13.37	8.69	18.88	9.44	6.14
C50-P3-R*-UR	21.25	4.35	8.70	5.65	6.88	6.88	4.48	9.72	4.86	3.16
C50-P3-R*-TR	28.24	5.78	11.56	7.51	9.15	9.15	5.95	12.92	6.46	4.20
C50-P3-R*-OR	35.36	7.24	14.47	9.41	11.46	11.46	7.45	16.18	8.09	5.26
C70-P1-R*-UR	40.22	8.23	16.46	10.70	13.03	13.03	8.47	18.40	9.20	5.98
C70-P1-R*-TR	54.82	11.22	22.44	14.59	17.76	17.76	11.55	25.08	12.54	8.15
C70-P1-R*-OR	75.75	15.50	31.01	20.16	24.55	24.55	15.96	34.66	17.33	11.26
C70-P2-R*-UR	32.87	6.73	13.45	8.75	10.65	10.65	6.92	15.04	7.52	4.89
C70-P2-R*-TR	42.99	8.80	17.60	11.44	13.93	13.93	9.06	19.67	9.84	6.39
C70-P2-R*-OR	57.76	11.82	23.64	15.37	18.72	18.72	12.17	26.43	13.21	8.59
C70-P3-R*-UR	28.82	5.90	11.80	7.67	9.34	9.34	6.07	13.19	6.59	4.29
C70-P3-R*-TR	37.74	7.72	15.45	10.04	12.23	12.23	7.95	17.27	8.63	5.61
C70-P3-R*-OR	46.12	9.44	18.88	12.27	14.95	14.95	9.71	21.10	10.55	6.86

6.6 PROBABILISTIC SIMULATION OF DEFLECTIONS OF FRP-RC BEAMS

Monte Carlo simulation was used in order to obtain the statistics of deflections for each of the eighty-one GFRP-RC beams designed according to ACI 440 provisions. Probabilities of failure (and corresponding reliability indexes) with respect to the limit state of excessive deflections have also been obtained. To this end: (i) the deterministic procedure presented in Figure 6.1, and (ii) generation of random variables consistent with the statistics presented in Table 6.5 were required. For each FRP-RC beam (see Table 6.6), a sample of 100,000 total deflection realizations was generated. This computacional procedure, presented in Appendix 1, was implemented using the Matlab software, version 7.0.1 (and *Statistics toolbox*). The main steps in the Monte Carlo simulation procedure are summarized in the flowchart presented in Figure 6.2.

A sample containing 100,000 realizations of the total deflections, Δ_{total}, was generated for each of the 81 GFRP-RC beams. In this process, each realization of the total deflection was computed using Eqs. (6.3), (6.4) and (6.5) (see Section 6.2.2), the random numbers generated according to the statistics presented in Table 6.5, and the considerations made in Section 6.2.2.2 with respect to long-term deflections ($\xi = 2.0$, 8-yr reference interval, and 20 % of sustained live load).

The statistics of the total deflections (minimum, mean, and maximum) corresponding to the 81 GFRP-RC beams considered in this study are presented in Tables 6.7 – 6.9. These tables also display the nominal value of the total deflection computed according to ACI 440, $\Delta_{total,ACI}$, and the ratio $\mu_{MSC} / \Delta_{total,ACI}$ (μ_{MSC} is the mean total deflection obtained via Monte Carlo simulation). From Table 6.7 it is observed that the ratios $\mu_{MSC} / \Delta_{total,ACI}$ are in the range:

- 0.99-1.34 for beams with $r = \mu_{DL} / \mu_{LL}$, equal to 0.5;

- 1.01-1.28 for beams with $r = \mu_{DL} / \mu_{LL}$, equal to 1.0; and

- 1.03-1.26 for beams with $r = \mu_{DL} / \mu_{LL}$, equal to 2.0.
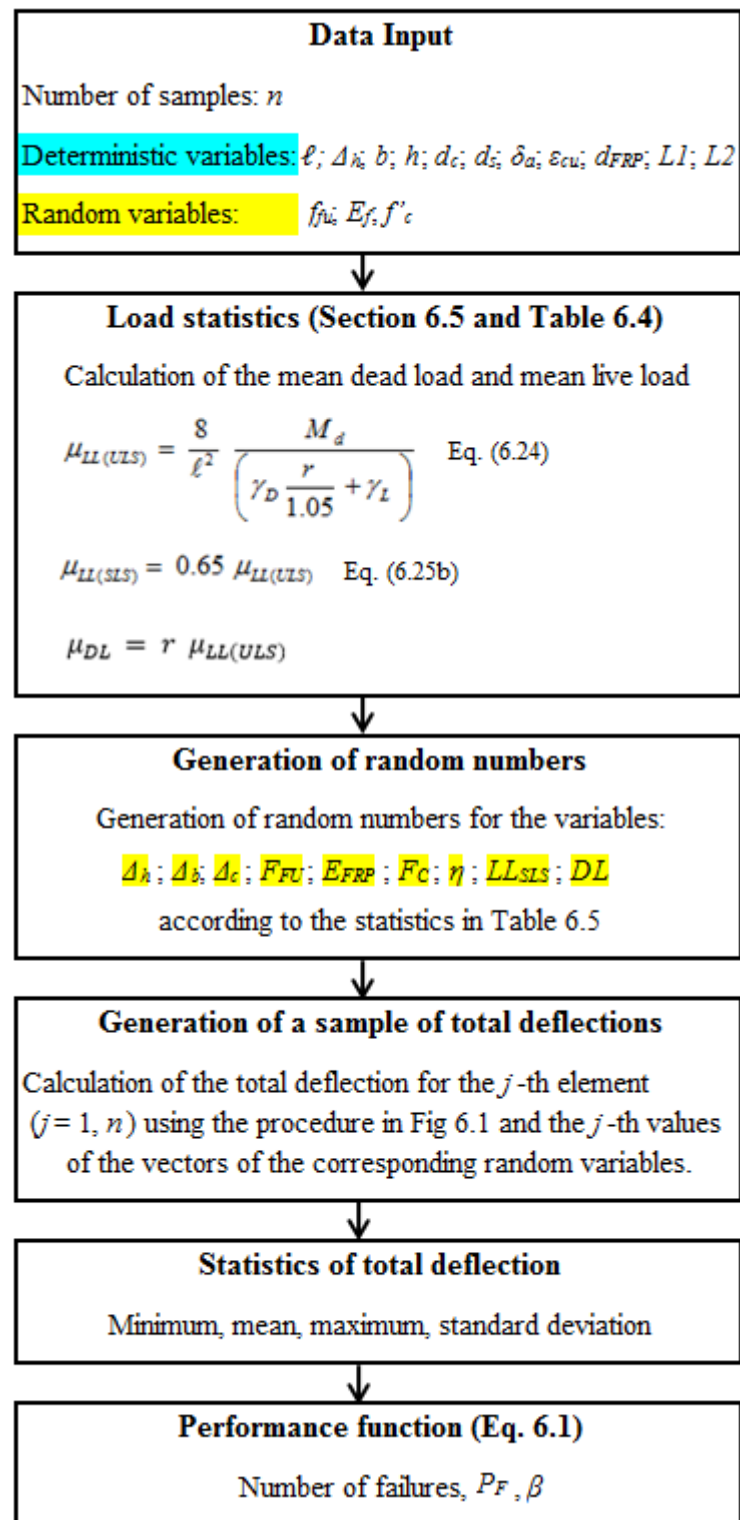
Figure 6.2 - Flowchart of Monte Carlo simulation procedure.

Additionally, it is seen that deflections increase as the load ratio increases, i.e., as more sustained loads act on the beam. Most importantly, it is seen that most over-reinforced beams,

- which correspond to the most desirable failure mode -, present larger deflections as compared to under-reinforced and transition zone beams. This results from the fact that comparatively more loads are allowed in over-reinforced beams, as well as, the use of larger strength-reduction factors for such beams (see Eqs. 3.12 (a)-(c)). Figures (6.3) - (6.8) show the histograms of deflections for selected beams. As a reference, the attendant allowable deflection is indicated in each histogram.

Table 6.7- Statistics of the total deflection of GFRP-RC beams ($r = 0.5$).

Beam	R5				
	Δ_{total} (m)			$\Delta_{total, ACI}$ (m)	μ_{MCS} / $\Delta_{total,ACI}$
	Min.	Mean	Max.		
C30-P1-R*-UR	0.0002	0.0041	0.0320	0.0038	1.0739
C30-P1-R*-TR	0.0011	0.0100	0.0375	0.0101	**0.9926**
C30-P1-R*-OR	0.0029	0.0117	0.0323	0.0116	1.0062
C30-P2-R*-UR	0.0002	0.0039	0.0404	0.0035	1.1126
C30-P2-R*-TR	0.0005	0.0077	0.0474	0.0074	1.0394
C30-P2-R*-OR	0.0010	0.0111	0.0490	0.0111	1.0041
C30-P3-R*-UR	0.0001	0.0025	0.0392	0.0022	1.1663
C30-P3-R*-TR	0.0002	0.0048	0.0498	0.0043	1.1123
C30-P3-R*-OR	0.0005	0.0081	0.0547	0.0077	1.0496
C50-P1-R*-UR	0.0003	0.0048	0.0337	0.0044	1.0834
C50-P1-R*-TR	0.0017	0.0117	0.0392	0.0117	1.0021
C50-P1-R*-OR	0.0038	0.0127	0.0342	0.0125	1.0150
C50-P2-R*-UR	0.0003	0.0047	0.0433	0.0042	1.1240
C50-P2-R*-TR	0.0006	0.0084	0.0493	0.0080	1.0544
C50-P2-R*-OR	0.0014	0.0129	0.0516	0.0128	1.0110
C50-P3-R*-UR	0.0001	0.0025	0.0397	0.0021	1.2004
C50-P3-R*-TR	0.0003	0.0059	0.0541	0.0053	1.1192
C50-P3-R*-OR	0.0007	0.0099	0.0584	0.0094	1.0530
C70-P1-R*-UR	0.0011	0.0101	0.0388	0.0093	1.0877
C70-P1-R*-TR	0.0028	0.0139	0.0407	0.0133	1.0413
C70-P1-R*-OR	0.0049	0.0141	0.0366	0.0136	1.0374
C70-P2-R*-UR	0.0004	0.0069	0.0481	0.0056	1.2306
C70-P2-R*-TR	0.0011	0.0120	0.0525	0.0108	1.1131
C70-P2-R*-OR	0.0027	0.0161	0.0509	0.0154	1.0478
C70-P3-R*-UR	0.0002	0.0046	0.0509	0.0034	**1.3363**
C70-P3-R*-TR	0.0006	0.0093	0.0606	0.0077	1.2051
C70-P3-R*-OR	0.0012	0.0135	0.0626	0.0120	1.1202

Table 6.8 - Statistics of the total deflection of GFRP-RC beams ($r = 1.0$).

Beam	R1				
	Δ_{total} (m)			$\Delta_{total, ACI}$ (m)	μ_{MCS} / $\Delta_{total,ACI}$
	Min.	Mean	Max.		
C30-P1-R*-UR	0.0006	0.0059	0.0303	0.0056	1.0520
C30-P1-R*-TR	0.0026	0.0131	0.0368	0.0130	**1.0105**
C30-P1-R*-OR	0.0053	0.0141	0.0321	0.0138	1.0251
C30-P2-R*-UR	0.0005	0.0059	0.0373	0.0054	1.0780
C30-P2-R*-TR	0.0013	0.0110	0.0454	0.0107	1.0315
C30-P2-R*-OR	0.0024	0.0150	0.0477	0.0148	1.0144
C30-P3-R*-UR	0.0003	0.0039	0.0344	0.0035	1.1159
C30-P3-R*-TR	0.0006	0.0071	0.0457	0.0066	1.0773
C30-P3-R*-OR	0.0013	0.0116	0.0519	0.0112	1.0368
C50-P1-R*-UR	0.0008	0.0069	0.0317	0.0064	1.0648
C50-P1-R*-TR	0.0038	0.0149	0.0385	0.0146	1.0211
C50-P1-R*-OR	0.0065	0.0152	0.0338	0.0147	1.0315
C50-P2-R*-UR	0.0007	0.0069	0.0397	0.0063	1.0922
C50-P2-R*-TR	0.0015	0.0119	0.0469	0.0113	1.0466
C50-P2-R*-OR	0.0033	0.0171	0.0502	0.0168	1.0238
C50-P3-R*-UR	0.0003	0.0038	0.0349	0.0033	1.1473
C50-P3-R*-TR	0.0009	0.0087	0.0496	0.0080	1.0881
C50-P3-R*-OR	0.0018	0.0139	0.0555	0.0133	1.0451
C70-P1-R*-UR	0.0026	0.0132	0.0377	0.0122	1.0871
C70-P1-R*-TR	0.0056	0.0171	0.0400	0.0162	1.0533
C70-P1-R*-OR	0.0077	0.0167	0.0362	0.0159	1.0494
C70-P2-R*-UR	0.0011	0.0099	0.0449	0.0083	1.1946
C70-P2-R*-TR	0.0027	0.0162	0.0507	0.0146	1.1051
C70-P2-R*-OR	0.0057	0.0202	0.0499	0.0191	1.0580
C70-P3-R*-UR	0.0006	0.0069	0.0461	0.0054	**1.2797**
C70-P3-R*-TR	0.0016	0.0133	0.0568	0.0113	1.1740
C70-P3-R*-OR	0.0029	0.0184	0.0602	0.0166	1.1098

Table 6.9 - Statistics of the total deflection of GFRP-RC beams (*r* = 2.0).

| Beam	R2				
	Δ_{total} (m)			$\Delta_{total, ACI}$ (m)	μ_{MCS} / $\Delta_{total,ACI}$
	Min.	Mean	Max.		
C30-P1-R*-UR	0.0012	0.0085	0.0306	0.0081	1.0511
C30-P1-R*-TR	0.0048	0.0166	0.0374	0.0162	**1.0273**
C30-P1-R*-OR	0.0075	0.0168	0.0326	0.0162	1.0384
C30-P2-R*-UR	0.0011	0.0087	0.0377	0.0081	1.0707
C30-P2-R*-TR	0.0027	0.0152	0.0460	0.0147	1.0378
C30-P2-R*-OR	0.0047	0.0197	0.0484	0.0191	1.0287
C30-P3-R*-UR	0.0006	0.0060	0.0346	0.0054	1.1016
C30-P3-R*-TR	0.0013	0.0106	0.0461	0.0099	1.0700
C30-P3-R*-OR	0.0027	0.0164	0.0526	0.0157	1.0409
C50-P1-R*-UR	0.0016	0.0097	0.0322	0.0091	1.0645
C50-P1-R*-TR	0.0066	0.0185	0.0391	0.0178	1.0364
C50-P1-R*-OR	0.0082	0.0179	0.0347	0.0172	1.0431
C50-P2-R*-UR	0.0015	0.0101	0.0401	0.0093	1.0853
C50-P2-R*-TR	0.0032	0.0163	0.0476	0.0155	1.0518
C50-P2-R*-OR	0.0063	0.0220	0.0510	0.0212	1.0375
C50-P3-R*-UR	0.0007	0.0059	0.0340	0.0052	1.1313
C50-P3-R*-TR	0.0019	0.0127	0.0502	0.0118	1.0820
C50-P3-R*-OR	0.0038	0.0192	0.0563	0.0183	1.0504
C70-P1-R*-UR	0.0048	0.0169	0.0383	0.0155	1.0883
C70-P1-R*-TR	0.0087	0.0205	0.0407	0.0193	1.0613
C70-P1-R*-OR	0.0092	0.0195	0.0371	0.0184	1.0580
C70-P2-R*-UR	0.0023	0.0141	0.0455	0.0119	1.1775
C70-P2-R*-TR	0.0052	0.0211	0.0515	0.0192	1.1026
C70-P2-R*-OR	0.0094	0.0247	0.0507	0.0232	1.0651
C70-P3-R*-UR	0.0013	0.0103	0.0455	0.0082	**1.2550**
C70-P3-R*-TR	0.0033	0.0186	0.0576	0.0161	1.1597
C70-P3-R*-OR	0.0057	0.0243	0.0611	0.0220	1.1064
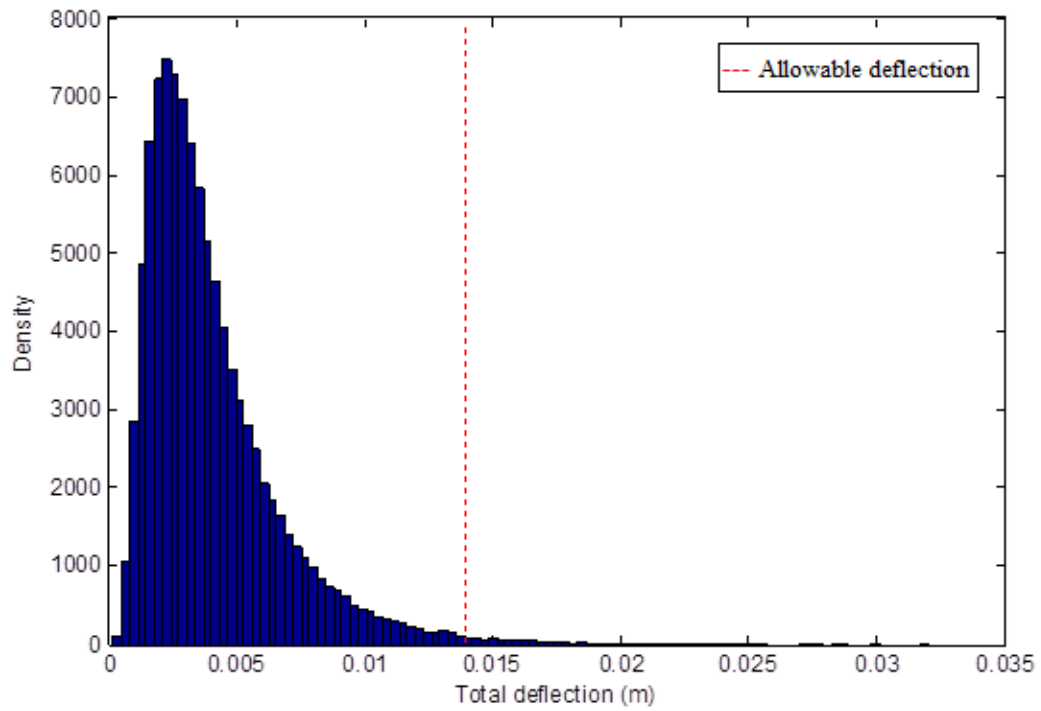
Figure 6.3 - Histogram of deflections: C30-P1-R5-UR beam.
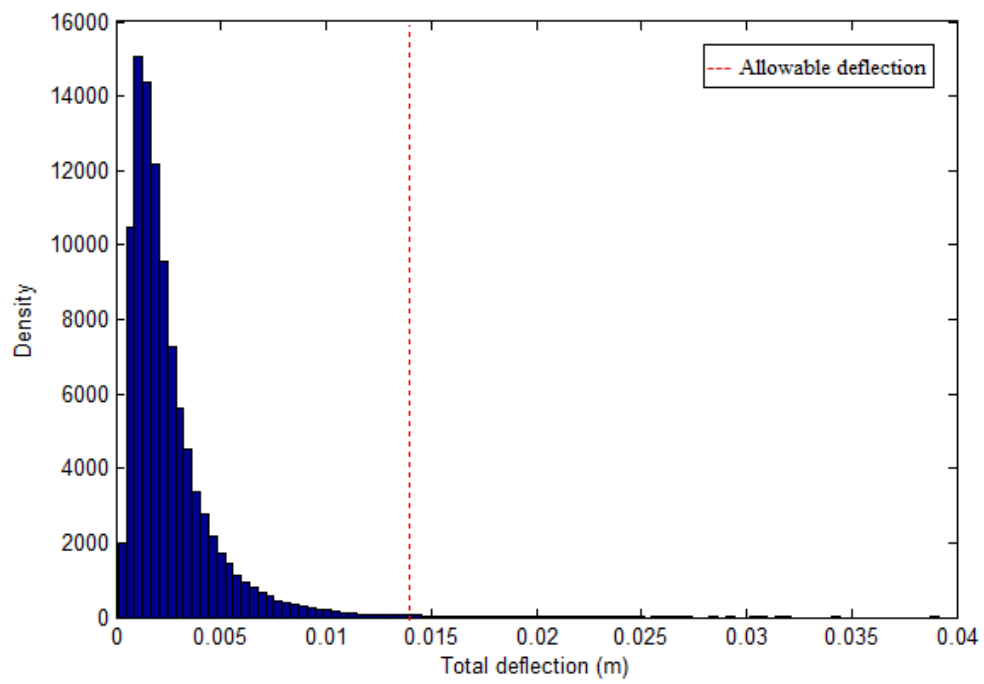

Figure 6.4 - Histogram of deflections: C30-P3-R5-UR beam.
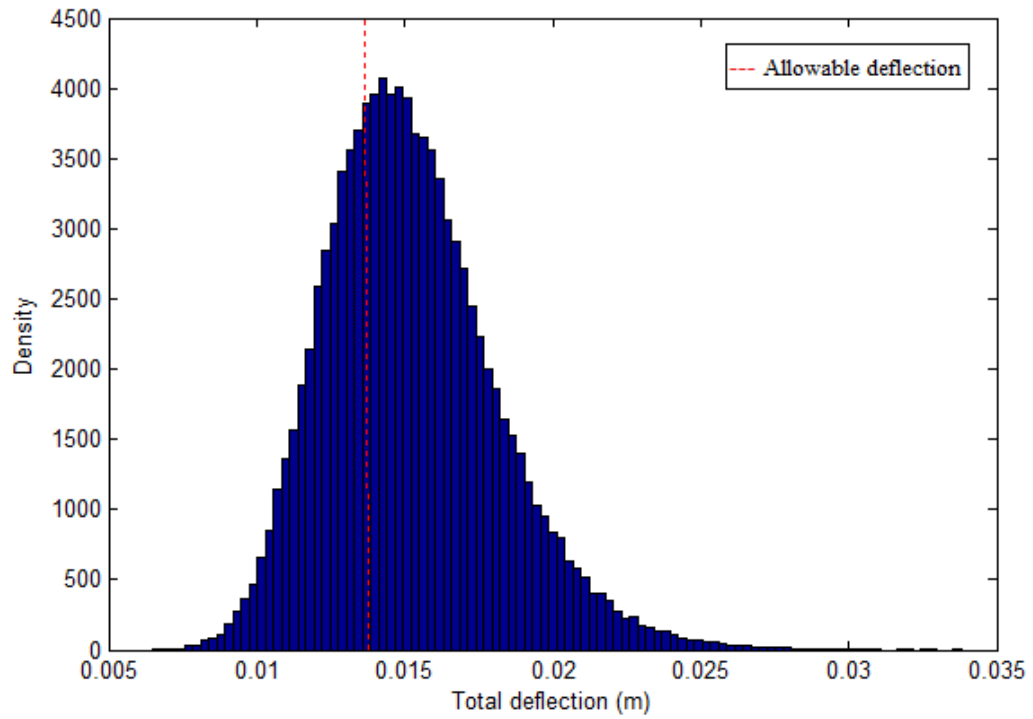
Figure 6.5 Histogram of deflections: C50-P1-R1-OR beam.
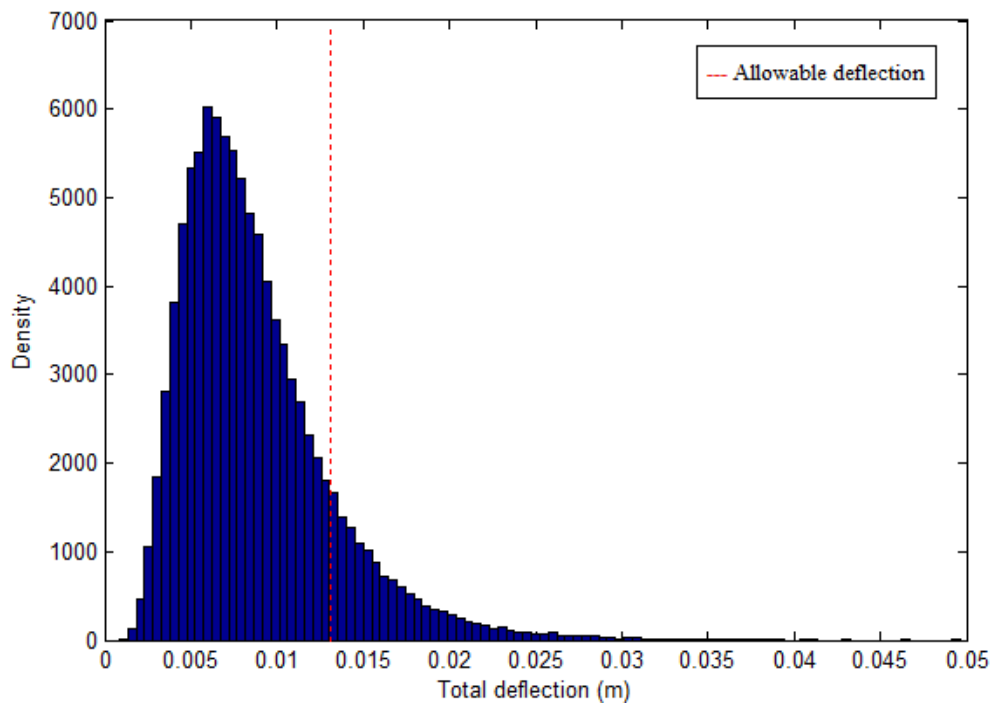

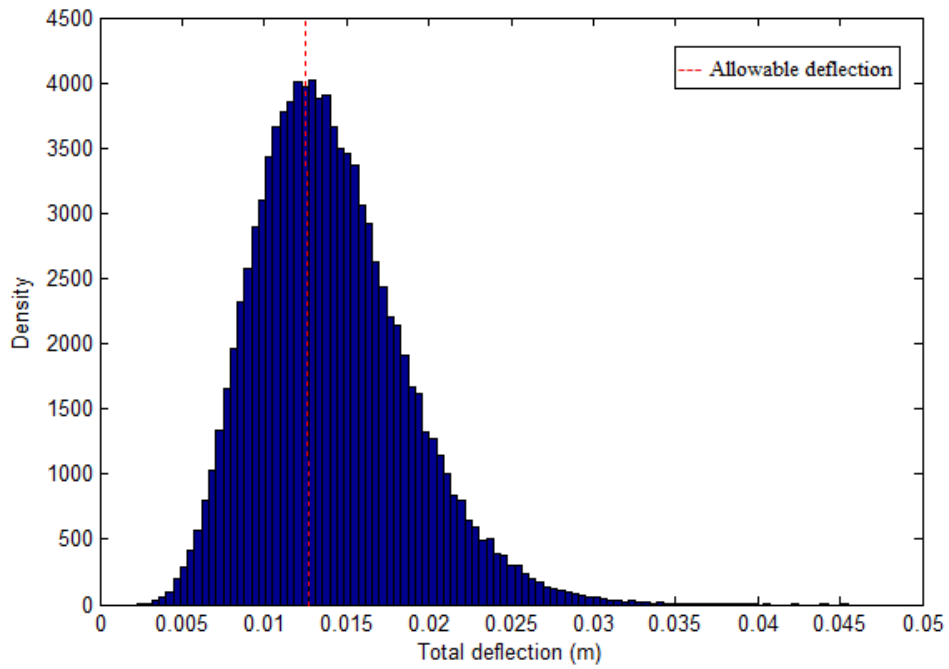**Figure 6.6 - Histogram of deflections: C50-P3-R1-TR beam.**

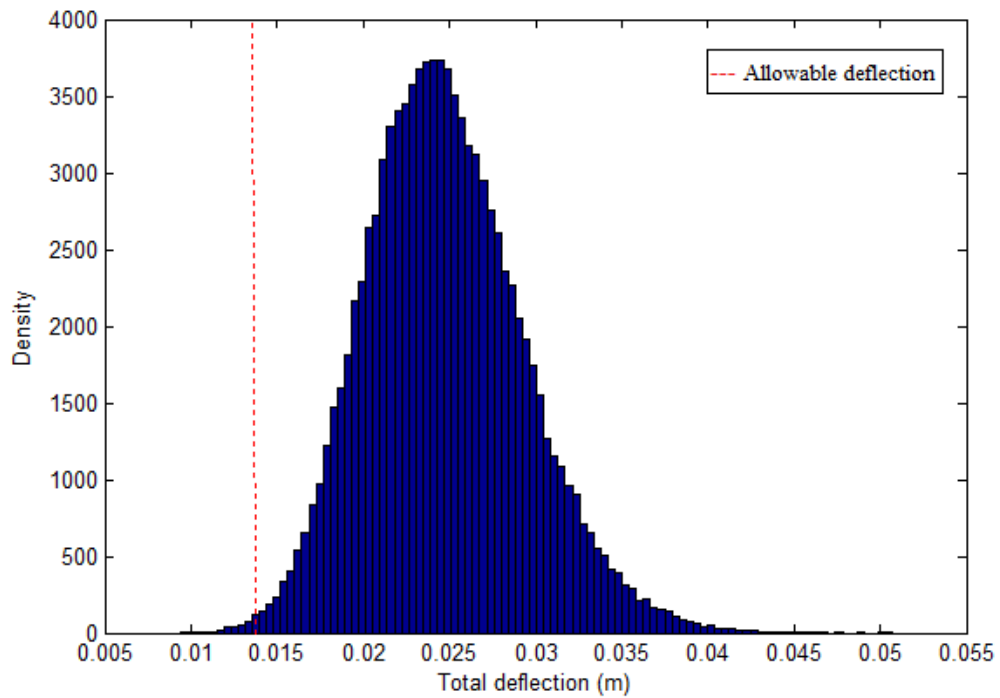**Figure 6.7 - Histogram of deflections: C70-P2-R2-UR beam.**

Figure 6.8 - Histogram of deflections: C70-P2-R2-OR beam.

6.7 PERFORMANCE FUNCTION

In this study, the performance function represented by the margin of safety, $g(\Delta) = \delta_a - \Delta_{total}$ [Eq. (6.1)] is used in the reliability assessment of the selected 81 GFRP-RC beams with respect to the limit state of excessive deflections. In Eq. (6.1), the allowable deflection, δ_a, is assumed as a deterministic variable taken as $\ell/240$ and the total deflection, Δ_{total}, is a derived random variable obtained by the procedure described in Section 6.2.2.

Figures (6.9)-(6.14) show the histograms of the margin of safety, $g(\Delta)$, for selected beams. As a reference, the line corresponding to the limit state condition, i.e. $g(\Delta) = 0$ is drawn in each histogram. The larger the area of the histogram in the $g(\Delta) < 0$ region, the larger the probability of excessive deflections.

Figure 6.9 - Histogram of the margin of safety: C30-P1-R2-OR beam.

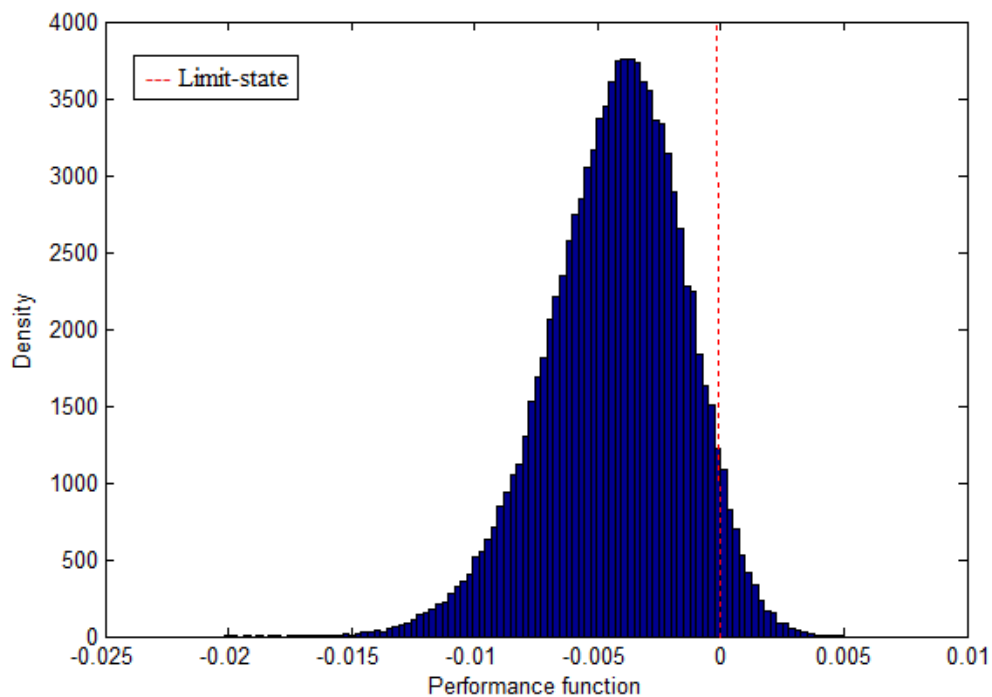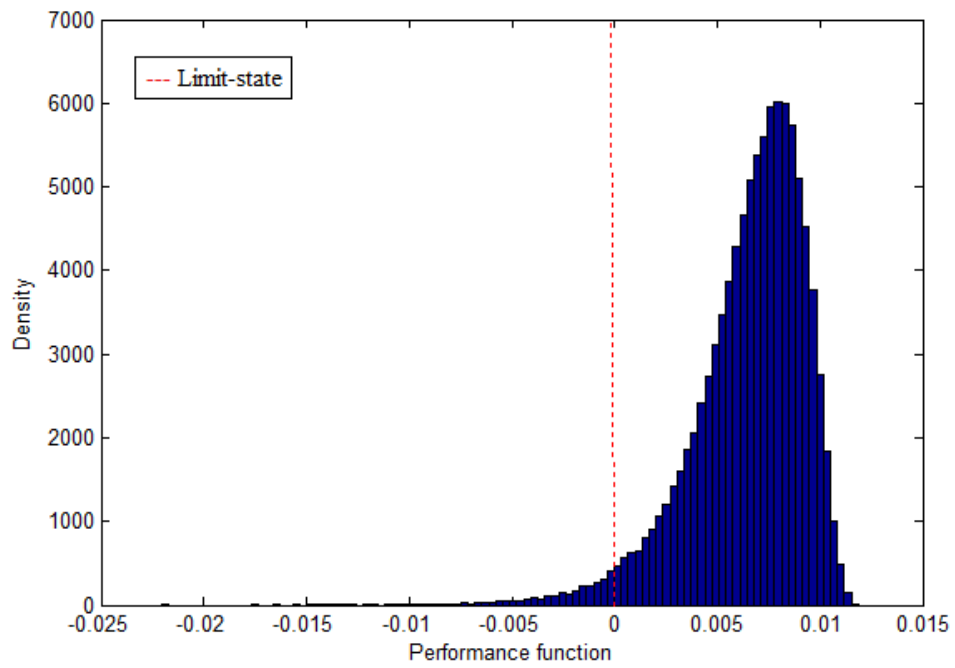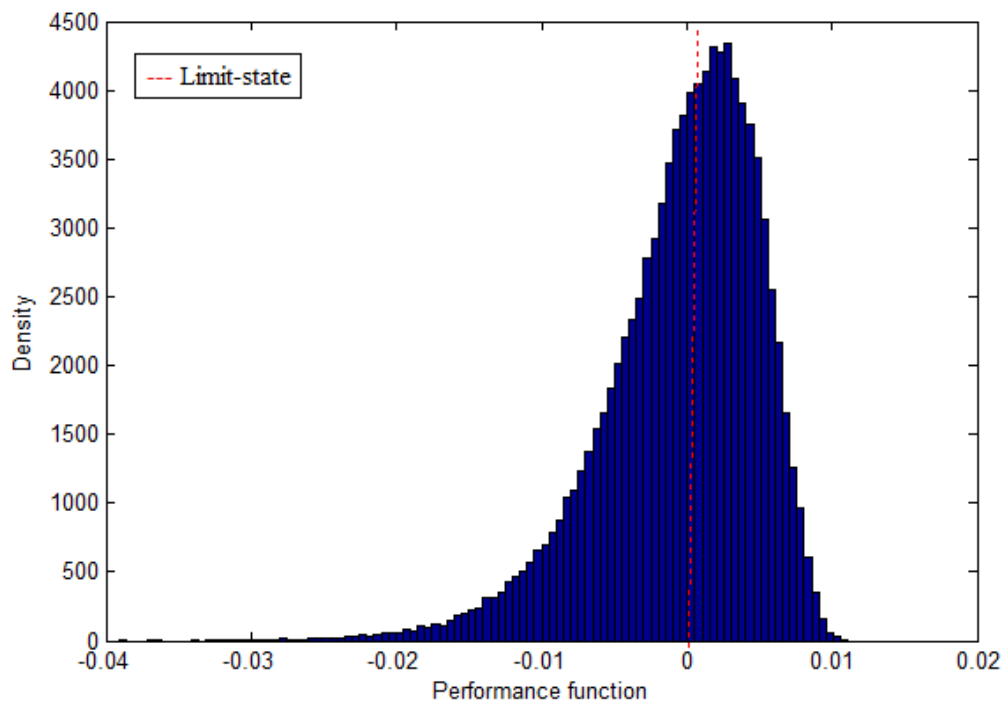**Figure 6.10 - Histogram of the margin of safety: C30-P3-R2-UR beam.**

Figure 6.11 - Histogram of the margin of safety: C50-P2-R5-OR beam.
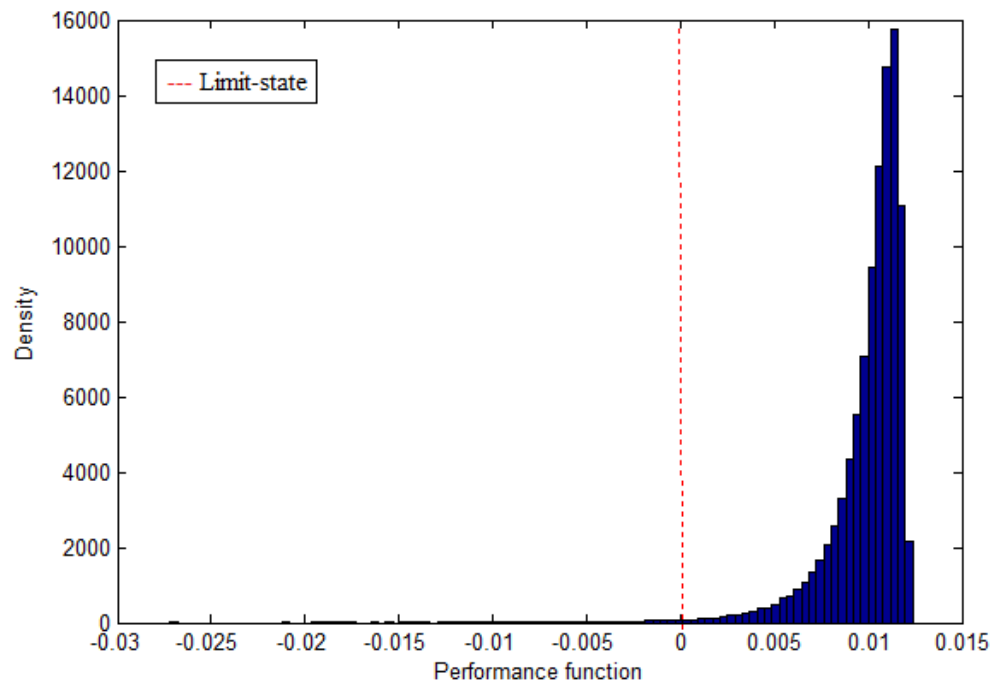
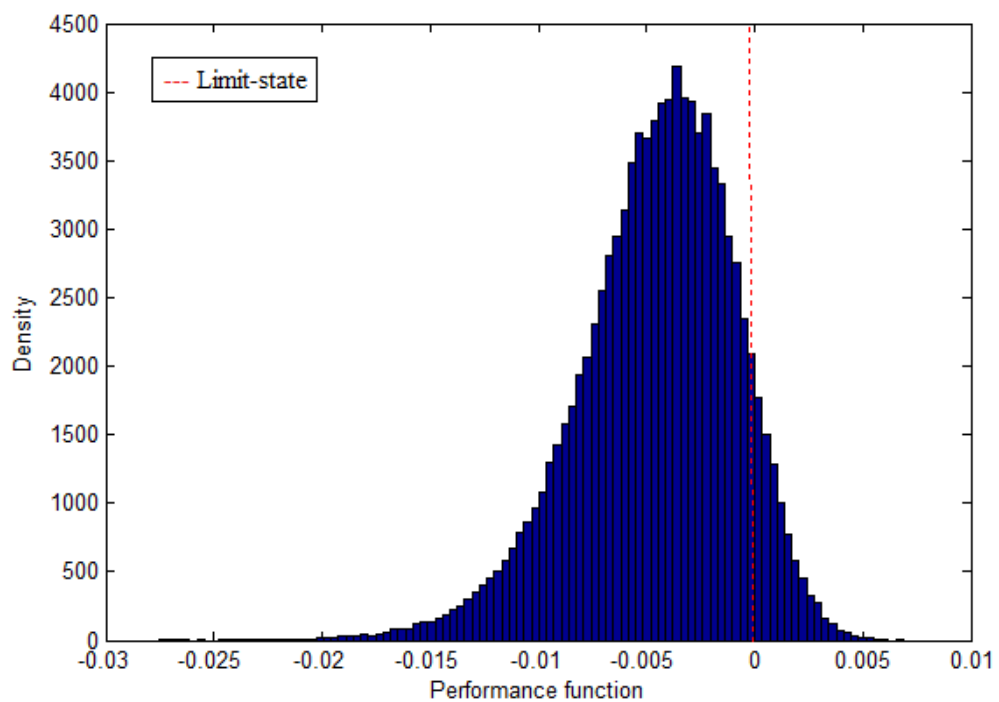**Figure 6.12 - Histogram of the margin of safety: C50-P3-R5-UR beam.**

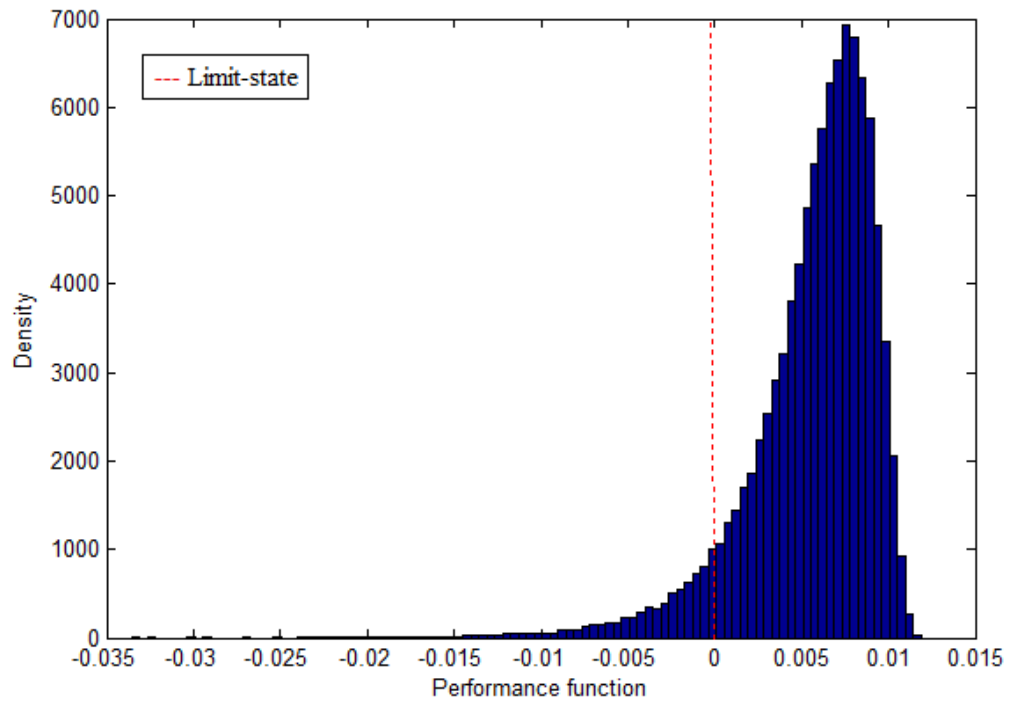**Figure 6.13 - Histogram of the margin of safety: C70-P1-R1-TR beam.**

Figure 6.14 - Histogram of the margin of safety: C70-P3-R1-UR beam.

6.8 PROBABILITY OF FAILURE AND RELIABILITY INDEX

By using Monte Carlo simulation, the number of unsatisfactory performances (number of simulations in which $\delta_a - \Delta_{total} < 0$) is counted, and the probability of failure, P_f, is obtained by the ratio of unsatisfactory performances (i.e., number of unsatisfactory performances, n_f, divided by the number of simulations, n_s). The corresponding reliability indexes are computed from the obtained P_f using the following relationship:

$$\beta = -\Phi^{-1} (P_f) \qquad\qquad (6.25)$$

Table 6.10 presents the probabilities of failure, P_f, obtained in the current study and the corresponding reliability indexes, β, associated to each of the 81 analyzed GFRP-RC beams. The results obtained in this study for the reliability indexes, β, are in the range:

- 2.48 up to negative values (corresponding to P_f in excess of 0.5) for beams with $r = \mu_{DL} / \mu_{LL}$, equal to 0.5;

- 2.35 up to negative values for beams with $r = 1.0$; and

- 1.95 up to negative values for $r = 2.0$.

From the aforementioned results, it is also observed that, for all other parameters remaining constant, beams with a larger load ratio, - i.e., more sustained loading -, present a smaller reliability index (and larger P_f). For instance, comparing beams C30-P1-R5-UR, C30-P1-R1-UR, and C30-P1-R2-UR, it is observed that β is equal to 2.15, 1.89, and 1.28, respectively.

For further analyses of the adequacy of the reliability levels obtained in this study for the deflections of GFRP-RC beams, a target reliability index, β_{target}, equal to 1.5, as suggested by Galambos and Ellingwood (1986) for the serviceability limit state, is considered. This target reliability index corresponds to floor beams under occupancy load for an eight-year reference period and is consistent with the analysis performed in this research (Section 6.3.5). Considering this target value, it is observed that out of the 81 beams designed according to ACI 440 provisions, the target is met in only **17** of such beams, none of them being over-reinforced. Considering that concrete crushing is the most desirable failure mode in flexural design of FRP-RC beams (over-reinforced beams), and that a beam must be safe and

serviceable, it is clear that the implicit reliability levels for the limit state of excessive deflections are unacceptable. Only one of the high-strength concrete GFRP-RC beams (C70 grade), out of the 27 of such beams, displays a reliability index above the selected target value.

The larger deflections of over-reinforced beams, - and consequently smaller reliability indexes -, are the result of comparatively more loads acting on over-reinforced beams, as a result of larger strength-reduction factors, ϕ, for such beams, as pointed out in Section 3.2.1.

Considering that the larger ϕ factors for over-reinforced beams are one of the reasons for larger deflections in such beams, the use of a constant ϕ factor equal to 0.55 in the design process was investigated. It is observed that there is an improvement in the resulting reliability levels. For example: C30-P3-R5-TR beam presents a reliability index, β, equal to 1.76 (see Table 6.10) for a variable ϕ factor, and for $\phi = 0.55$, β increases and is equal to 2.06 (see Table 6.11). For the target reliability index equal to 1.5, it is observed that with the change of the ϕ factor, **19** of the 81 GFRP-RC beams presents reliability indexes that meet this target value and one beam is over-reinforced.

In an attempt to further improve the implicit reliability levels for the limit state of excessive deflections, the use of a constant and smaller ϕ factor is also investigated. From the results presented in Table 6.12 for $\phi = 0.50$, it is observed that there is a significant improvement in the resulting reliability levels and the target reliability index ($\beta_{target} = 1.5$) is met in **34** out of the 81 GFRP-RC beams, 6 of them being over-reinforced. For a variable ϕ factor, $\phi = 0.55$ and $\phi = 0.50$, C30-P3-R1-OR beam have reliability indexes equal to 0.36, 1.41 and 1.95, respectively. For ϕ factor equal to 0.50, 3 of the high-strength concrete GFRP-RC beams (C70 grade), among of these 34 beams, display a reliability index above the selected target value.

Based on these results, it is possible to observe that the smaller the strength reduction factor, the greater the improvement in the reliability index and the implicit reliability levels for the limit state of excessive deflections.

Table 6.10 - Probabilities of failure (and reliability indexes) associated to serviceability limit state.

Beam	R5		R1		R2	
	P_f	β	P_f	β	P_f	β
C30-P1-R*-UR	0.0157	**2.1530**	0.0294	**1.8892**	0.1011	1.2753
C30-P1-R*-TR	0.2307	0.7366	0.5267	-0.0669	0.8844	-1.1972
C30-P1-R*-OR	0.3445	0.4002	0.7027	-0.5321	0.9527	-1.6717
C30-P2-R*-UR	0.0201	**2.0509**	0.0388	**1.7644**	0.1327	1.1136
C30-P2-R*-TR	0.1280	1.1360	0.3082	0.5011	0.7001	-0.5247
C30-P2-R*-OR	0.3232	0.4587	0.6693	-0.4379	0.9474	-1.6202
C30-P3-R*-UR	0.0068	**2.4656**	0.0099	**2.3305**	0.0282	**1.9084**
C30-P3-R*-TR	0.0390	**1.7629**	0.0845	1.3752	0.2764	0.5937
C30-P3-R*-OR	0.1516	1.0297	0.3590	0.3612	0.7566	-0.6955
C50-P1-R*-UR	0.0249	**1.9612**	0.0517	**1.6283**	0.1800	0.9154
C50-P1-R*-TR	0.3645	0.3463	0.7278	-0.6061	0.9648	-1.8093
C50-P1-R*-OR	0.4736	0.0662	0.8310	-0.9580	0.9832	-2.1246
C50-P2-R*-UR	0.0325	**1.8451**	0.0688	**1.4846**	0.2327	0.7299
C50-P2-R*-TR	0.1597	0.9956	0.3799	0.3059	0.7810	-0.7754
C50-P2-R*-OR	0.4638	0.0908	0.8253	-0.9359	0.9854	-2.1794
C50-P3-R*-UR	0.0065	**2.4832**	0.0093	**2.3547**	0.0255	**1.9522**
C50-P3-R*-TR	0.0681	**1.4900**	0.1577	1.0041	0.4629	0.0932
C50-P3-R*-OR	0.2435	0.6951	0.5427	-0.1073	0.8974	-1.2666
C70-P1-R*-UR	0.2354	0.7212	0.5369	-0.0927	0.8927	-1.2411
C70-P1-R*-TR	0.5964	-0.2441	0.9155	-1.3757	0.9951	-2.5814
C70-P1-R*-OR	0.6565	-0.4029	0.9368	-1.5282	0.9962	-2.6711
C70-P2-R*-UR	0.0954	1.3081	0.2288	0.7428	0.5962	-0.2436
C70-P2-R*-TR	0.3846	0.2933	0.7485	-0.6698	0.9706	-1.8901
C70-P2-R*-OR	0.7461	-0.6624	0.9719	-1.9093	0.9992	-3.1382
C70-P3-R*-UR	0.0353	**1.8084**	0.0749	1.4402	0.2508	0.6720
C70-P3-R*-TR	0.2138	0.7933	0.4894	0.0265	0.8648	-1.1020
C70-P3-R*-OR	0.4832	0.0421	0.8414	-1.0004	0.9876	-2.2445

Table 6.11 - Probabilities of failure (and reliability indexes) associated to serviceability limit state (ϕ = 0.55).

Beam	$\phi = 0.55$					
	R5		**R1**		**R2**	
	P_f	β	P_f	β	P_f	β
C30-P1-R*-UR	0.0157	**2.1530**	0.0294	**1.8892**	0.1011	1.2753
C30-P1-R*-TR	0.2008	0.8386	0.4719	0.0705	0.8499	-1.0360
C30-P1-R*-OR	0.1126	1.2129	0.2908	0.5512	0.6778	-0.4615
C30-P2-R*-UR	0.0201	**2.0509**	0.0388	**1.7644**	0.1327	1.1136
C30-P2-R*-TR	0.0757	1.4346	0.1804	0.9139	0.5063	-0.0157
C30-P2-R*-OR	0.1012	1.2747	0.2451	0.6901	0.6208	-0.3075
C30-P3-R*-UR	0.0068	**2.4656**	0.0099	**2.3305**	0.0282	**1.9084**
C30-P3-R*-TR	0.0198	**2.0575**	0.0378	**1.7766**	0.1289	1.1317
C30-P3-R*-OR	0.0367	**1.7908**	0.0791	1.4114	0.2644	0.6297
C50-P1-R*-UR	0.0249	**1.9612**	0.0517	**1.6283**	0.1800	0.9154
C50-P1-R*-TR	0.2990	0.5274	0.6424	-0.3650	0.9392	-1.5480
C50-P1-R*-OR	0.1823	0.9066	0.4452	0.1379	0.8246	-0.9332
C50-P2-R*-UR	0.0325	**1.8451**	0.0688	**1.4846**	0.2327	0.7299
C50-P2-R*-TR	0.1183	1.1837	0.2845	0.5694	0.6772	-0.4597
C50-P2-R*-OR	0.1709	0.9505	0.4072	0.2347	0.8075	-0.8687
C50-P3-R*-UR	0.0065	**2.4832**	0.0093	**2.3547**	0.0255	**1.9522**
C50-P3-R*-TR	0.0366	**1.7917**	0.0789	1.4125	0.2610	0.6402
C50-P3-R*-OR	0.0677	1.4934	0.1582	1.0018	0.4673	0.0820
C70-P1-R*-UR	0.2354	0.7212	0.5369	-0.0927	0.8927	-1.2411
C70-P1-R*-TR	0.5143	-0.0359	0.8660	-1.1076	0.9900	-2.3248
C70-P1-R*-OR	0.3155	0.4802	0.6665	-0.4304	0.9384	-1.5411
C70-P2-R*-UR	0.0954	1.3081	0.2288	0.7428	0.5962	-0.2436
C70-P2-R*-TR	0.3023	0.5178	0.6420	-0.3637	0.9400	-1.5544
C70-P2-R*-OR	0.3909	0.2770	0.7588	-0.7025	0.9729	-1.9251
C70-P3-R*-UR	0.0353	**1.8084**	0.0749	1.4402	0.2508	0.6720
C70-P3-R*-TR	0.1267	1.1421	0.3039	0.5133	0.7014	-0.5284
C70-P3-R*-OR	0.1818	0.9084	0.4273	0.1834	0.8238	-0.9301

Table 6.12 - Probabilities of failure (and reliability indexes) associated to serviceability limit state (ϕ = 0.50).

Beam	R5		R1		R2	
	P_f	β	P_f	β	P_f	β
C30-P1-R*-UR	0.0057	**2.5333**	0.0081	**2.4057**	0.0229	**1.9969**
C30-P1-R*-TR	0.0976	1.2955	0.2421	0.6995	0.6172	-0.2982
C30-P1-R*-OR	0.0506	**1.6388**	0.1290	1.1312	0.4048	0.2409
C30-P2-R*-UR	0.0074	**2.4372**	0.0112	**2.2845**	0.0336	**1.8310**
C30-P2-R*-TR	0.0318	**1.8553**	0.0678	**1.4925**	0.2313	0.7347
C30-P2-R*-OR	0.0441	**1.7051**	0.1002	1.2805	0.3288	0.4433
C30-P3-R*-UR	0.0020	**2.8829**	0.0023	**2.8296**	0.0046	**2.6068**
C30-P3-R*-TR	0.0073	**2.4422**	0.0107	**2.3001**	0.0315	**1.8593**
C30-P3-R*-OR	0.0143	**2.1901**	0.0255	**1.9510**	0.0849	1.3727
C50-P1-R*-UR	0.0092	**2.3571**	0.0154	**2.1609**	0.0496	**1.6485**
C50-P1-R*-TR	0.1593	0.9975	0.3888	0.2824	0.7900	-0.8063
C50-P1-R*-OR	0.0872	1.3581	0.2284	0.7440	0.5930	-0.2353
C50-P2-R*-UR	0.0124	**2.2445**	0.0216	**2.0227**	0.0706	1.4714
C50-P2-R*-TR	0.0527	**1.6194**	0.1204	1.1730	0.3811	0.3027
C50-P2-R*-OR	0.0803	1.4033	0.1944	0.8619	0.5407	-0.1021
C50-P3-R*-UR	0.0018	**2.9112**	0.0021	**2.8597**	0.0041	**2.6454**
C50-P3-R*-TR	0.0143	**2.1884**	0.0249	**1.9612**	0.0826	1.3881
C50-P3-R*-OR	0.0279	**1.9123**	0.0579	**1.5731**	0.1986	0.8467
C70-P1-R*-UR	0.1178	1.1859	0.2921	0.5474	0.6883	-0.4911
C70-P1-R*-TR	0.3176	0.4744	0.6701	-0.4401	0.9475	-1.6206
C70-P1-R*-OR	0.1732	0.9416	0.4282	0.1809	0.8088	-0.8735
C70-P2-R*-UR	0.0411	1.7378	0.0907	1.3365	0.3011	0.5212
C70-P2-R*-TR	0.1604	0.9929	0.3844	0.2939	0.7869	-0.7957
C70-P2-R*-OR	0.2223	0.7645	0.5147	-0.0369	0.8811	-1.1805
C70-P3-R*-UR	0.0139	**2.2012**	0.0236	**1.9849**	0.0772	1.4240
C70-P3-R*-TR	0.0569	**1.5818**	0.1310	1.1217	0.4059	0.2381
C70-P3-R*-OR	0.0865	1.3626	0.2071	0.8164	0.5638	-0.1606

6.9 SUMMARY OF THE CHAPTER

In this chapter, Monte Carlo simulation was used in order to obtain the statistics of deflections of the eighty-one GFRP-RC beams designed according to ACI 440 (2006) and the corresponding probabilities of failure (and reliability indexes) with respect to the limit state of excessive deflections. Several important results were obtained:

- over-reinforced beams present larger deflections - and consequently smaller reliability indexes - as compared to under-reinforced and transition zone beams;

- the load ratio has a great influence in the implicit reliability levels. It was observed that the higher the load ratio μ_{DL} / μ_{LL} (i.e., more sustained loading), the smaller the reliability index, and, consequently, the larger the probability of failure;

- the highest probabilities of failure (exceeding 0.5), are found for high-strength concrete GFRP-RC beams (C70 grade). The worst results correspond to $\mu_{DL} / \mu_{LL} = 2.0$;

- considering a target reliability index, β_{target}, equal to 1.5, only 17 GFRP-RC beams (out of the 81 selected beams) present reliability indexes that meet this target value, none of them being over-reinforced;

- the use of a constant and smaller strength-reduction factor ($\phi= 0.50$ and $\phi= 0.55$) lead to a significant improvement in the resulting reliability levels for GFRP-RC beams, and particularly for beams paired with higher strength of FRP.

7

SUMMARY, CONCLUSIONS AND SUGGESTIONS FOR FURTHER RESEARCH

7.1 SUMMARY

A major problem in the durability of RC structures is the corrosion of reinforcing steel. In this light, Fiber Reinforced Polymers (FRP), as noncorrosive materials, provide a promising prospect for use as reinforcement in concrete construction. FRP reinforcement may offer not only greater durability but also higher resistance and, consequently, potential gains throughout the lifecycle of the structure.

Although the use of FRP bars as structural reinforcement shows great promise in terms of durability, the characteristics of this material led to new challenges in the design of FRP-RC components. Design of RC beams usually results in under-reinforced beams, where the failure mode is governed by the yielding of steel, while in the design of FRP-RC beams concrete crushing is a more desirable failure mode. Design recommendations of steel reinforced members are commonly based on limit state design principles in that the member is designed based on its required strength and then checked for serviceability criteria. On the other hand, in many instances, serviceability criteria may control the flexural design of FRP-RC members.

While a reasonable body of knowledge has been gathered regarding the reliability of FRP-RC beams with respect to ultimate limit state, the same is not true for serviceability of FRP-RC beams. Therefore, the main objective of this work was to contribute to the development of semi-probabilistic design recommendations for FRP-RC beams with respect to serviceability limit states (excessive deflections). To this end, the following steps were followed:

- the main mechanical properties of concrete and FRP bars were studied;

- ACI 440 provisions for flexural design of FRP-reinforced concrete (FRP-RC) members were reviewed;

- general considerations on deflections of FRP-reinforced concrete beams were detailed. Calculation of the total deflection (and consequently of the immediate and long-term deflections) was presented. In particular, proposed equations to compute the effective moment of inertia of FRP-RC beams were compiled from the literature;

- a brief review of the basic reliability concepts and tools was presented;

- eighty-one GFRP-RC beams were selected for the analysis;

- a deterministic relationship for the performance evaluation of the selected beams was established;

- an equation to calculate the effective moment of inertia was selected. Special attention was given to the availability of the corresponding statistics of the model error;

- the probabilistic description of the basic variables of the problem (compressive strength and modulus of elasticity of concrete, cracking moment, tensile strength and modulus of elasticity of FRP, cross section geometry, model error, dead load, and live load at service), and their statistics (mean, coefficient of variation, and type of distribution) were obtained and a summary was presented. Special attention was given to the statistics of live loads at service condition;

- a computational procedure for the reliability analysis of GFRP-RC beams, for the limit state of excessive deflections was implemented. This computational procedure uses Monte Carlo simulation in the estimation of probabilities of failure of such beams;

- 81 GFRP-RC beams were designed according to ACI 440 (2006) recommendations, representing different concrete compressive strengths (from normal- to high- strength concrete), strength and stiffness of FRP, expected failure mode (under-reinforced, in the transition region, and over-reinforced beams), and ratio mean dead load to mean live load. In the absence of Brazilian recommendations for FRP-RC construction, the selected beams were designed according to ACI 440 (2006) guidelines;

- the reliability of GFRP-RC beams designed according to ACI 440 (2006) recommendations, with respect to the limit state of excessive deflections, was assessed.

7.2 CONCLUSIONS

In this research, the reliability of GFRP-RC beams designed according to ACI 440 (2006) recommendations, with respect to the limit state of excessive deflections, was assessed. To this end, samples of the deflections of selected beams were generated by Monte Carlo simulation, which was also used in the computation of the corresponding probabilities of excessive deflections.

Based on the results obtained and reported in the previous chapter, the following conclusions can be drawn:

- It was observed that total deflections (immediate plus long-term deflections) increase as the load ratio increases, i.e., as more sustained loads act on the beam.

- A comparison of the nominal value of the total deflection computed according to ACI 440 recommendations, $\Delta_{total,ACI}$, and the mean total deflection obtained via Monte Carlo simulation, μ_{MSC}, demonstrated that the ratios $\mu_{MSC} / \Delta_{total,ACI}$ are in the range:

  o 0.99-1.34 for beams with $r = \mu_{DL} / \mu_{LL}$, equal to 0.5;

  o 1.01-1.28 for beams with $r = \mu_{DL} / \mu_{LL}$, equal to 1.0; and

  o 1.03-1.26 for beams with $r = \mu_{DL} / \mu_{LL}$, equal to 2.0.

- Considering that the ratios $\mu_{MSC} / \Delta_{total,ACI}$ are mostly larger than the unit, it can be concluded that there is a trend for the mean total deflection to be larger than those predicted by ACI 440 procedures. The level of conservatism in the computation of the total deflection $\Delta_{total,ACI}$ is about the same for the all values of the load ratio r considered in this study.

- By using Monte Carlo simulation in the generation of samples of the total deflection, the corresponding histogram was obtained. Considering that the main goal in this study was the assessment of reliability levels corresponding to the limit state of

excessive deflections, distribution fitting of the generated samples was not pursued herein.

Regarding the reliability levels associated to the limit state of excessive deflections, the computed reliability indexes, β, are in the range:

- 2.48 up to negative values (corresponding to P_f in excess of 0.5) for beams with $r = \mu_{DL} / \mu_{LL}$, equal to 0.5;

- 2.35 up to negative values for beams with $r = 1.0$; and

- 1.95 up to negative values for $r = 2.0$.

It is observed that the load ratio has a great influence on the implicit reliability levels; all other parameters remaining constant, the higher the load ratio μ_{DL} / μ_{LL} (i.e., more sustained loading), the smaller the reliability index, and, consequently, the larger the probability of failure.

Several additional important results were obtained:

- over-reinforced beams present larger deflections - and consequently smaller reliability indexes - as compared to under-reinforced and transition zone beams;

- the highest probabilities of failure (exceeding 0.5), are found for high-strength concrete GFRP-RC beams (C70 grade). The worst results correspond to $\mu_{DL} / \mu_{LL} = 2.0$;

- for a target reliability index, β_{target}, equal to 1.5 (as suggested by Galambos and Ellingwood, 1986), only 17 GFRP-RC beams (out of the 81 selected beams) present reliability indexes that meet this target value, none of them being over-reinforced;

- considering that concrete crushing is the most desirable failure mode (corresponding to over-reinforced beams), it is clear that the implicit reliability levels for the limit state of excessive deflections are unacceptable;

- only one of the high-strength concrete GFRP-RC beams (C70 grade), out of the 27 of such beams, displays a reliability index above the selected target value. Therefore, the use of the concrete with higher strengths should be avoided in GFRP-RC beams;

- the use of a constant and smaller strength-reduction factor (ϕ= 0.50) lead to a significant improvement in the resulting reliability levels for GFRP-RC beams, and particularly for C50 beams paired with higher FRP strengths (P2 and P3);

- considering the large probabilities of failure obtained, use of Monte Carlo simulation with a sample size of 100,000 elements was able to provide results with acceptable accuracy for the limit state of excessive deflections of GFRP-beams.

7.3 SUGGESTIONS FOR FURTHER RESEARCH

This research focused on the reliability analysis of GFRP-RC beams for the limit state of excessive total deflections, for beams designed according to ACI 440 recommendations.

Suggestions for future research may include:

- more studies are required on the factors that influence long-term deflections of FRP-RC beams (e.g. creep of FRP);

- more studies are required in the characterization of the random variable "model error" as related to the ratio experimental to predicted deflections;

- more studies are required in the characterization of live loads at service condition and the corresponding statistics (reference period, ratio mean to characteristic);

- considering the importance of the load ratio r on the resulting reliability levels, more studies are required in the characterization of such ratio for FRP-RC construction;

- the target reliability index for the limit state of excessive deflections;

- reliability analysis of FRP-RC beams considering customized allowable deflections (i.e. other than those cases predicted in a design code);

- reliability analysis of FRP-RC beams considering other design provisions with the same scope;

- reliability analysis of FRP-RC beams considering other materials for FRP bars (e.g. CFRP).

- reliability analysis of FRP-RC beams considering other serviceability limit states (e.g. cracking).

REFERENCES

ACI COMMITTEE 318, Building Code Requirements for Structural Concrete (ACI 318-2014) and Commentary (ACI 318-08). American Concrete Institute. Farmington Hills MI, 2008.

ACI COMMITTEE 318, Building Code Requirements for Structural Concrete (ACI 318-2014) and Commentary (ACI 318R-14). American Concrete Institute. Farmington Hills MI, 2014.

ACI COMMITTEE 440. Guide for the Design and Construction of Structural Concrete Reinforced with FRP Bars. ACI 440.1R-03, 2003.

ACI COMMITTEE 440. Guide for the Design and Construction of Structural Concrete Reinforced with FRP Bars. ACI 440.1R-06, 2006.

ACI COMMITTEE 440, Guide for the Design and Construction of Structural Concrete Reinforced with FRP Bars. ACI 440.1R-15, 2015.

ANG, A.H.; and TANG, W.H. Probability Concepts in Engineering Planning and Design - Decision, Risk and Reliability, Vol. II, John Wiley & Sons. EUA, 1990.

AROCKIASAMY, M.; AMER, A.; and SHAHAWY, M. Environmental and Long-Term Studies on CFRP Cables and CFRP Reinforced Concrete Beams, Proceedings of the First International Conference on Durability of Composites for Construction, B. Benmokrane and H. Rahman, eds., Sherbrooke, Quebec, pp. 599-610, 1998.

AZEVEDO, C.P.B.; and DINIZ, S.M.C. Estudo Probabilístico da Resistência à Compressão de Concretos Utilizados em Fundações. 50º Congresso Brasileiro do Concreto, 5 a 9 de setembro, Salvador, 2008.

BENMOKRANE, B.; CHAALLAL, O.; and MASMOUDI, R. Flexural Response of Concrete Beams Reinforced with FRP Reinforcing Bars. ACI Structural Journal, V. 93, No. 1, Jan.-Feb., pp. 46-55, 1996.

BISCHOFF, P.H.; and GROSS, S.P. Equivalent Moment of Inertia Based on Integration of Curvature. Journal of Composites for Construction, ASCE, 2011a.

BISCHOFF, P.H.; and GROSS, S.P. Design Approach for Calculating Deflection of FRP-Reinforced Concrete. Journal of Composites for Construction, ASCE, 2011b.

BISCHOFF, P. H.; and SCANLON, A. Effective Moment of Inertia for Calculating Deflections of Concrete Members Containing Steel Reinforcement and FRP Reinforcement. ACI Struct. J., 104(1), 68–75, 2007.

BRANSON, D.E. Instantaneous and Time-Dependent Deflections of Simple and Continuous Reinforced Concrete Beams. HPR Rep. No. 7, Part 1, Alabama Highway Dept., Bureau of Public Roads, Montgomery, AL, 1965.

BROWN, V. Sustained Load Deflections in GFRP Reinforced Concrete Beams, Proceedings of the Third International Symposium on Non-Metallic (FRP) Reinforcement for Concrete Structures (FRPRCS-3), V. 2, Japan Concrete Institute, Tokyo, Japan, pp. 495-502, 1997.

BROWN, V.L.; and BARTHOLOMEW, C.L. Long-term Deflections of GFRP-Reinforced Concrete Beams. Proc., ICCI, Tucson, Ariz., 389–400, 1996.

CANADIAN STANDARDS ASSOCIATION (CAN/CSA-S6-06), Canadian Highway Bridge Design Code, CSA International, Rexdale, Ontario, Canada, 2006.

CANADIAN STANDARDS ASSOCIATION (CSA S806), Canadian Highways Bridge Design Code, section 16- Fiber Reinforced Structures. Final draft, 2012.

COMITÉ EURO-INTERNATIONAL DU BÉTON, CEB-FIP Model Code, 1990.

COMITÉ EURO-INTERNATIONAL DU BÉTON, FRP Reinforcement in RC Structures, CEB Bulletin n. 40, 2007.

COMITÉ EURO-INTERNATIONAL DU BÉTON, CEB-FIP Model Code, 2010.

DINIZ, S.M.C.; and FRANGOPOL, D.M. Reliability Bases for High-Strength Concrete Columns, Journal of Structural Engineering, ASCE, Vol. 123, number 10, 1997.

DINIZ, S.M.C. Structural Reliability: Rational Tools for Design Code Development, ASCE Structures Congress, ASCE, 2008.

FICO, R. Limit States Design of Concrete Structures Reinforced with FRP Bars. Thesis, University of Naples Federico II, 2007.

GALAMBOS, T.V.; ELLINGWOOD, B.R.; MacGREGOR, J.G.; and CORNELL, C.A. Probability-Based Load Criteria: Assessment of Current Design Practice, Journal of the Structural Division, ASCE, 108(5), 1982.

GALAMBOS, T.V.; and ELLINGWOOD, B.R. Serviceability limit states: Deflection, J. Struct. Eng., 10.1061/ (ASCE) 0733-9445(1986)112: 1(67), 67–84, 1986.

GANGARAO, H.V.S.; and VIJAY, P.V. Design of Concrete Members Reinforced with GFRP Bars, Proceedings of the Third International Symposium on Non-Metallic (FRP) Reinforcement for Concrete Structures (FRPRCS-3), V. 1, Japan Concrete Institute, Tokyo, Japan, pp. 143-150, 1997.

GAO, D.; BENMOKRANE, B.; and MASMOUDI, R. A Calculating Method of Flexural Properties of FRP-Reinforced Concrete Beam: Part 1: Crack Width and Deflection, Technical Report, Department of Civil Engineering, University of Sherbrooke, Sherbrooke, Québec, Canada, 24 p., 1998.

JAEGER, L.G.; MUFTI, A.; and TADROS, G. The Concept of the Overall Performance Factor in Rectangular-Section Reinforced Concrete Beams, Proceedings of the Third International Symposium on Non-Metallic (FRP) Reinforcement for Concrete Structures (FRPRCS-3), V. 2, Japan Concrete Institute, Tokyo, Japan, pp. 551-558, 1997.

JAPAN SOCIETY OF CIVIL ENGINEERS (JSCE), Recommendation for Design and Construction of Concrete Structures Using Continuous Fiber Reinforcing Materials. Concrete Engineering Series 23, Tokyo, 1997.

MACHADO, A.P. Reforço de Estruturas de Concreto Armado com Fibras de Carbono. São Paulo: Pini, 282 p., 2002.

MALLICK, P.K. Fiber Reinforced Composites, Materials, Manufacturing, and Design, Marcell Dekker, Inc., New York, 469 p., 1988.

MELCHERS, R.E. Structural reliability analysis and prediction, 2nd Ed., Wiley, New York, 1999.

MIRZA, S.A.; and MacGREGOR, J.G. Variability of Mechanical Properties of reinforced Bars. Journal of the Structural Division, ASCE, 105(5), pp. 921-937, 1979.

MOTA, C.; ALMINAR, S.; and SVECOVA, D. Critical Review of Deflection Formulas for FRP-RC Members, Journal of Composites for Construction, ASCE, 10(3), pp. 183-194, 2006.

NANNI, A. Flexural Behavior and Design of Reinforced Concrete Using FRP Rods, Journal of Structural Engineering, V. 119, No. 11, pp. 3344-3359, 1993.

NAWY, E.; and NEUWERTH, G. Fiberglass Reinforced Concrete Slabs and Beams, Journal of the Structural Division, ASCE, V. 103, No. ST2, pp. 421-440, 1977.

NOWAK, A.S. and COLLINS, K.R. Reliability of Structures, McGraw Hill, 2000.

PILAKOUTAS, K.; NEOCLEOUS, K.; and GUADAGNINI, M. Design Philosophy Issues of Fiber Reinforced Polymer Reinforced Concrete Structures. Journal of Composites for Construction, ASCE, 6(3), pp. 154-161, 2002.

RIBEIRO, S.E.C. Análise de Confiabilidade de Vigas de Concreto Armado com Plástico Reforçado por Fibras. Tese de Mestrado, Universidade Federal de Minas Gerais, 2009.

RIBEIRO, S.E.C.; and DINIZ, S.M.C. Reliability-based design recommendations for FRP-reinforced concrete beams. Engineering Structures, V. 52, 273-283, 2013.

RIZKALLA, S.; and MUFTI, A. Reinforcing Concrete Structures with Fiber Reinforced Polymers. Design Manual No. 3, ISIS Canada, Winnipeg, Man., Canada, 2001.

SHIELD, C.K.; GALAMBOS, T.V.; and GULBRANDSEN, P. On the History and Reliability of the Flexural Strength of FRP Reinforced Concrete. Members in ACI 440.1R, SP-275: Fiber-Reinforced Polymer Reinforcement for Concrete Structures, 2011.

SHOOMAN M. L. Probabilistic Reliability: An Engineering Approach, McGrawHill Book Co., New York, N.Y., 1968.

SZERSZEN, M.; and NOWAK, A. Calibration of Design Code for Buildings (ACI 318): Part 2 - Reliability Analysis and Resistance Factors. ACI Structural Journal, American Concrete Institute, 100(3), pp. 383-391, 2003.

TEGOLA, A. Actions for Verification of RC Structures with FRP Bars. Journal of Composites for Construction, ASCE, 2(3), pp. 145-148, 1998.

THERIAULT, M.; and BENMOKRANE, B. Effects of FRP Reinforcement Ratio and Concrete Strength on Flexural Behavior of Concrete Beams, Journal of Composites for Construction, V. 2, No. 1, pp. 7-16, 1998.

THORENFELDT, E., TOMASZEWICZ, A. E JENSEN, J.J., Mechanical Properties of High Strength Concrete and Application to Design, Proceedings of the Symposium: 121 Utilization of High-Strength Concrete", Stavanger, Norway, Tapir, Trondheim, pp. 149-159, 1987.

TIGHIOUART, B.; BENMOKRANE, B.; and MUKHOPADHYAYA, P. Bond Strength of Glass FRP Rebar Splices in Beams Under Static Loading, Construction and Building Materials, V. 13, No. 7, pp. 383-392, 1999.

TOUTANJI, H.; and SAAFI, M. Flexural Behavior of Concrete Beams Reinforced with Glass Fiber-Reinforced Polymer (GFRP) Bars, ACI Structural Journal, V. 97, No. 5, Sept.-Oct., pp. 712-719, 2000.

VIJAY, P. V.; GANGARAO, H. V. S.; and KALLURI, R. Hygrothermal Response of GFRP Bars under Different Conditioning Schemes, Proceedings of the First International Conference (CDCC 1998), Sherbrooke, Canada, pp. 243-252, 1998.

WU, W. P. Thermomechanical Properties of Fiber Reinforced Plastic (FRP) Bars, PhD dissertation, West Virginia University, Morgantown, W.Va., 292 p., 1990.

YAMAGUCHI, T.; KATO, Y.; NISHIMURA, T.; and UOMOTO, T. Creep Rupture of FRP Rods Made of Aramid, Carbon and Glass Fibers, Proceedings of the Third International Symposium on Non-Metallic (FRP) Reinforcement for Concrete Structures (FRPRCS-3), V. 2., Japan Concrete Institute, Tokyo, Japan, pp. 179-186, 1997.

YOST, J. R.; GROSS, S. P.; and DINEHART, D. W. Effective moment of inertia for glass fiber-reinforced polymer-reinforced concrete beams. ACI Struct. J., 100-6, 732–739, 2003.

APPENDIX 1 – FRPSERV PROGRAM

% FRPSERV program for the reliability analysis of serviceability of GFRP-RC beams implemented using Monte Carlo simulation in order to obtain the statistics of deflections of GFRP-RC beams and the corresponding probabilities of failure (and reliability indexes) with respect to the limit state of excessive deflections of simply-supported GFRP-RC beams subjected to uniformly distributed loads.

clc , clear all

% DETERMINISTIC VARIABLES

% Span: L = 3 m
% Width: B = 0.2 m
% Depth: H = 0.3 m
% Cover: dc = 35 mm
% Stirrups: ds = 9.5 mm
% Allowable deflection: dmax = L/240 (m)
% Maximum compressive strain in the concrete: ecmax = 0.003
%_____
% RANDOM VARIABLES

% STATISTICS OF DEPTH VARIATION (deltah)
% Normal distribution
% Standard deviation = 0.25 in = 0.25*25.4 mm
% Mean = 0.06in = 0.06*25.4 mm

% STATISTICS OF WIDTH VARIATION (deltab)
% Normal distribution
% Standard deviation = 0.25 in = 0.25*25.4 mm
% Mean = 0.06in = 0.06*25.4 mm

% STATISTICS OF COVER VARIATION (deltaC)
% Normal distribution
% Standard deviation = 4.22 mm
% Mean = (6.35+0.004*H) mm

% TENSILE STRENGTH OF FRP
% Normal distribution
% Coefficient of variation = 0.05
% Means = 500 MPa, 1000 MPa and 1500 MPa

% MODULUS OF ELASTICITY OF FRP
% Normal distribution
% Coefficient of variation = 0.05
% Means = 35 GPa, 42.5 GPa, and 50 GPa

% COMPRESSIVE STRENGTH OF CONCRETE
% Lognormal distribution
% Coefficient of variation = 0.10 - Excellent quality control

% Means of specified compressive strength of concrete = 30 MPa, 50 MPa, and 70 MPa

% MODEL ERROR
% Normal distribution
% Standard deviation = 0.066
% Mean = 0.95

% STATISTICS OF LIVE LOADS (SLS)
% Extreme Value Type I (Gumbel) Distribution
% Coefficient of variation = 0.32
% Reference period = 8 years
% Ratio of mean to unfactored nominal load = 1.00
% ratio mean dead load to mean live load = 0.5, 1.0 and 2.0

% Extreme Value Type I (Gumbel) Distribution
% Coefficient of variation = 0.32
% Reference period = 8 years
% Ratio of mean to unfactored nominal load = 1.00
% ratio mean dead load to mean live load = 0.5, 1.0, and 2.0

% STATISTICS OF DEAD LOAD (ULS)
% Normal distribution
% Coefficient of variation = 0.10
% Ratio of mean to unfactored nominal load = 1.05
% ratio mean dead load to mean live load = 0.5, 1.0, and 2.0

%_____
% DATA INPUT

samples = input('Number of simulations: ');

dfrp = input('FRP diameter (mm): ');

l1 = input('Number of FRP bars in the first layer: ');

l2 = input('Number of FRP bars in the second layer: ');

ffu = input('Design tensile strength of FRP, ffu, (MPa): ');

E = input('Design modulus of elasticity of FRP (MPa) : ');

fc = input('Specified compressive strength of concrete (MPa): ');
%===
% Flexural strength

% FRP reinforcement ratio (pf):

Afrp = (((l1+l2)*pi*(dfrp^2))/4)*0.000001;
d = H-((dfrp/2)/1000)-ds-(dc/1000);
pf = Afrp/(B*d);
%_____
% Balanced FRP reinforcement ratio (pfb):

 if fc < 27.6

```
  beta1 = 0.85;
 else
  Beta1 = (0.85-(0.05*((fc-27.6)/6.9)));
  if Beta1 < 0.65
    beta1 = 0.65;
  else
    beta1 = Beta1;
  end
 end
```

```
pfb = (0.85*beta1*(fc/ffu))*((E*ecmax)/((E*ecmax)+ffu));
%_____
% Stress in FRP reinforcement in tension, ff (MPa):
```

```
p1 = ((E*ecmax)^2)/4;
p2 = (0.85*beta1*fc)/pf;
p3 = E*ecmax;
p4 = 0.5*E*ecmax;
```

```
FF = (sqrt(p1+(p2*p3)))-p4;
```

```
if FF < ffu
   ff = FF;
  else
   ff = ffu;
end
%_____
% Nominal moment capacity, Mn (kNxm):
```

```
p1 = pf*ff;
p2 = 1-(0.59*((pf*ff)/fc));
p3 = B*(d^2); % m3
```

```
Mn = (p1*p2*p3)*1000;
%_____
% Strength reduction factor, fi (kNxm):
```

```
 if pf <= pfb
     fi = 0.55
 elseif pf > pfb && pf < 1.4*pfb
     fi = 0.3+(0.25*(pf/pfb))
 elseif pf >= 1.4*pfb
     fi = 0.65
 end
```

```
fiMn = fi*Mn;
%_____
% Design moment capacity, Md (kNxm):
```

```
Md = fiMn;
%_____
% Calculation of means of the load:
```

```
% Mean of the live load (ULS):

% - r = 0.5:
mi_LL5 = (8*Md)/((L^2)*((1.2*(0.5/1.05))+1.6));

% - r = 1.0:
mi_LL1 = (8*Md)/((L^2)*((1.2*(1/1.05))+1.6));

% - r = 2.0:
mi_LL2 = (8*Md)/((L^2)*((1.2*(2/1.05))+1.6));
%----------------------------------------------------------------------------------------------
% Mean of the live load (SLS):

% - r = 0.5:
mi_LL5_SLS = mi_LL5*0.65;

% - r = 1.0:
mi_LL1_SLS = mi_LL1*0.65;

% - r = 2.0:
mi_LL2_SLS = mi_LL2*0.65;
%----------------------------------------------------------------------------------------------
% Mean of the dead load (ULS) = mean of the dead load (SLS):

r = 0.5;
mi_DL5 = r*mi_LL5;

r = 1.0;
mi_DL1 = r*mi_LL1;

r = 2.0;
mi_DL2 = r*mi_LL2;
%=========================================================
% GENERATION OF RANDOM NUMBERS

% Depth, h (m)
randn('seed',1)
deltaH = 0.06*0.0254;
sd = 0.25*0.0254;
cov = sd/deltaH;
deltah = deltaH+cov*deltaH*randn(1,samples);
h = H+deltah;
%_____
% Width, b (m)
randn('seed',2)
deltaB = 0.06*0.0254;
sd = 0.25*0.0254;
cov = sd/deltaB;
deltab = deltaB+cov*deltaB*randn(1,samples);
b = B+deltab;
%_____
% Cover, d_cover (m)
randn('seed',3)
deltaC = 6.35+0.004*(H*1000);
```

```
sd = 4.22;
cov = sd/deltaC;
deltac = deltaC+cov*deltaC*randn(1,samples);
d_cover = (35+deltac)/1000;
%_____
% Tensile strength of FRP, TS_FRP  (MPa)
randn('seed',4)
tsFRP = ffu*1000;
TS_FRP = tsFRP+0.05*tsFRP*randn(1,samples);
%_____
% Modulus of elasticity of FRP, E_FRP (MPa)
randn('seed',4)
eFRP = E*1000;
E_FRP = eFRP+0.05*eFRP*randn(1,samples);
%_____
% Compressive strength of concrete, fc_cilinder (MPa)
rand('seed',5)
cov = 0.10;
fcm = fc/(1-1.34*cov);
mu = log((fcm^2)/sqrt(((cov*fcm)^2)+(fcm^2)));
sigma = sqrt(log((((cov*fcm)^2)/(fcm^2))+1));
fc_cilinder = lognrnd(mu,sigma,1,samples);
%_____
% Model error, delta_error
randn('seed',8)
sd = 0.066;
mi_model_error = 0.95;
cov = sd/mi_model_error;
delta_error = mi_model_error+cov*mi_model_error*randn(1,samples);
%_____
% Live load (kN/m)

% - r = 0.5;

rand('seed',6)
sd = 0.32*mi_LL5_SLS;
sig = (sqrt(6)*sd)/pi;
mu = mi_LL5_SLS-(0.5772*sig);
u = rand(1,samples);
LL5 = mu-(sig.*(log(-log(u))));

% Dead load (kN/m)

randn('seed',7)
DL5 = mi_DL5+0.1*mi_DL5*randn(1,samples);
%--------------------------------------------------------------------------------------------------
% Live load (kN/m)

% - r = 1.0;

% Live load
rand('seed'.6)
sd = 0.32*mi_LL1_SLS;
sig = (sqrt(6)*sd)/pi;
```

```
mu = mi_LL1_SLS-0.5772*sig;
u = rand(1,samples);
LL1 = mu-sig.*(log(-log(u)));

% Dead load (kN/m)
randn('seed',7)
DL1 = mi_DL1+0.1*mi_DL1*randn(1,samples);
%------------------------------------------------------------------------------------------------
% Live load (kN/m)

% - r = 2.0;

% Live load
rand('seed',6)
sd = 0.32*mi_LL2_SLS;
sig = (sqrt(6)*sd)/pi;
mu = mi_LL2_SLS-0.5772*sig;
u = rand(1,samples);
LL2 = mu-sig.*(log(-log(u)));

% Dead load (kN/m)
randn('seed'.7)
DL2 = mi_DL2+0.1*mi_DL2*randn(1,samples);
%===========================================================
% Computation of the total deflection

% Moment due to service loads

% r = 0.5
M_LL5 = (LL5*(L^2))/8;
M_DL5 = (DL5*(L^2))/8;
M_SERV5 = M_LL5+M_DL5;

% r = 1.0
M_LL1 = (LL1*(L^2))/8;
M_DL1 = (DL1*(L^2))/8;
M_SERV1 = M_LL1+M_DL1;

% r = 2.0
M_LL2 = (LL2*(L^2))/8;
M_DL2 = (DL2*(L^2))/8;
M_SERV2 = M_LL2+M_DL2;

j = 1;

while j<samples+1

  % Computation of in situ concrete compressive strength

  fcci = fc_cilinder(1.j);
  if fcci < 55
    alfa = 0.85;
    fcc = fcci*alfa;
  else
```

```
  alfa1 = (0.85-0.004*(fcci-55));
  if alfa1 < 0.75
    alfa = 0.75;
  else
    alfa = alfa1;
  end
  fcc = fcci*alfa;
end

if fcci < 27.6
  beta1 = 0.85;
 else
  Beta1 = (0.85-(0.05*((fcci-27.6)/6.9)));
  if Beta1 < 0.65
    beta1 = 0.65;
  else
    beta1 = Beta1;
  end
  index = 0.85*beta1;
end

hb = h(1.j);
bb = b(1.j);
d_c = d_cover(1.j);
TSFRP = TS_FRP(1.j);
EFRP = E_FRP(1.j);
MLL5 = M_LL5(1.j);
MDL5 = M_DL5(1.j);
Ma_5 = M_SERV5(1.j);
MLL1 = M_LL1(1.j);
MDL1 = M_DL1(1.j);
Ma_1 = M_SERV1(1.j);
MLL2 = M_LL2(1.j);
MDL2 = M_DL2(1.j);
Ma_2 = M_SERV2(1.j);
fconc(j) = fcc;
deltaERRO = delta_error(1.j);

% Calculation of the centroid of tension reinforcement (m)
C =((l1*(d_c+ds+(dfrp/(2*1000))))+(l2*(d_c+ds+(dfrp/(2*1000)))))/(l1+l2);

% Distance from extreme compression fiber to centroid of tension reinforcement (m)
d = hb - C;

% Gross moment of inertia (m^4)
Ig = (bb*hb^3)/12;

% Modulus of rupture (MPa)
fr = 0.62*sqrt(fcc);

% Cracking moment (kN.m)
Mcr = (2*(fr*1000)*Ig)/(hb);

% FRP reinforcement ratio
```

```
pf = Afrp/(bb*d);

% Elastic Modulus of concrete (MPa)
Ec = 4700*sqrt(fcc);

% Tensile strength of FRP to modulus of concrete ratio
nf = EFRP/(Ec*1000);

% The depth of the neutral axis to the depth of the reinforcement
k = sqrt((2*pf*nf)+(pf*nf)^2)-pf*nf;

% Moment of inertia of transformed cracked section (m^4)
Icr = (((bb*d^3)/3)*(k^3))+((nf*Afrp*(d^2)*((1-k)^2)));

% Balanced FRP reinforcement ratio
pfb = (index*((fcc*1000)/TSFRP))*((EFRP*ecmax)/((EFRP*ecmax)+TSFRP));

% Effective moment of inertia (m^4)
alfa = (0.064*(pf/pfb))+0.13;
Bd = alfa*((EFRP/(21000/0.0001))+1);
% r = 0.5
Ie_5 = (((Mcr/Ma_5)^3)*Bd*Ig)+((1-((Mcr/Ma_5)^3))*Icr);
% r = 1.0
Ie_1 = (((Mcr/Ma_1)^3)*Bd*Ig)+((1-((Mcr/Ma_1)^3))*Icr);
% r = 2.0
Ie_2 = (((Mcr/Ma_2)^3)*Bd*Ig)+((1-((Mcr/Ma_2)^3))*Icr);

% Immediate deflection
% r = 0.5
% Immediate deflection due to live load (m)
Im_LL5 = ((5*MLL5*(L^2))/(48*(Ec*1000)*Ie_5))*deltaERRO;
% Immediate deflection due to dead load (m)
Im_DL5 = ((5*MDL5*(L^2))/(48*(Ec*1000)*Ie_5))*deltaERRO;

% r = 1.0
% Immediate deflection due to live load (m)
Im_LL1 = ((5*MLL1*(L^2))/(48*(Ec*1000)*Ie_1))*deltaERRO;
% Immediate deflection due to dead load (m)
Im_DL1 = ((5*MDL1*(L^2))/(48*(Ec*1000)*Ie_1))*deltaERRO;

% r = 2.0
% Immediate deflection due to live load (m)
Im_LL2 = ((5*MLL2*(L^2))/(48*(Ec*1000)*Ie_2))*deltaERRO;
% Immediate deflection due to dead load (m)
Im_DL2 = ((5*MDL2*(L^2))/(48*(Ec*1000)*Ie_2))*deltaERRO;
%_____
% Long-term deflection (20% sustained of live load) (m)
Lt_5 = 0.6*2*(Im_DL5+0.2*Im_LL5);
Lt_1 = 0.6*2*(Im_DL1+0.2*Im_LL1);
Lt_2 = 0.6*2*(Im_DL2+0.2*Im_LL2);
%_____
% Total deflection (m)

Td_5 = (0.8*Im_LL5)+Lt_5;
```

```
  Td_1 = (0.8*Im_LL1)+Lt_1;
  Td_2 = (0.8*Im_LL2)+Lt_2;

  Total_deflection_5(j) = Td_5;
  Total_deflection_1(j) = Td_1;
  Total_deflection_2(j) = Td_2;
  %_____
  % Performance function

  % r = 0.5
  PF_5 = dmax - Total_deflection_5;
  % r = 1.0
  PF_1 = dmax - Total_deflection_1;
  % r = 2.0
  PF_2 = dmax - Total_deflection_2;

  j= j+1;

end
%=========================================================
% STATISTICS OF TOTAL DEFLECTIONS (m):

% r = 0.5

Min_Deflection_5 = min(Total_deflection_5)
Mi_Deflection_5 = mean(Total_deflection_5)
Max_Deflection_5 = max(Total_deflection_5)
SD_Deflection_5 = std(Total_deflection_5)
failures_5 = PF_5 < 0;
Num_Failures_5 = sum(failures_5(:))
Reliability_Index_5 = -norminv(Num_Failures_5/samples)
Prob_failure_5 = Num_Failures_5/samples
%_____
% r = 1.0

Min_Deflection_1 = min(Total_deflection_1)
Mi_Deflection_1 = mean(Total_deflection_1)
Max_Deflection_1 = max(Total_deflection_1)
SD_Deflection_1 = std(Total_deflection_1)
failures_1 = PF_1 < 0;
Num_Failures_1 = sum(failures_1(:))
Reliability_Index_1 = -norminv(Num_Failures_1/samples)
Prob_failure_1 = Num_Failures_1/samples
%_____
% r = 2.0

Min_Deflection_2 = min(Total_deflection_2)
Mi_Deflection_2 = mean(Total_deflection_2)
Max_Deflection_2 = max(Total_deflection_2)
SD_Deflection_2 = std(Total_deflection_2)
failures_2 = PF_2 < 0;
Num_Failures_2 = sum(failures_2(:))
Reliability_Index_2 = -norminv(Num_Failures_2/samples)
Prob_failure_2 = Num_Failures_2/samples
```

APPENDIX 2 – WORKED EXAMPLE: RELIABILITY ASSESSMENT OF C30-P2-R2-UR BEAM

This example of beam design follows the procedure adopted in this work for the probabilistic assessment of total deflections of FRP-RC beams designed according to ACI 440 (2006).

It is assumed that C30-P2-R2-UR is an interior beam, simply-supported, subjected to uniformly distributed load (dead load, *DL*, and live load, *LL*), and is reinforced with GFRP bars. It is assumed that 20 % of the live load is sustained.

A2.1 Geometric characteristics and mechanical properties of materials

- Span of the beam: $\ell = 3$ m;
- Total area of FRP reinforcement: $A_f = 2.13$ cm^2 (3 ϕ 9.5);
- Design modulus of elasticity of FRP: $E_f = 42.5$ GPa;
- Guaranteed tensile strength of FRP bar: $f^*_{fu} = 850$ MPa;
- Thickness of stirrups: $d_s = 9.5$ mm;
- Thickness of concrete cover: $d_c = 35$ mm;
- Cross section: 20 x 30 cm^2;
- Specified compressive strength of concrete: $f'_c = 30$ MPa;
- Load ratio: $\mu_{DL} / \mu_{LL} = 2.0$.

A2.2 Deterministic procedure for calculation of the design moment

A2.2.1 Design tensile strength of FRP, f_{fu}

Design tensile strength of FRP considering reductions for service environment, f_{fu}, is given by Eq. (3.14), and the environmental reduction factor is equal to 0.8 (see Table 3.1). Thus: f_{fu} = 0.8 x 850 MPa = 680 MPa.

A2.2.2 FRP reinforcement ratio, ρ_f

FRP reinforcement ratio, ρ_f, is computed by Eq. (3.2). The distance from extreme compression fiber to centroid of tension reinforcement, d, is equal to 25.075 cm. Therefore ρ_f = 0.0042.

A2.2.3 FRP reinforcement balanced ratio, ρ_{fb}

FRP reinforcement balanced ratio, ρ_{fb}, computed by Eq. (3.3), is ρ_{fb} = 0.0049. The ratio ρ_f / ρ_{fb} is 0.86.

A2.2.4 Failure mode

For C30-P2-R2-UR beam, $\rho_f < \rho_{fb}$; so, the failure mode is governed by FRP rupture. The strength reduction factor suggested by ACI 440 (2006) is 0.55 [Eq. (3.12a)].

A2.2.5 Stress in FRP reinforcement in tension, f_f

Stress in FRP reinforcement in tension, f_f, computed by Eq. (3.7) is equal to 737.80 MPa. However, in order to meet design requirements, the stress in FRP bar has to be less than or equal to the design tensile strength, f_{fu},. As this condition is not met, f_f is taken to be equal to 680 MPa.

A2.2.6 Nominal moment capacity, M_n

Nominal moment capacity of the beam, M_n, is obtained by Eq. (3.8) and is equal to 34.20 kN.m.

A2.2.7 Design moment, M_d

Design moment, M_d, is computed by multiplying the nominal moment with the strength reduction factor corresponding to the failure mode of the beam (defined in section A2.2.4). Thus: $M_d = 0.55 \times 34.20$ kN.m = 18.81 kN.m.

A2.3 Deterministic procedure for calculation of mean dead loads and mean live loads at service

A2.3.1 Mean live load at ultimate limit state, $\mu_{LL(ULS)}$

From the deterministic procedure described in Section 6.5, the mean live load at ultimate state is computed by Eq. (6.24), where $\phi = 0.55$, $M_n = 34.20$ kN.m, $r = 2.0$, $\gamma_D = 1.2$, and $\gamma_L = 1.6$. It is found that $\mu_{LL(ULS)} = 4.30$ kN/m.

A2.3.2 Mean dead load, μ_{DL}

Given the ratio $r = \mu_{DL} / \mu_{LL}$, with $r = 2.0$ and $\mu_{LL} = 4.30$ kN/m, the mean dead load is equal to 8.60 kN/m. The mean dead load at ultimate limit state is the same as the mean dead load at service.

A2.3.3 Mean of the live load to serviceability limit state, $\mu_{LL(SLS)}$

The mean live load at service, $\mu_{LL(SLS)}$, is computed by Eq. (6.25b) and is equal to 2.80 kN/m.

A2.4 Monte Carlo Simulation

Two items are required for the reliability assessment of deflections of GFRP-RC beams: (i) the statistics of the random variables involved in calculation of the total deflection (summarized in Table 6.5), and (ii) the deterministic procedure to compute the total deflection (described in Figure 6.1).

Program FRPSERV (see Appendix 1) was used in the simulation of total deflections; sample size was taken as 100,000.

A2.4.1 Generation of random numbers

A2.4.1.1 Generation of random numbers related to the depth

The random variable "Depth" is taken as the sum of the nominal depth (30 cm) and the corresponding deviation (see Table 6.5). Figure A2.1 shows the corresponding histogram for C30-P2-R2-UR beam and superimposed normal distribution.
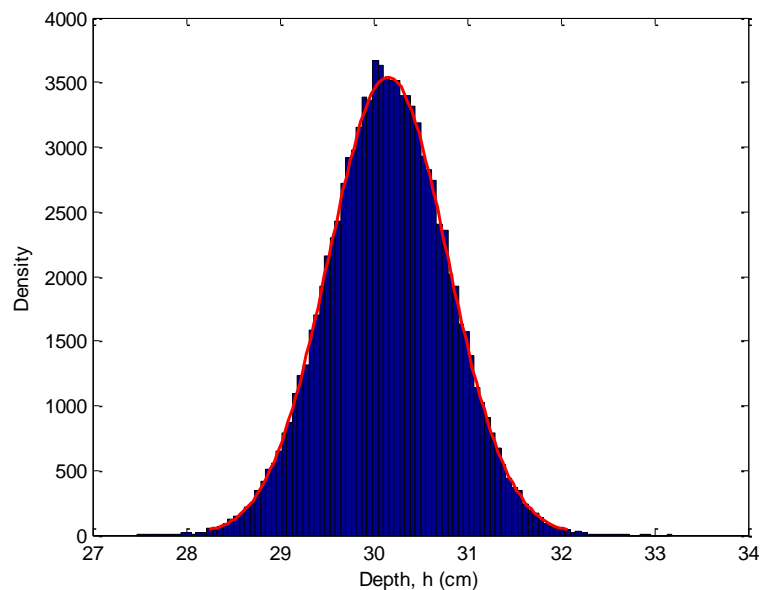

Figure A2.1 - Histogram of depth.

A2.4.1.2 Generation of random numbers related to the width

The random variable "Width" is taken as the sum of the nominal width (20 cm) and the corresponding deviation (see Table 6.5). Figure A2.2 shows the corresponding histogram for C30-P2-R2-UR beam and superimposed normal distribution.
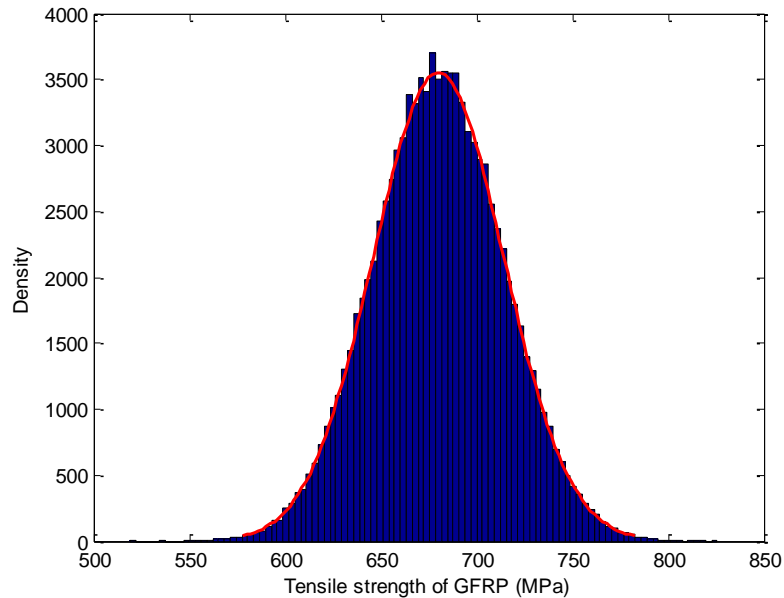
A2.4.1.3 Generation of random numbers related to concrete cover

The random variable "Cover" is taken as the sum of the nominal cover (35 mm) and the corresponding deviation (see Table 6.5). For $h = 300$ mm, the mean is $\mu = 6.35 + (0.004 \times 300) = 7.55$ mm, and the standard deviation, σ, equal to 4.22 mm. Figure A2.3 shows the corresponding histogram for C30-P2-R2-UR beam and superimposed normal distribution.
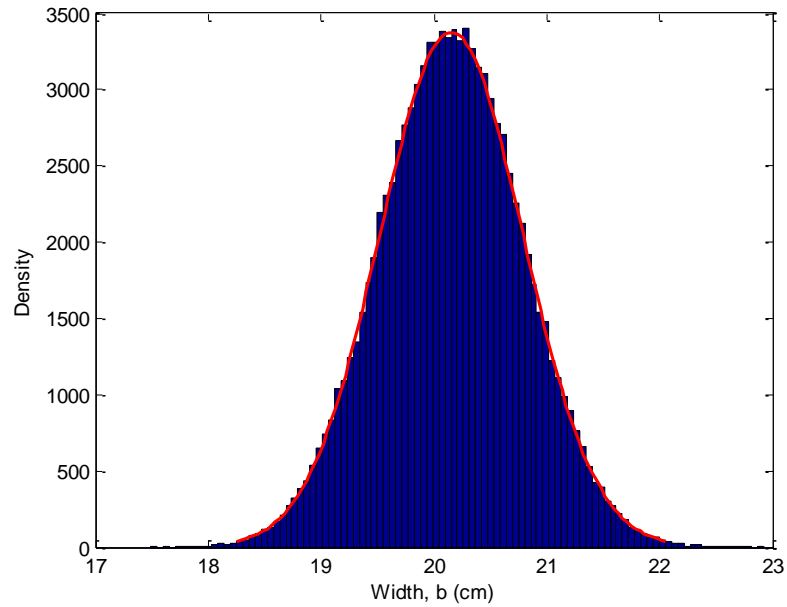
Figure A2.2 - Histogram of width.
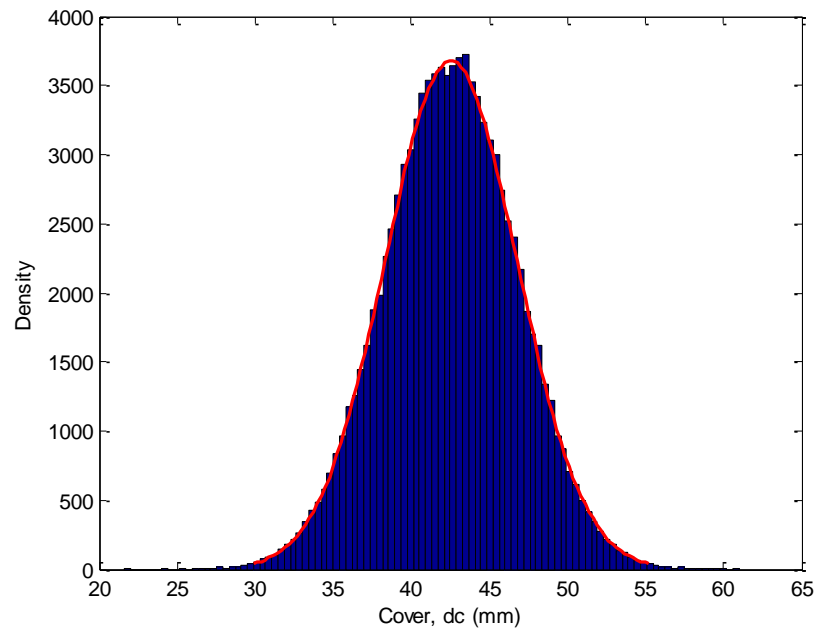
Figure A2.3 - Histogram of cover.

A2.4.1.4 Generation of random numbers related to the tensile strength of FRP

Design tensile strength of FRP (f_{fu}) is equal to the guaranteed tensile strength of FRP bar (f^*_{fu}) multiplyed by the environmental reduction factor (C_E). In this case, $f_{fu} = 0.8$ x 850 MPa = 680 MPa. Random numbers are generated according to the statistics in Table 6.5. Figure A2.4

shows the corresponding histogram for C30-P2-R2-UR beam and superimposed normal distribution.

Figure A2.4 - Histogram of FRP tensile strength.

A2.4.1.5 Generation of random numbers related to the modulus of elasticity of FRP

Figure A2.5 shows the corresponding histogram of the FRP modulus of elasticity for C30-P2-R2-UR beam and superimposed normal distribution.

A2.4.1.6 Generation of random numbers related to the concrete compressive strength

Figure A2.6 shows the histogram of the compressive strength of concrete from cylindrical specimens, where $f'_c = 30$ MPa. *In situ* concrete compressive strength (f_c) is computed by Eq. (6.7).
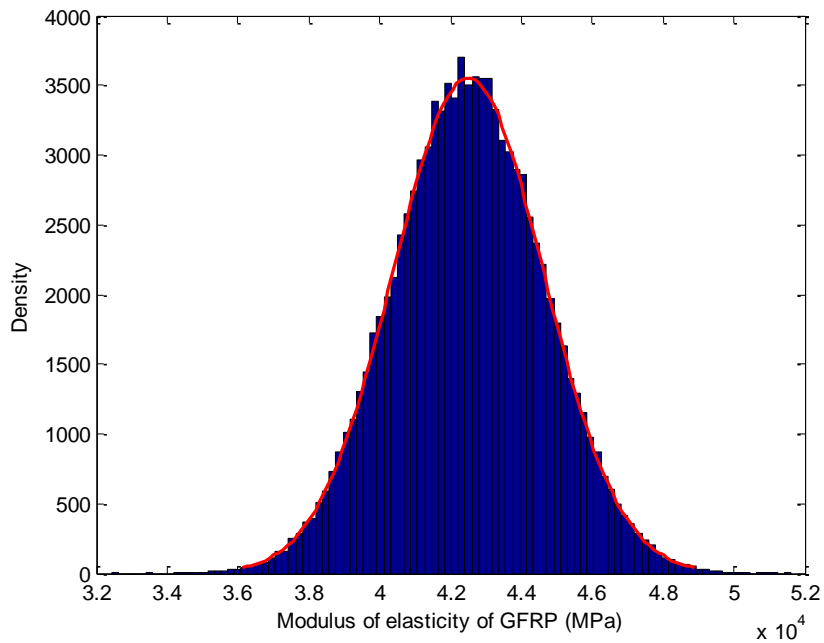
Figure A2.5 - Histogram of FRP modulus of elasticity.
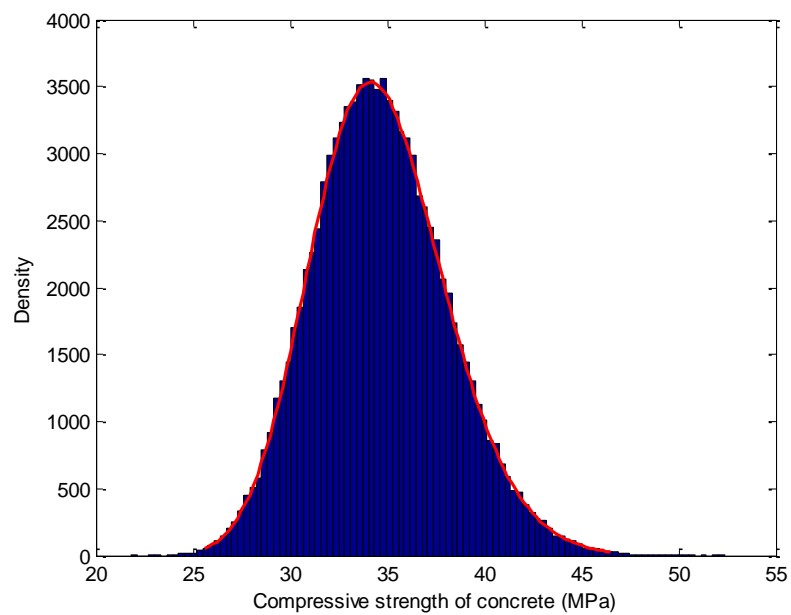
Figure A2.6 - Histogram of the compressive strength of concrete.

A2.4.1.7 Generation of random numbers related to the model error

Model error is a random variable to adjust the calculated total deflection, given by the ratio experimental/ calculated deflection. Figure A2.7 shows the histogram of the model error.
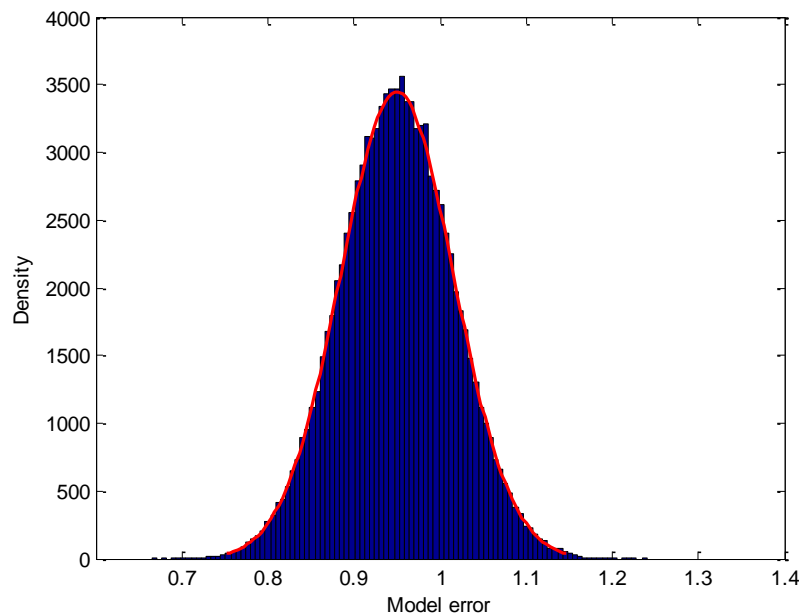
Figure A2.7 - Histogram of model error.

A2.4.1.8 Generation of random numbers related to live load at service

Random numbers corresponding to the random variable live load at service, LL_{SLS}, are generated using the mean value obtained in A2.3.3 and the corresponding statistics (COV and type of distribution) given in Table 6.5. Figure A2.8 shows the histogram of live load at service for C30-P2-R2-UR beam and superimposed Extreme Value Type I (Gumbel) distribution.

A2.4.1.9 Generation of random numbers related to dead load

Random numbers corresponding to the random variable dead load, *DL*, are generated using the mean value obtained in A2.3.2 and the corresponding statistics (COV and type of distribution) given in Table 6.5. Figure A2.9 shows the histogram of dead load for C30-P2-R2-UR beam and a superimposed Normal distribution.
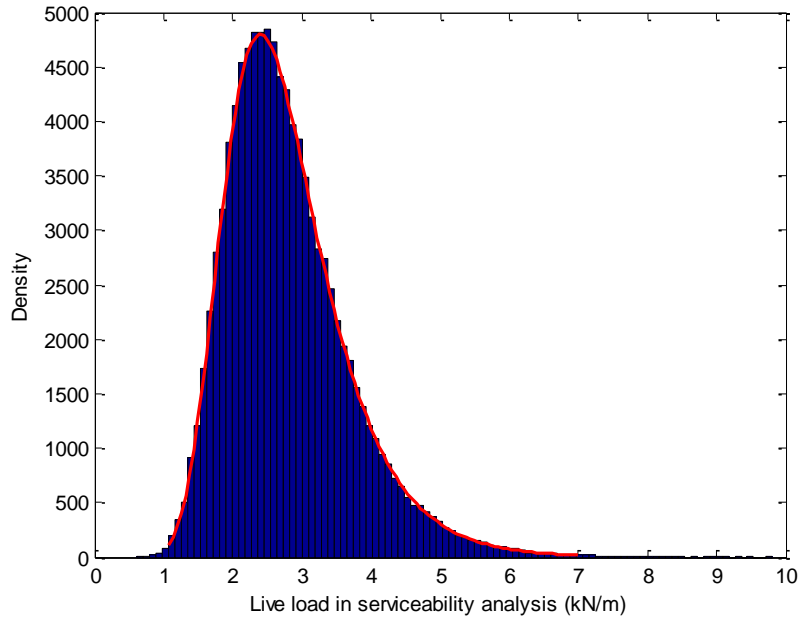
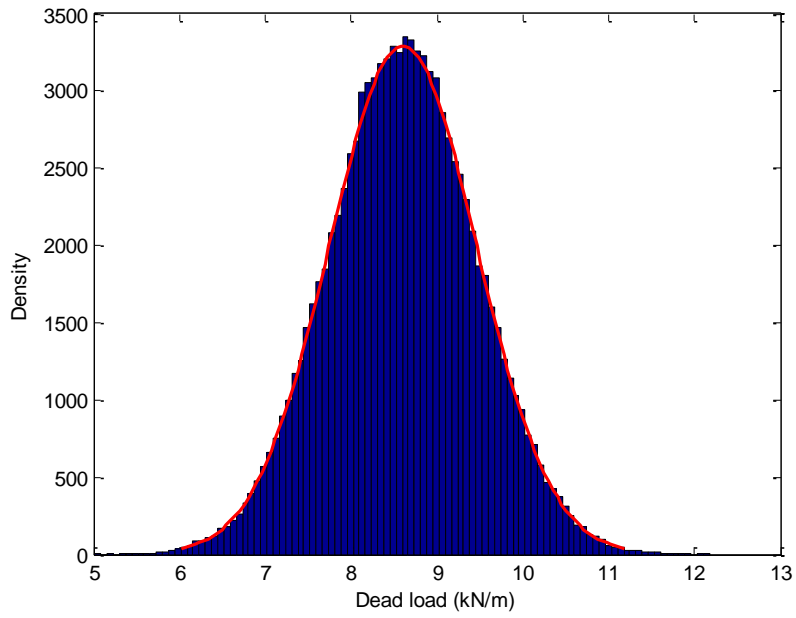**Figure A2.8 - Histogram of live load at service.**

Figure A2.9 - Histogram of dead load.

A2.4.1.10 Statistics of the total deflection

Repeating the procedure described in Figure 6.1 for the 100,000 elements of the sample (beam realizations), statistics of the total deflection are obtained. These statistics of C30-P2-R2-UR beam are listed in Table A2.1; Figure A2.10 shows the histogram of the total deflection. The ratio $\mu_{MSC} / \Delta_{total.ACI}$ is equal to 1.0707 (μ_{MSC} is the mean total deflection obtained via Monte Carlo simulation, and $\Delta_{total,ACI}$ is the nominal value of the total deflection computed according to ACI 440 recommendations). The dashed line in Figure A2.10 corresponds to the allowable deflection.

Table A2.1 - Statistics of total deflection of C30-P2-R2-UR beam.

Total deflection, Δ_{total} (m)			Standard deviation (σ)	COV
Minimum	**Mean**	**Maximum**		
0.0011	0.0087	0.0377	0.0035	0.4023

A2.4.1.11 Performance function and probability of failure

The performance function used in the current study is defineb by Eq. (6.1). The allowable deflection, δ_a, is taken as $\ell/240$, with $\ell = 3$ m, thus resulting in $\delta_a = 0.0125$ m. Figure A2.11 shows the histogram of the margin of safety, g(Δ), for C30-P2-R2-UR beam.

For this particular beam, the number of unsatisfactory performances (i.e., $\Delta_{total} > \delta_a$) is 13,272 out of 100,000 realizations of the performance function. The probability of failure, P_F, for this beam is 0.1327 (ratio unsatisfactory performances to number of simulations, i.e. 13,272/ 100,000), and the corresponding reliability index, β, calculated using Eq. (6.25), is 1.1136. This value of β is below the target reliability index, β_{target}, taken as 1.5.
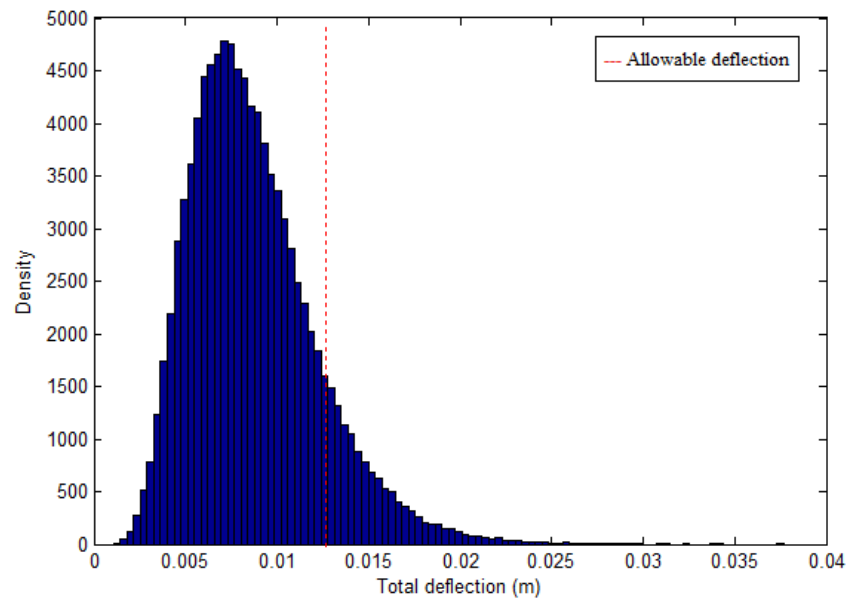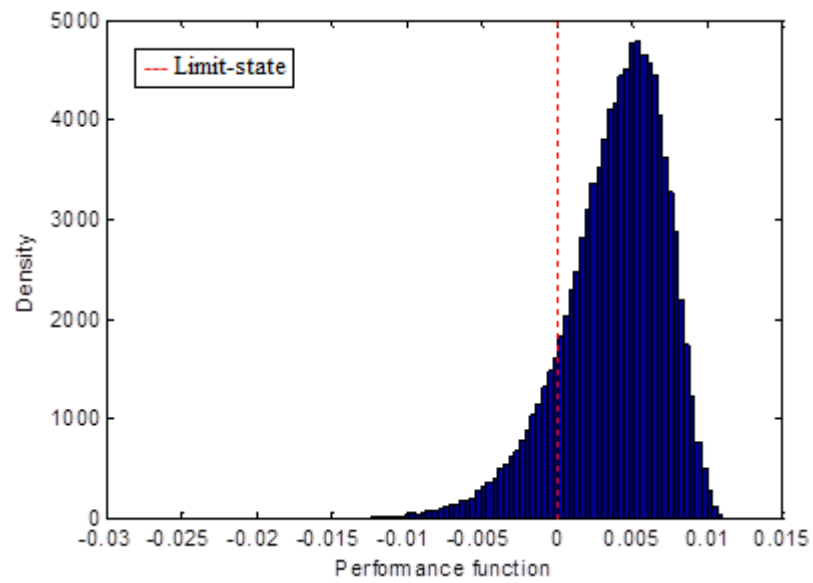
Figure A2.10 - Histogram of total deflections.

Figure A2.11 - Histogram of the margin of safety.